Development of an In-line CIP Sensor.

by

Richard J. Croy

B.Tech.

A dissertation submitted in partial satisfaction of the
requirements for the degree of
Masters of Technology

in

Food Engineering

MASSEY UNIVERSITY at PALMERSTON NORTH

2000

Abstract

Development of an In-line CIP Sensor.

by

Richard J. Croy
Masters of Technology in Food Engineering

Massey University (Palmerston North)

The need to spend a few hours cleaning milk powder plants at least once every 24 hours is the cause of a significant amount of downtime for a plant. This downtime is worth millions of dollars of lost production time to the New Zealand dairy industry each year.

Optimisation of the cleaning-in-place (CIP) systems used to clean milk powder factories has been limited by the lack of a method for measuring the amount of fouling throughout a plant without dismantling equipment for visual inspection. A sensor that could measure the amount of fouling remaining on a plant surface during CIP would allow cleaning rates and cleaning times to be determined for each cleaning cycle. Areas of intense fouling within the plant could also be mapped out using such a sensor.

Research was conducted to develop a method for using a heat flux sensor to measure the amount of fouling remaining on a stainless steel surface during CIP. A pilot plant was built to replicate the pre-heating and fouling processes in a milk powder plant. The pilot plant had a cleaning-in-place system that cleaned the plant in a manner as similar as possible to that used in the dairy industry.

Results from pilot plant trials showed that the heat flux sensor reflected changes in the fouling mass during cleaning. The heat transfer coefficient was low in the presence of fouling on the measured surface. As fouling was removed during CIP the overall heat transfer coefficient would increase. The probe allowed the estimation of the cleaning rate and cleaning time of the measured surface. The extent of fouling removed during cleaning could also be determined. Cleaning was found to be a relatively rapid process. Fouling layers of about 1 mm thickness took about 5 minutes of washing with 1.0% w/w caustic to become almost visually clean. Visual observations of a fouling layer during cleaning showed that cleaning was a process of attrition of the fouling surface. No lumps of fouling were seen breaking off the fouling layer during cleaning.

Accurate and fast-responding temperature sensors to measure the CIP fluid tem-

perature were found to be essential to the performance of the CIP monitoring system. When commercial Resistance Temperature Detectors (RTDs) mounted in a stainless steel sheath were used to measure the CIP fluid temperature the slow response time of the RTDs caused anomalies in the heat transfer coefficient trace. Heat loss from the RTD tip to its surroundings was also found to cause offset in temperature measurements. These anomalies were not seen when naked thermocouples were used to measure the CIP fluid temperature.

The effect of changes in the thermophysical properties of the CIP solutions on the heat transfer coefficient during cleaning was also investigated. Changes in temperature were found to have the largest effect on the heat transfer coefficient. A method for compensating the heat transfer coefficient trace for changes in CIP fluid temperature was developed. The compensation was justified by predictions calculated from fundamental heat transfer theory. The concentration of soil or nitric acid did not significantly affect the heat transfer coefficient. The addition of caustic soda to the process fluid caused a very small decrease in the heat transfer coefficient.

An industrial trial of the heat flux sensor was made at Kiwi Coop. Dairies Ltds Pahiatua Milk Powder Factory. The heat flux sensor was attached to the pipe directly following the direct steam injection unit (DSI) used to pre-heat milk before it entered the evaporator. The heat transfer coefficient was measured using the heat flux sensor and an existing RTD temperature probe measuring the process fluid temperature downstream of the direct steam injection unit. The CIP monitoring system was able to measure the build up of fouling during milk processing. However instability in the DSI during CIP lead to fluctuating process fluid temperatures during CIP making accurate measurement of the heat transfer coefficient impossible. A fast-response temperature sensor close to the heat flux sensor would have been needed for an accurate measurement. The existing RTD was however of a type similar to those that had given problems in earlier laboratory experiments.

Much of the data collected from the heat flux sensor and the process fluid temperature sensor at Pahiatua contained significant noise or interference. The cause of this interference is unknown but it was likely due to electrical interference from powerful electrical devices within the plant. Amplification of the signal from the heat flux sensor is therefore recommended for industrial environments along with special attention to signal wire sheilding.

To my parents.

Contents

Abstract i

List of Figures viii

List of Tables xii

Acknowledgements xiii

1 Introduction 1

2 Literature Review 3
2.1 Introduction . . . 3
2.1.1 The value and cost of cleaning . . . 3
2.1.2 Definition of the problem . . . 4
2.2 Introduction to fouling . . . 6
2.2.1 Composition . . . 6
2.2.2 Distribution . . . 7
2.2.3 Mechanisms . . . 8
2.3 How clean is clean? . . . 9
2.4 Cleaning-in-Place (CIP) . . . 11
2.4.1 Introduction . . . 11
2.4.2 Current practice and procedure . . . 12
2.4.3 Current CIP knowledge . . . 15
2.5 Monitoring CIP processes . . . 25
2.5.1 Requirements of a CIP monitor . . . 25
2.5.2 Current methods of monitoring CIP . . . 27
2.5.3 Industrial methods . . . 36
2.6 Heat flux sensors . . . 37
2.6.1 Thermocouples . . . 37
2.6.2 Thick film heat flux sensors . . . 38
2.6.3 Previous studies using heat flux probes . . . 39
2.7 Conclusions. . . . 43

3 Theory 45

4 Materials and Methods **48**
4.1 Introduction. . . . 48
4.2 Materials. . . . 48
4.2.1 Milk. . . . 48
4.2.2 CIP solutions. . . . 48
4.2.3 Steam. . . . 49
4.2.4 Water. . . . 49
4.2.5 Concentrated soiled caustic (Retentate). . . . 49
4.2.6 Heat transfer paste. . . . 49
4.2.7 Adhesive tape. . . . 49
4.3 Design and construction of the pilot plant. . . . 49
4.3.1 Objectives. . . . 50
4.3.2 Overview of the Pilot Plant. . . . 50
4.3.3 Design or selection of major items. . . . 55
4.4 Process control and instrumentation. . . . 70
4.4.1 Process control computers. . . . 70
4.4.2 Flowmeters. . . . 75
4.4.3 Temperature sensors. . . . 75
4.4.4 Heat flux sensors. . . . 82
4.5 Experimental techniques. . . . 87
4.5.1 Instrumentation used. . . . 87
4.5.2 Methods of plant operation. . . . 89
4.5.3 Cleaning-in-place procedure. . . . 92
4.5.4 Effect of process fluid thermophysical properties. . . . 95
4.5.5 Details of experimental procedures 96

5 Results and Discussion **99**
5.1 Mathematical Analysis 99
5.1.1 Heat transfer coefficient normalisation. . . . 99
5.1.2 Temperature compensation of traces 100
5.2 Effect of changing properties of the process fluid on the heat transfer coefficient trace. . . . 103
5.2.1 Effect of process fluid temperature 103
5.2.2 Effect of soil concentration in the caustic solution. . . . 106
5.2.3 Effect of nitric acid concentration. . . . 106
5.2.4 Effect of caustic concentration 110
5.3 Effect of flowrate on HTC. . . . 112
5.4 Sensitivity of the HF sensor to the presence of fouling. . . . 115
5.4.1 Comparison of the traces of clean and fouled plates. . . . 115
5.4.2 Estimate of fouling thickness from the HTC trace. . . . 117
5.4.3 Fouling resistance and visual observations. . . . 119
5.4.4 Visual evidence of the end of the caustic wash. . . . 128
5.5 Effect of lag in process temp measurement on monitor performance 130

6 Industry Trial **135**
6.1 The trial site. . . . 135
6.2 Sensor setup and data collection . . . 136
6.2.1 Attachment of the heat flux sensor to the DSI. . . . 136
6.2.2 Data logger. . . . 136
6.2.3 Data collected. . . . 136
6.2.4 Plant sensors. . . . 137
6.2.5 Data storage. . . . 138
6.3 Data manipulation. . . . 140
6.4 Results and Discussion. . . . 141
6.4.1 Interference and noise in the collected data. . . . 141
6.4.2 Sensitivity of the HF sensor to fouling. . . . 147
6.4.3 Summary discussion. . . . 151

7 Conclusions & Recommendations. **152**
7.1 Conclusions . . . 152
7.1.1 Performance of the heat flux sensor during CIP. . . . 152
7.1.2 Factors affecting the NHTC trace during cleaning. . . . 153
7.1.3 Performance of the process fluid temperature sensor. . . . 153
7.1.4 Limitations of the sensor . . . 154
7.2 Recommendations for further work. . . . 154
7.2.1 Using the HF sensor to map fouling within a plant. . . . 154
7.2.2 Development of a data gathering and control system using the HF sensor. . . . 154
7.2.3 Development of fast-response temperature sensors. . . . 155

Bibliography **156**

A Abbreviations and Nomenclature **160**
A.1 Abbreviations . . . 160
A.2 Nomenclature. . . . 161

B Example Calculations. **163**
B.1 Calculation of heat transfer coefficient for fouling modules. . . . 163
B.2 Effect of flowrate on HTC. . . . 164

C Computer Programming. **165**
C.1 CR10X Datalogger program. . . . 165
C.2 Programs for arranging data from the industrial trial. . . . 169
C.2.1 Program to patch raw data to make it a regular pattern. . . . 169
C.2.2 Removing data recorded between 8 second intervals. . . . 171
C.2.3 Organising data into straight columns. . . . 171

D Chemical analysis. **173**
D.1 Mojonnier method for fat. AACC Method 30-10. . . . 173
D.1.1 Apparatus. . . . 173
D.1.2 Reagents. . . . 173

D.1.3 Preparation of flour, bread or baked cereal products. 174
D.1.4 Majonnier fat extraction procedure (all samples). 174
D.1.5 Results - fat content. 175
D.2 Protein Analysis - Kjeldahl Method. 175
D.2.1 Apparatus. 175
D.2.2 Reagent. 175
D.2.3 Digestion. 176
D.2.4 Distillation and titration. 176
D.2.5 Results - protein content. 177
D.2.6 Caustic analysis - retentate. 177

E Contents of the CD-ROM **179**

List of Figures

2.1 Evolution of soiling along the pasteurizer (C and D sections) and the UHT sterilizer (E, F and H sections) with presentation of bulk milk temperature, of the dry weight (DW) deposit and of main component composition of dry deposit recovered per plate. (After Tissier et al., 1984). 7
2.2 Observed removal pattern for whey and whole milk protein deposits cleaned from stainless steel surfaces. (after Bird, 1997c). 16
2.3 (a) and (b). SEM's of whey protein concentrate deposit contacted with 0.1 wt% sodium hydroxide at 50°C for 2 minutes. (after Bird 1997c) 18
2.4 (a) and (b). SEM's of whey protein concentrate deposit contacted with 0.5 wt% sodium hydroxide at 50°C for 2 minutes. (after Bird 1997c) 19
2.5 Schematic representation of the milk deposit removal during alkaline cleaning. (After Jeurnink and Brinkman, 1994). 21
2.6 Performance comparison of sodium hydroxide and LI chemicals cleaning WPC deposit at 50°C and 0.175 m/s. (After Bird, 1997c). 23
2.7 Effect of flowrate on cleaning time. (after Timperley and Smeulders, 1988). 24
2.8 Influence of the acid/alkaline sequence on the removal in multiphase cleaning. (After Grasshoff, 1997). 26
2.9 Cross-section of the AERE Harwell heated radial flow cell showing the heating oil recirculation system. (After Fryer and Pritchard, 1989). 28
2.10 Surface temperature variation during the operation of the RFC. The inset shows the fouled plate and positions A, B, C and D (48.5, 28.5, 13.5 and 38.5 mm from the centre, respectively). (After Fryer and Pritchard, 1989) 29
2.11 Schematic diagram of the tapered tube. (After Fryer and Pritchard, 1989). 30
2.12 An ultrasonic transmission system for detecting a fouling deposit. (After Withers, 1996). 31
2.13 Change in time of flight of the ultrasonic signal against fouling film thickness for a artificial fouling film (layers of adhesive film) in a water filled pipe. (after Withers, 1996). 32
2.14 Frequency response of the vibration sensor plotted against a function of signal amplitude for cleaned and fouled states. (after Withers, 1996). 33
2.15 Output from the optical sensor (in millivolts) against fouling film thickness (expressed in terms of mass per unit area). The product used was skim milk. (Withers, 1996). 35
2.16 The Seebeck effect. (after Carstens 1993) 37
2.17 Diagram of a heat flux sensor. (after Rhopoint Ltd.) 39

2.18 Cross section through the heated block and cut-out pipe arrangement. (after Jones et al., 1996). 40
2.19 Schematic diagram of thermal resistance measurement cell. (after Davies et al. 1997) 42
2.20 Plot of corrected fouling resistance against wet deposit coverage. (After Davies et al., 1997). 42
2.21 Variation of deposition along heat exchanger. Re = 5000; oil temperature = 97°C, solid circles–run 1; open circles–run 2. (After Davies et al., 1997). . . 43

3.1 Diagram of the experimental system showing the sensor setup on a fouled wall. 46
3.2 Schematic diagram of the heat transfer system showing the individual heat transfer resistances. 47

4.1 Process flow diagram for milk processing on the Pilot Plant. 51
4.2 Photo of the Pilot Plant. 53
4.3 Process and Instrumentation Diagram of the Pilot Plant. 54
4.4 Process flow diagram for clean-in-place system of the Pilot Plant. 56
4.5 Process and Instrumentation diagram of the pilot plant with the flow path of CIP solutions marked in bold. 58
4.6 A 3D model of the fouling module developed for the study of fouling and CIP cleaning. 60
4.7 The array of the six fouling modules. Each module has six valves that allow it to be isolated from the main flow at any time without disturbing the other modules. (Drawing by H. Bennett.) 61
4.8 Photograph of the fouling rig containing the six fouling modules. 62
4.9 Photo of the Plate Heat Exchanger (PHE) and surrounding equipment. [A] Plate Heat Exchanger. [B] DSI that provided hot water to the PHE. [C] Milk pump. [D] Milk vat. 63
4.10 Photo of the inside of the milk vat. [A] Agitator paddle. [B] Temperature sensor column (filled with heat transfer oil and an RTD). [C] Tank outlet to plant. 65
4.11 Photo of the refrigeration unit for the milk vat. [A] Refrigeration unit with shroud. [B] Exterior pipe to milk vat. Used to fill the milk vat from a truck parked outside. 66
4.12 Photo of the holding tubes before the evaporator. [A] Holding tube 1, 50 seconds. [B] Holding tube two, 25 seconds. 69
4.13 Photo of the pilot plant with the hot water circuit marked in white. [1] Hot water heater. [2] Hot water pump. [3] Fouling rig. [4] Fouling tubes. 71
4.14 Photo of the Allen Bradley Programmable Logic Controller (PLC). 72
4.15 Screen shot of one of the control screens on the micro-computer used to monitor plant data and control the plant. 74
4.16 Screen shot of one of the historical trend graphs on the micro-computer. . . 74
4.17 Photo of a RTD temperature sensor mounted in a fouling module. The RTD is measuring the process fluid chamber. [A] Swagelok fitting welded to the fouling module holds the RTD. [B] The shaft of the RTD and the sensor wire. 76
4.18 Photo of the three types of temperature sensors used. [A] RTD. [B] thermocouple. [C] Heat flux sensor, containing a thermocouple on-board. 78

4.19 Photo of a HF sensor applied to a block of Perspex using the standard application technique. [A] HF sensor (outline can just be seen). [B] Heat transfer paste between the HF sensor and the Perspex. 85
4.20 Photo of a heat flux (HF) sensor of the type used in all experimentation. The sensor contains a thermopile [a] that measures the HF at the tip and an thermocouple [b] in the centre of the probe to measure the probe temperature. 89
4.21 P&ID diagram of the pilot plant showing the path taken by milk during milk processing. 91

5.1 Plot of HTC against temperature for water moving across a clean plate. The data is from five separate runs. 101
5.2 Comparison of two CIP monitor traces (Module 1, Run 30) with and without the temperature correction factor (TCF). (A) Traces without temperature correction. (B) Traces with TCF. 104
5.3 Plot of HTC (U) against temperature for four water runs. Predicted values of U are also shown for each water run. Water run 3 has been removed as the data overlaps run 2 making the plot too cluttered. 107
5.4 Plot of HTC against temperature for 4 solutions containing increasing concentrations of soiled caustic (retentate). 108
5.5 Plot of HTC against temperature for 3 solutions containing increasing concentrations of nitric acid. 109
5.6 Plot of HTC against temperature for 4 solutions of increasing concentrations of caustic. 111
5.7 Plot of HTC against flowrate for four fluid types used in CIP. A theoretical prediction for water is also plotted. 113
5.8 Normalised and temperature corrected HTC traces of three plates during a complete CIP cycle. Cleaning of two fouled plates (F1 & F2) and a clean plate (C). 116
5.9 Plot of NHTC before and after cleaning. The NHTC was measured during the rinses before and after cleaning. 118
5.10 A plot of estimated fouling resistance against time for Run 35. The flowrate is also plotted. The numbers from [1] to [11] refer to the stills reproduced from Figure 5.11 to 5.21 121
5.11 1st rinse. Time 0:22s. White areas indicate positions where there is no fouling and the stainless steel plate shines through. Light grey indicates fouling. The black frame indicates the location of the HF sensor on the opposite side of the plate. 121
5.12 1st rinse. Time 1:17s. Note that the white areas have not changed. 122
5.13 Caustic wash. Time 1:51s. Note that the white areas have decreased in area. Right at the probes thermopile location they have disappeared altogether. This is due to swelling of the fouling layer. 122
5.14 Caustic wash. Time 2:11s. Note that white areas have expanded indicating that cleaning has begun. The white areas during the caustic wash are at the same position as was observed during water rinse 1. Cleaning expands the white areas. 122
5.15 Caustic wash. Time 2:30s. White areas have expanded significantly from their original size. 123

5.16 Caustic wash. Time 3:01s. 123
5.17 Caustic wash. Time 4:01s. 123
5.18 Caustic wash. Time 5:00s. 124
5.19 Caustic wash. Time 7:26s. Near the end of the caustic wash. 124
5.20 Water rinse 2. Time 8:11s. Note that the grey specs are no longer shrinking. The water rinse does not clean any further. 124
5.21 Water rinse 21. Time 9:17s. 125
5.22 A plot of cleaning rate against time for Run 35. 127
5.23 HTC trace of a initially fouled plate during a caustic wash cycle. 129
5.24 Photograph of the plate (Run 35) after the post-caustic rinse. Some fouling can be seen still remaining of the plate after cleaning. 130
5.25 Comparison of two temperature sensor types. Both sensors are measuring the same flow. The RTD suffers from both a long response time and an offset error caused by heat loss. 131
5.26 Photograph of the two sensor types used. Sensor A is a RTD shielded in a stainless steel sheath. Sensor B is a T-type thermocouple with plastic insulation. 132
5.27 Comparison of HTC traces on a clean plate as measured by two different temperature probes: a thermocouple and an RTD. 134

6.1 A plot of process fluid temperature against time. The data shows three periods of severe interference in the data. 142
6.2 A plot of heat flux against time. The plot shows that the noise levels in the HF data increase during cleaning-in-place. 143
6.3 Plot of the time (in days) recorded by the data logger. Step changes in the recorded time suggest that the data loggers clock suffered interference or malfunctioned during the trial. 143
6.4 A plot of HF sensor temperature, process fluid temperature and flowrate during cleaning-in-place. 145
6.5 Detail of the plot of HF sensor temperature, process fluid temperature and flowrate during cleaning-in-place. 145
6.6 A plot of the conductivity of the process fluid along with the process fluid temperature and the HF sensor temperature during a CIP cycle. 146
6.7 Plot of the temperature of the process fluid and the HF sensor during milk processing. 149
6.8 Plot of the overall heat transfer coefficient(U) of the pipe at the exit of the Direct Steam Injection unit during milk processing. Two (2) degrees K has been added to the temperature of the process fluid temperature for each calculation of U. 149
6.9 Plot of process fluid temperature and HF sensor temperature during a CIP cycle. The difference between the two temperatures provide an indication of the amount of fouling on the inside pipe surface adjacent to the HF sensor. 150

List of Tables

2.1 Food deposit constituent characteristics (after Bird, 1997a) 11

4.1 Modules within the Allen Bradley Programmable Logic Controller. 72
4.2 Variables controlled using the micro-computer. 73
4.3 Initial temperature sensor locations. 79
4.4 Changes made to the locations of temperature sensors. 80
4.5 Calibration data for fouling module RTD sensors. 80
4.6 Calibration data for heat flux sensor thermocouples. 81
4.7 Calibration data for thermocouples used to measure the process fluid temperature in fouling modules 1, 2 & 3. 81
4.8 Calibration results for TC3, TC4 and TC5 with thermocouples for measuring process fluid temperature in fouling modules 1, 2 & 3. 82

5.1 Table of calculated h_p values for temperatures from 20 to 90°C. 105
5.2 The composition of the soiled solutions used in the Soil Effect experiments . 106

6.1 Plant sensor signal outputs, resistors and linear equations. 138

B.1 Calculations of U for flow velocities of 0.4, 0.5, 0.6, 0.7 and 0.8 m/s. 164

D.1 Retentate fat content results. 175
D.2 Retentate protein composition results. 177
D.3 Titration results for caustic concentration in the retentate. 178

Acknowledgements

I would like to acknowledge and thank the following people for their help with this project:

- Trinh, Khanh Tuoc, for his challenging and supportive supervision and the opportunity he provided with this project.
- Orica Chemnet Ltd, for their sponsorship and support for the project.
- Foundation for Research, Science and Technology for this opportunity provided through the GRIF project.
- Terry Smith, for his support for the project and help with obtaining supplies and equipment for the experimental work. Thanks also for his help with editing my thesis.
- Byron McKillop, for his extensive assistance and advice in building the pilot plant.
- Hayden Bennett, Andrew Hinton and Carol Ma for their help in the group project to build the pilot plant. Thanks to Carol also for her help in the chemistry lab.
- Binh Trinh, for his assistance in the pilot plant.
- Don McClean, for his help with welding for the pilot plant.
- Steve Glasgow, for his help with the handling of the CIP chemicals.
- Garry Radford, for helping with lots of little queries in the lab and with getting milk for the pilot plant.
- Geedha Sivalingham-Reid, for her help in the chemistry lab.
- Hong Chen, Scott Houston and Bruce Manson at Kiwi Dairies Ltd. for their support in trialing the sensor at Pahiatua.
- Neville Burgess and Les Welch for their assistance in installing the sensor at Pahiatua.
- Gerard Harrigan, for his assistance with datalogging equipment for the factory trial and with the signal conditioner.
- Thanks also to Mike and Troy at Pahiatua for their help in the plant.
- Alison Spurway and Richard Webb, for their introduction to the Hawera site and offers of support throughout the project.

Chapter 1

Introduction

The dairy industry is a major contributer to the New Zealand economy. More than a billion litres of milk are processed annually (NZDB 2000). The total revenue from exports of milk products for the New Zealand dairy industry in 1997/98 was $NZ 4.6 billion.

Milk powder exports account for $1.6 billion of this revenue. 525,000 tonnes of milk powder were produced in 1997/98 (NZDB 2000). Because the throughput of milk powder plants is large and the processing operations essentially continuous downtime for these plants is worth millions of dollars each year (Fung 1997).

The cleaning of milk powder plants is necessary. Failure to clean dairy processing equipment will lead to a failure of the process and possibly unsafe product (Bird 1997a). The need for cleaning causes 2-3 hours of downtime for a milk powder plant about every 18 hours. This loss of production time is a huge cost to the dairy industry.

Current CIP systems used in milk powder plants use very little or no real-time feed back control. Cleaning cycles are recipe based with a preset duration for each cleaning step. Cleaning times for each plant are determined empirically. Some plant equipment can be opened for inspection to determine if there is any fouling remaining after CIP but this process is too time consuming to be done for every cleaning cycle. Therefore it is not possible to tell if all surfaces within the plant are clean from run to run.

Some technologies are used in industry for making global measurements of CIP processes within a milk processing plant. Measurement of the turbidity of the CIP process stream provides an indication of the soil concentration during CIP. Measurement of the conductivity and pH of the CIP stream allows the concentration of chemical cleaning agents to be monitored. These parameters provide measurements of the CIP stream but not of the fouled surfaces directly. They reveal the rate at which fouling is being removed from the

plant as a whole rather than whether localised surfaces within the plant are clean.

The availability of a sensor that could provide local measurements of fouling would allow the cleaning process to be measured on a local scale, thus providing better opportunities for process optimisation and feed-back control. Measurement of the amount of fouling remaining on a process surface during cleaning would allow local cleaning rates and cleaning times to be determined for each cleaning cycle. A local measurement of fouling would also allow the amount of fouling removed during cleaning to be determined. This would allow positions of excessive fouling within a plant to be mapped out.

This project aimed to develop a method for using a heat flux sensor to provide a local measurement of fouling on a process surface during cleaning-in-place. Heat flux sensors have been used to monitor fouling development within milk powder plants in the past (Truong et al. 1998). Several added complexities have prevented the methods used to measure fouling being directly applied to cleaning-in-place. The most significant of these is the changing thermophysical properties of cleaning-in-place solutions during a cleaning cycle. To develop a method for using a heat flux sensor to monitor cleaning two main areas of research were required:

- To develop an understanding of how to interpret changes in the measured trace in terms of the removal of fouling from the measured surface during cleaning-in-place.
- To develop methods for compensating for unwanted changes in the measured trace caused by changes in the thermophysical properties of CIP solutions during cleaning.

This thesis first discusses literature on cleaning-in-place knowledge and systems used in dairy plants with an emphasis on experimental and industrial techniques for monitoring cleaning-in-place. Chapter 3 discusses the theoretical background underlying the use of a heat flux sensor to measure fouling. Chapter 4 then discusses the construction of the pilot plant used for this research and the experimental techniques and procedures used for pilot plant based research. Chapter 5 discusses the results of the research conducted on the pilot plant beginning with the effect of changing thermophysical properties of the the CIP solutions on the heat sensor trace and then discussing the performance of the sensor during cleaning. The following chapter discusses the site, methods, and results of an industrial trial of the sensor. Conclusions and recommendations for future work are then given in Chapter 7.

Chapter 2

Literature Review

2.1 Introduction

2.1.1 The value and cost of cleaning

Cleaning in the food industry has traditionally been as much of an art as a science. 'Rules of thumb', such as the widely quoted minimum cleaning velocity of 1.5 m/s, are still in use industrially. The empirical approach to cleaning in industry is due to the fact that cleaning systems were designed before scientific studies of the fundamental mechanisms of cleaning were made. This has resulted in effective but wasteful cleaning systems. The cost of cleaning is high and the expenses come from a number of sources (Bird, 1997a):

- chemical, the cost of the cleaning chemicals themselves.
- loss of production, as a result of down time. In some segments of the dairy industry, up to 42% of the available production time may be taken up with cleaning and sterilising.
- energy, needed to heat cleaning solutions and run pumps.
- product loss, food contaminated by cleaning chemicals is unmarketable.
- effluent treatment, the handling of cleaning chemicals prior to discharge and the environmental consequences of the discharge.

Cleaning in the dairy industry is particularly expensive due to the rapid formation of fouled deposits on heated surfaces within the plant, for example heat exchangers and evaporators. Whereas the removal of fouling in some chemical plants is done a few times a year, the rapid fouling of milk processing plant means that they must be cleaned once

a day (Fryer and Belmar-Beiny, 1991). Such an expense must be justified, and it can be: failure to clean dairy processing equipment will lead to a failure of the process and possibly unsafe product. Even before the product safety is compromised, fouling will progressively reduce the performance of heat transfer equipment, causing increased processing costs.
It is necessary to clean for two reasons (Bird, 1997a):

- to control microorganisms, which can cause contamination
- to remove fouled deposit from heat exchange surfaces.

Fouled deposit results in:

- increased pressure drop causing flow problems (in the dairy industry, pressure drop generally limits the operation of process plant)
- reduced heat transfer efficiency.

The cost of fouling to process industries is very high. It has been estimated to cost the New Zealand dairy industry around $140 million per year (Steinhagen et al., 1990).

2.1.2 Definition of the problem

A soiled system is made up of three phases:

- a solid phase, the equipment of the food processing plant.
- an adherent soil phase, which may be liquid or solid.
- a liquid phase, the cleaning solution.

The system involves three interfaces between (1) wall and soil, (2) soil and cleaning solution, and eventually (3) between the cleaning solution and the wall. Cleaning is the results of a series of processes:

- the diffusion of cleaning solution to the surface,
- wetting of the surface, i.e. contact between the cleaning solution and the deposit
- penetration of the cleaning solution into the deposit
- reaction between the cleaning solution and the deposit
- removal of deposit

Difficulties with any one of these steps, such as poor mass transfer in low shear areas of a heat exchanger, low diffusivity of cleaning chemicals through compacted deposits, or slow reaction, can be rate controlling steps, and can result in slow cleaning (Bird, 1997). The rate of cleaning is therefore dependent on several factors, the most common variables of which are:

- the nature of the fouling: its structure, composition and thickness, which is dependent on the process
- the concentration and composition of detergents in the cleaning solution, especially the concentration of sodium hydroxide
- the temperature of the cleaning solution
- the velocity of the flow of the cleaning solution

The last three of these items are the parameters which can be varied in a CIP cycle. These variables mean that required cleaning times can vary greatly depending on parameter values.

The chemistry of the milk fouling process is now fairly well understood, and models have been developed (Paterson and Fryer, 1988, de Jong et al., 1992, Toyoda et al., 1994). The natural variations in milk composition give rise to variations in rate of fouling development (Burton, 1968). These variations make it uncertain whether a fouling model would be directly useful in predicting fouling under all practical cases (Jones et al., 1996). This is also true in the case of the cleaning of fouled surfaces. Several models have been proposed (Gallot-Lavallee et al., 1984a, Jeurnink and Brinkman, 1994, Bird, 1997b). However variations in fouling thickness and type as well as the effects of local geometry of equipment make it very difficult, if not impossible, to accurately predict the cleaning time required. There is, therefore, a need for an on-line device that can measure the development and removal of fouling deposits (Jones et al., 1996). This device would be useful for determining when cleaning should be begun and when it may be safely ended. If local on-line measurements of fouling can not be made at critical areas of the plant then the CIP process will remain inefficient, relying on 'overkill' to ensure plant performance and product safety. The use of an on-line fouling monitor has the potential to greatly reduce the cost of cleaning and reduce the effect of cleaning on the environment.

2.2 Introduction to fouling

2.2.1 Composition

Two types of milk deposit have been described (Burton, 1968). Type A deposit is formed at temperatures above about 75°C and below 110°C and is a soft, voluminous, curd-like material, white or cream in colour, which may overlay a harder base. At higher temperatures, especially above 110°C, a second type of deposit is formed (type B). This is brittle, gritty and grey in colour except where is has been overheated at the surface. This deposit has a higher ash content than type A (about 70%) and a lower protein content (15-20%) (Burton 1968).

Type A deposit is largely made up of protein (50-60%), but also contains mineral matter (30-35%) (Burton (1968), Tissier and Lalande (1986), Gallot-Lavallee et al. (1984)) reported a composition of approximately 60% protein, 30% fat, 10% minerals for fouling in the holding section of a pasteuriser. The variation in composition during this study was about 10% for protein, 15% for fat, and 20% for minerals. Burton (1968) reports a fat content of 4-8% although this has been found to vary greatly depending on such variables as the source and processing history of the milk. Other workers have reported fat contents of more than 45% in dry deposits (Fung, 1998).

Tissier and Lalande (1986) found that this deposit, when forming on a heated surface had two layers. Initially a rugged and dense deposit forms within the first minute of contact. The thickness of this layer increases with the duration of the heat treatment. Simultaneously the roughness of this deposit increases. This deposit is mainly composed of minerals.

The second layer that forms on the first is a spongy deposit only weakly bound to the mineral rich layer. This spongy layer consists mainly of protein in which fat globules are enclosed (Tissier & Lalande, 1986). The protein phase consists of at least seven different proteins: the four basic caseins and three whey proteins β-lactoglobulin, α-lactalbumin and immunoglobulins (Tissier et al., 1984). Casein is found in the deposit in the form of micelles (Jeurnink and Brinkman, 1994). β-lactoglobulin accounts for more than half of the protein found in a type A deposit. In the case of a type B deposit the largest protein component is β-casein at about 50% (Tissier et al, 1984). The spongy deposit is very heterogeneous. Minerals are present in the form of very small particles or large aggregates whose size can reach sizes of several tens of μm. Mineral deposit is mostly tricalcium phosphate. Microorganisms and large spheric fat globules are also present (Tissier & Lalande, 1986).

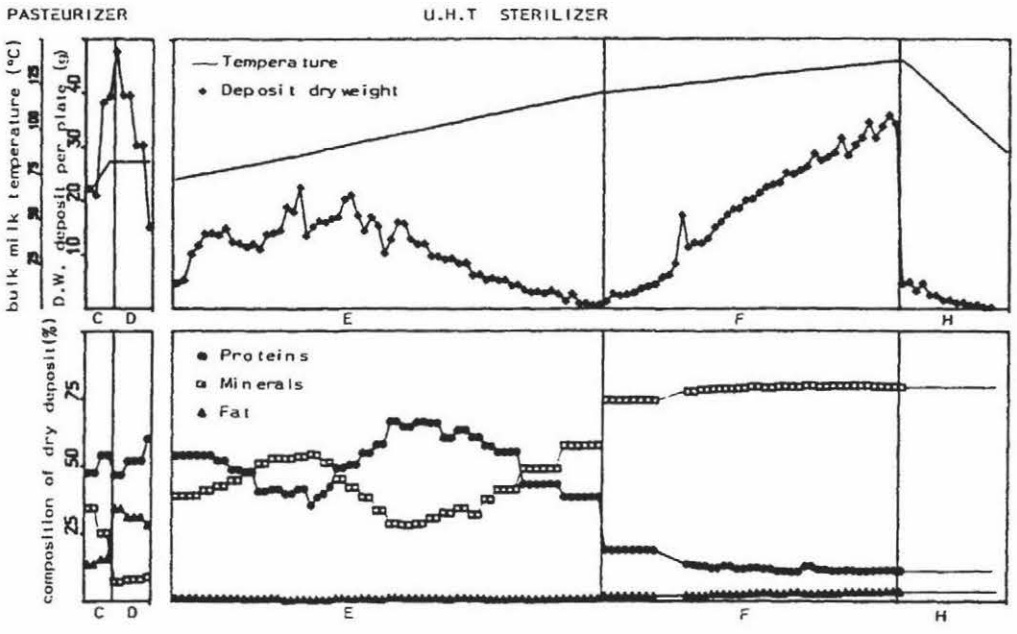

Figure 2.1: Evolution of soiling along the pasteurizer (C and D sections) and the UHT sterilizer (E, F and H sections) with presentation of bulk milk temperature, of the dry weight (DW) deposit and of main component composition of dry deposit recovered per plate. (After Tissier et al., 1984).

Proteins seem to be responsible for the cohesion of the deposit. Mineral content increases with the depth of the deposit and mineral content is greatest near the stainless steel surface (Fryer and Belmar-Beiny, 1991).

2.2.2 Distribution

Tissier et al. (1984) showed that fouling is not homogeneously distributed along a plate heat exchanger. Figure 2.1 shows the distribution of fouling across the various sections of the pasteuriser and steriliser.

For the pasteurizer, deposit dry weight increased first with bulk milk temperature along the heat section (C), then was higher at the beginning of the holding section (D), and finally steadily decreased.

For the sterilizer two kinds of deposit were formed on two heat exchanger zones. E section was covered mostly with type A deposit and had the greatest deposit weight at about 90°C. The second type of deposit was roughly located in section F and was like a type B deposit. In the sections where the milk temperature remained lower than 70°C no solid deposit could be seen after water rinsing.

Truong (1997) described the fouling that developed along the pipe of a fouling rig. Fouling was found to cover all the periphery of the pipe. The surface of deposit was a matrix of large porous particles, but became smaller in the area of the middle section. The thickness of the deposit varied along the length of pipe: 6 mm at inlet, 2 mm in centre and 5 mm at outlet. The total length of the pipe was 250 mm.

Davies et al. (1997) showed that the rate of mass of fouling deposit per area formation was dependent on the temperature of the bulk fluid as well as the surface temperature. When the bulk temperature is lower than 75°C the reaction rate is controlled by surface reactions, and can be seen to be relatively slow. Where bulk temperature is above 75°C the fouling rate is controlled by bulk reaction rates and is more rapid. (NB. more details of this study are given in section 2.6.3). Paterson and Fryer (1988) described a model that would explain a decrease in fouling rate for surface controlled reactions. As the bulk fluid would have a lower foulant concentration than the laminar surface layer of fluid, foulant would flow from the laminar region into the bulk fluid. This would reduce the amount of foulant available in the laminar sub-layer to make contact with the heated surface.

These studies show that the rate of deposit formation is dependent on geometry and bulk fluid and surface temperatures. The variation in fouling thickness throughout the plant means that the location of a fouling monitor will have to be carefully chosen so that it is placed at the point of slowest cleaning. To complicate matters further, the location of slowest cleaning may not be the place of maximum fouling thickness.

2.2.3 Mechanisms

Fryer and Bird (1994) state that there are four stages to fouling:

- denaturation and aggregation of proteins in the hot fluid
- mass transfer to the deposit surface
- surface incorporation of protein into the deposit; a further reaction
- possible transfer of proteins back to the bulk.

The denaturation of proteins can occur in the bulk fluid or at the liquid solid interface. If the temperature of bulk fluid is less than about 75°C then protein denaturation will not occur. However if the metal surface is heated, such as in a heat exchanger, then the boundary layer of fluid by the wall may be above 75°C, even when the bulk fluid is significantly cooler than this. In this situation the first stage suggested by Fryer and Bird

will change slightly; protein will only become denatured close to the wall and will have a relatively short distance to traverse to deposit on the surface. Davies et al. (1997) called this system surface reaction controlled. When the temperature of the bulk fluid is above 75°C the system is said to be bulk reaction controlled.

Under conditions of surface reaction control the deposit is relatively smooth and consists of small aggregates of denatured protein. Deposits formed under bulk reaction control conditions feature significantly larger aggregates in a less densely packed arrangement (Davies et al., 1997). The rate of fouling is greater under conditions of bulk reaction control.

Above 70-71°C the fouling rate increases as the protein denatures, and a complex series of reactions takes place. The protein first partially unfolds, exposing reactive sulphydryl groups, and then polymerises (aggregates), either with other β-Lactoglobulin molecules or with other proteins such as α-lactalbumin (Fryer and Belmar-Beiny, 1991). Fouling may have a lengthy induction period with no fall in heat exchanger performance followed by a rapid decline in performance (Fryer and Bird, 1994, Grandison, 1988a and Truong, 1997).

Davies et al. (1997) found that the total amount of protein present as deposit is a small fraction of the total mass of protein moving through the pipe. This result confirms that protein denaturation is not the rate limiting step in the fouling process. They suggest the mass transport and attachment mechanisms are also significant.

2.3 How clean is clean?

The determination of plant cleanliness

Grasshoff (1997) states there are three aims to a proper cleaning procedure:

- a physically clean surface, that is, the absence of an optically detectable or physically measurable deposit.
- a chemically clean surface, that is, the absence of analytically detectable foreign chemical materials.
- a biologically clean surface that is free of viable microorganisms.

The meeting of one of these criteria does not ensure the meeting of the others. For example an optically clean surface does not ensure that no viable microorganisms are living on it. Some methods for making a food contact surface sterile, also, do very little to

make the surface physically or chemically clean. An example of this is a heat treatment to kill microorganisms, which will actually exacerbate fouling. Processes aimed at removing physical soil may not successfully dislodge microorganisms which can become very firmly attached to a surface especially in the case of biofilm formation.

There are alternative definitions of cleaning. In some process industries, equipment may be considered sufficiently clean when its subsequent fouling behaviour is the same as a new surface (Bird, 1997a). In food industries the cleaning procedure must not leave any deposit which can damage the product, or promote the next fouling cycle.

Although a variety of possible definitions of cleanliness are available no one definition has been argued by researchers as more useful than others. From a safety and quality point of view it is clear that the very highest standards should be set. As Grasshoff (1997) summarises: a surface should be in a condition which excludes any possibility that the quality of a product to be processed will undergo undesirable changes, either immediately or at a later stage. This would require that the equipment is free from all microorganisms, as one microorganism is enough to contaminate the product and bacteria multiply exponentially if given suitable conditions. But the degree of chemical cleanliness required is unclear.

From the view point of product quality the purpose of cleaning is to remove material from the equipment that could become re-entrained in the product. The mineral sub-layer is optically difficult to detect but it is firmly attached to the surface of heat exchangers and may not recontaminate the product if left accidently in the heating surface. Leaving a mineral sublayer remaining after cleaning may provide a primary layer for the growth of the next fouling deposit, and with this head start, growth during the next run will be faster with a much shorter lag phase. Economically this is a case of giving with one hand and taking with the other, as the shorter cleaning times will lead to more frequent cleaning.

If there is a spongy protein layer remaining after cleaning it will have to be removed as it may absorb CIP solution which could become re-entrained in the product during the next run. As well as this, milk fouling, having being treated with caustic solution, is swollen and very susceptible to the shear forces of a fluid moving past it and could easily make its way back into the product.

Monitoring the cleanliness of one item of equipment may not ensure the cleanliness of the entire plant. Areas of food contact surfaces may have cleaning rates significantly lagging behind the plant average due to variations in local cleaning conditions. The cleaning process involves steps which may be governed by mass transfer, diffusion and reaction and

any of these could become a limiting process (Fryer and Bird, 1994). For example:

- mass transfer in low-shear areas, such as contacts between exchanger plates, could be slow, limiting both contact and removal.
- non-wetting deposit surface will resist cleaning.
- cleaning materials will diffuse only slowly through hard non-porous deposit, such as that formed by over-cooking.
- some forms of deposit, again perhaps formed by over-cooking, may be resistant to chemical attack.

It should be possible, however, to find a section of the process equipment that will be the last to become clean for a given cleaning process. Various components of foods are also more difficult to remove than others (Bird, 1997a). Table 2.1 presents examples of deposit components and their characteristics. The most difficult component of fouling to remove is the protein, according to Bird.

Table 2.1: Food deposit constituent characteristics (after Bird, 1997a)

Component on surface	Solubility	Ease of removal	Changes induced by heating
Sugar	water soluble	easy	caramelisation
Fat	water insoluble	difficult	polymerisation
Protein	water insoluble alkali soluble	very difficult	denaturation
Salts	water soluble acid soluble	easy to difficult	interaction

2.4 Cleaning-in-Place (CIP)

2.4.1 Introduction

Cleaning-in-place systems are those which allow food plants to be cleaned without the dismantling of equipment, which is time consuming and labour intensive. CIP systems in the dairy industry involve a set of pumps, tanks and heat exchangers which allow hot cleaning solutions to be pumped and sprayed through processing equipment. CIP systems use fully automated cleaning routines which facilitate the removal of complex food soils by using set cleaning and rinsing cycles (Bird 1997a).

The cleaning of process plant has been automated, but not optimised (Bird, 1997a). Most CIP systems are operated on a semi-empirical basis; cleaning schedules are fixed irrespective of the amount of fouling present, or the type of soil to be removed.

Sodium hydroxide forms the basis of many, but not all, cleaning compounds used in the food industry. Sodium hydroxide breaks down proteins, saponifies fats, has good disinfectancy properties, and is a relatively low cost product. Grasshoff (1997) identifies several characteristic CIP cleaning systems:

- single use cleaning, in which chemicals are only passed once through the system and then discarded to the drain or a waste treatment system.
- re-use systems in which the cleaning chemicals are stored and used several times.
- centralised cleaning, in which the whole process, independent of the object to be cleaned is controlled by a central cleaning station with a central supply of cleaning solutions via stationary pipelines.
- decentralised cleaning, in which smaller cleaning units are installed close to the objects to be cleaned, each with its own operational program.

2.4.2 Current practice and procedure

Fryer and Bird (1994) identify two types of CIP cleaning processes:

- two-stage cleaning: using both acid and alkali, commonly sodium hydroxide, followed, after rinsing, with nitric or phosphoric acid. The sodium hydroxide removes the protein whilst acid dissolves the mineral scale.
- single stage cleaning with formulated detergents, which contain compounds to enhance cleaning, such as surface active and chelating agents. These enable both protein and mineral to be removed.

A typical two-stage procedure involves five steps:

- first there is a water rinse to remove liquid milk from the equipment.
- then a heated alkali, usually sodium hydroxide, is circulated to remove the protein and fat from the deposit.
- another water rinse is made to remove all alkali.

- a hot acid is then circulated, usually nitric or phosphoric acid, to removed remaining mineral deposits.
- a final water rinse is made to remove acid before processing restarts.

It should be noted, however, that there are different views on whether the acid step should be undertaken before the alkali one. Perlat et al. (1986) found that using an acid-alkali process gave both a more effective clean in terms of amount of soil removed and a faster clean in a indirect UHT process using a plate heat exchanger.

Grasshoff (1997) gives a list of chemicals likely to be found in alkaline and acid cleaners. Alkaline cleaners may contain:

- strong alkalis, e.g. sodium hydroxide and or potassium hydroxide, for the degradation of organic soils including denatured proteins.
- weak alkalis, for example sodium silicate, to keep the removed soil dispersed.
- sequestering agents, e.g. polyphosphates, salts of nitrilotriacetic acid (EDTA), gluconates, phosphonates and polyacrylates for binding water hardness, for example salts of Ca and Mg, and to prevent the formation of scale and insoluble precipitates.
- surface active agents, generally of the non-ionic type, to lower the interfacial tension, emulsifying fatty components, and to control the foam properties, desirable for foam cleaners, undesirable for circulation cleaning.
- stabilisers such as phosphonates for solutions to be stored at elevated temperatures.
- oxidizers, such as hydrogen peroxide and sodium hypochlorite, to intensify the cleaning effect.
- corrosion inhibitors, for example sodium silicate and sodium gluconate.
- solubilizer to stabilise cleaning solution concentrates.

Components of acid cleaners are:

- strong acids, for example nitric acid and phosphoric acid (non-ferrous, free of chlorides and arsenic (danger of corrosion!)), to extract mineral components from a complex soil matrix.
- inhibitors, such as urea and hydrazine compounds, to bind nitrous fumes.

- dispersing agents to prevent precipitation during the neutralisation process at the end of the acid cleaning phase.
- anionic surfactants.

Enzymatic cleaners are not commonly used because of their high price, about three times higher than conventional cleaners. They require considerably more time for disintegrating encrusted soil structures than conventional strong alkalis or acids.

Grasshoff (1997) recommends a cleaning temperature in the range of 65-70°C for the cleaning of pasteurising equipment. Experience has shown that at 70°C the gasket elastomers are still resistant to the chemical which are generally used for cleaning purposes.

Single stage processes are made possible by the addition of chelating agents, such as EDTA, to NaOH solutions. In this way the chelating agents remove mineral deposits while the alkali removes fat and protein. Timperley et al. (1994) found that cleaning a plate heat exchanger with 2% w/w concentration of sodium hydroxide for 20 mins resulted in the plates being completely covered with white deposit. When the process was repeated with a single stage detergent the pressure drop across the heat exchanger fell to the clean level within minutes.

Although the chemicals needed for single-stage cleaning are more expensive, they offer the opportunity of reduced total cleaning costs by more economical use of chemicals, wash water, labour and down time.

The over-ride method for H.T.S.T pasteurisers

The over-ride method utilises a defoamed acid detergent and a highly caustic alkaline detergent. The over-riding is achieved by first circulating acid detergent for the recommended time and at a recommended temperature; then alkali is added slowly and directly in to the acid solution (Gilbert et al., 1979). Using the acid first ensures that mineral bonds within the fouling are broken, making the remaining protein and fat deposit easily removable. The acid detergent is a blend of cleaning acid and non-foaming (above 55°C) wetting agent. The alkaline detergent is a blend of sodium hydroxide, a caustic stable defoamer and sequesterants. The over-ride method method offers savings by reducing the amount of water used during cleaning.

2.4.3 Current CIP knowledge

Process Visualisation (Bird, 1997c)

A visual description of cleaning is given in Bird (1997c): The sequence of events during cleaning is shown in Figure 2.2. Times quoted are representative of those occurring for cleaning WPC deposit with a 0.5 wt% sodium hydroxide solution at 50°C and Re = 1750 (velocity = 0.075 m/s).

At time = 0, sodium hydroxide contacts the deposit, and a very small amount of weakly bound deposit is flushed from the matrix. The concentration or type of detergent used does not effect this initial flushing and it occurs even when pure water is used. Only 2% of the original mass of deposit is removed this way. During the next 2 minutes the deposit swells and becomes translucent. Material leaves the surface in aggregates rather than uniformly. Some small aggregates are removed during the swelling stage; their size ranges from about 0.2 mm at 40°C to greater than 0.1 mm at 70°C; the higher the temperature, the smaller the aggregates. For time greater than 2 minutes, the surface of the deposit continues to break up. In these later stages of cleaning, large sections of deposit can become partially detached from the surface, and aggregates can be shed from the ends of the 'fingers' that result. Maximum aggregate sizes removed during this period range from 0.5 mm at 70°C to 1.0 mm at 40°C. After 10 minutes, deposit removal is complete. A thin layer of mineral is left attached to the surface of the stainless plate.

The removal of large lumps explains why minerals are also removed during the NaOH cleaning (Jeurnink and Brinkman, 1994). Because some minerals are bound to the protein they become trapped in a relatively large piece of deposit that is dislodged by the flow.

Cleaning mechanisms

The first process necessary in the removal of milk deposit from a metal surface is the delivery of sodium hydroxide (and other possible ingredients) to the surface of the deposit. Although rinsing with water will remove a small amount of loosely bound deposit from its surface, no amount of pure water flowing past the fouling will remove a significant amount. Bird (1997c) found that the initial flow of water only removed 2% of the initial mass of fouling. In order for more deposit to be removed it is necessary to change it into a form that is made more vulnerable to the weak shear forces of the cleaning solution flow. While the mechanical action of a scrubbing brush has a high shear force of more than 100

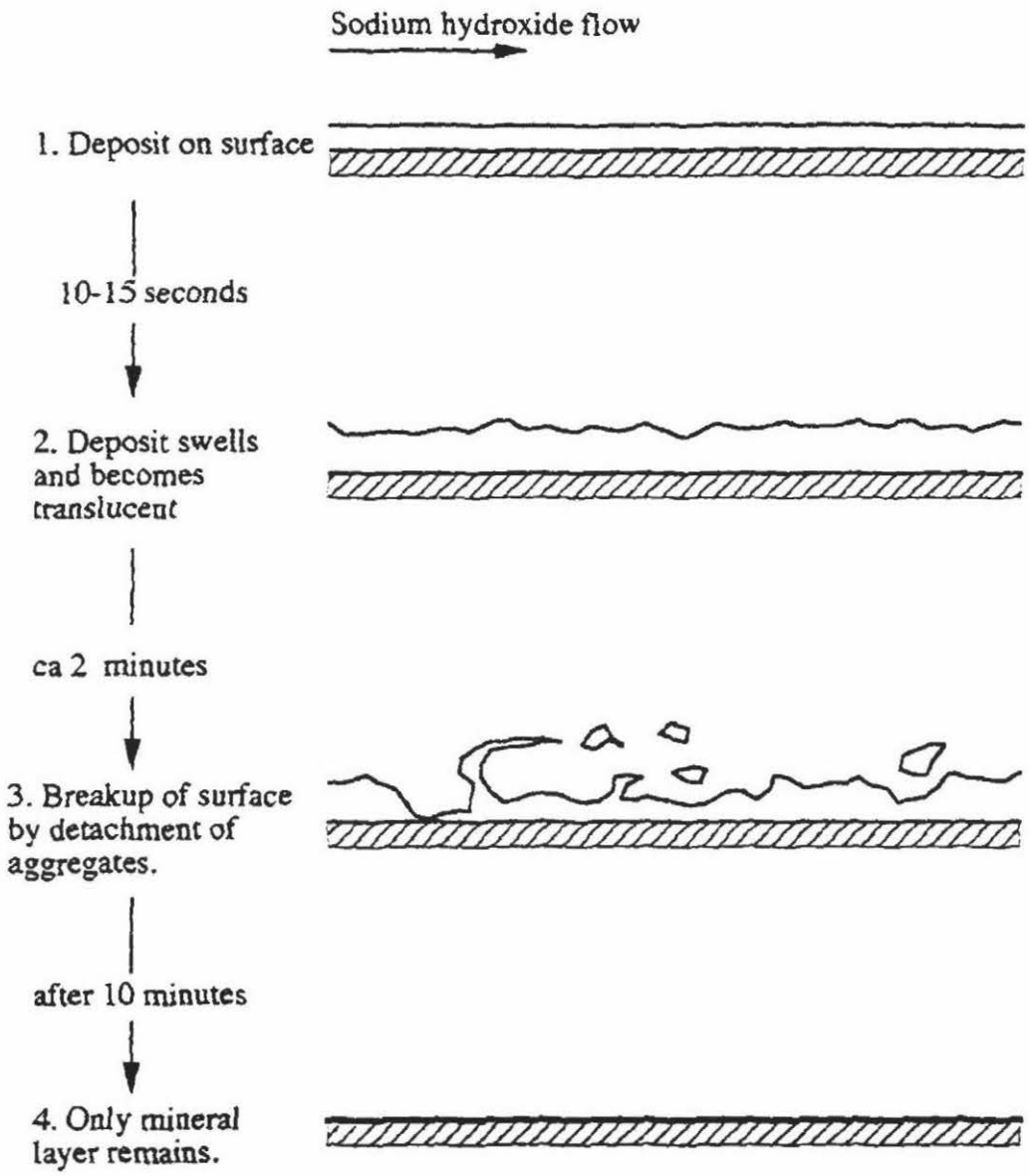

Figure 2.2: Observed removal pattern for whey and whole milk protein deposits cleaned from stainless steel surfaces. (after Bird, 1997c).

nm^{-2}, the shear force of a CIP flow has been estimated to be mostly between 1-10 nm^{-2} (Grasshoff 1997).

When an alkaline cleaning solution comes into contact with the deposit surface a swelling is observed and the deposit becomes translucent (Fryer and Bird, 1994). This swelling process has been photographed using Scanning Electron Microscopy (SEM). Figures 2.3 (a) and (b) show a whey protein concentrate (WPC) deposit. Figures 2.4 (a) and (b) show the deposit after being contacted with 0.1 wt% sodium hydroxide. It can be seen that after contact the distinction between platelets has disappeared. Holes have been formed and the surface is smoother. Figure 2.3(b) also shows that the structure has also become wrinkled. The void fraction of the surface is quite low and was estimated by Bird (1997c) to be about 0.25. Swelling of the deposit layer may be a result of breakage of a number of deposit-deposit attachments or of an increased repulsion in the deposit layer due to the high pH of the alkaline cleaning solution (Jeurnink and Brinkman 1994). Experiments in which there was no flow of cleaning fluid across the deposit illustrate this initial stage of cleaning well. Bird (1997b) did such experiments and found that the deposit initially swelled, and very slowly began to break up. However, in the absence of flow, material was extremely slow to diffuse away from the surface. A deposit of whey protein concentrate (WPC) swelled to 2.5 times its initial size. A whole milk deposit swelled to 1.45 times its initial size.

The use of a higher concentration than 0.5% produced changes that are deleterious to the cleanability of the deposit (Figure 2.4 (a), (b)). The honeycomb structure begins to collapse and become shrunken. The surface voidage falls from the optimum of 0.7 to a value of 0.6, in the case of the use of 1.0% caustic, or 0.5, in the case of 2.0% sodium hydroxide being used.

In order for all of the deposit to become swollen it is necessary that the cleaning solution diffuses through to contact all of the fouling. Jeurnink and Brinkman (1994) found that the diffusion of the alkaline cleaning solution into the deposit layer is slow; reasonable values for the thickness of the fouling layer and for the effective diffusion coefficient are 10 mm and 10^{-8} m^2/s, respectively. This means that it would take at least 1 hour before the cleaning solution reached the stainless steel wall by diffusion. The removal process, however, takes only a few minutes.

Observation has shown that the caustic solution does not penetrate the deposit all the way through to the metal surface before the fouling begins to break up (Fryer and Bird, 1994). Jeurnink and Brinkman (1994) suggested that the swelling caused cracks to form which, in turn, accelerated the further penetration of the cleaning solution. This is

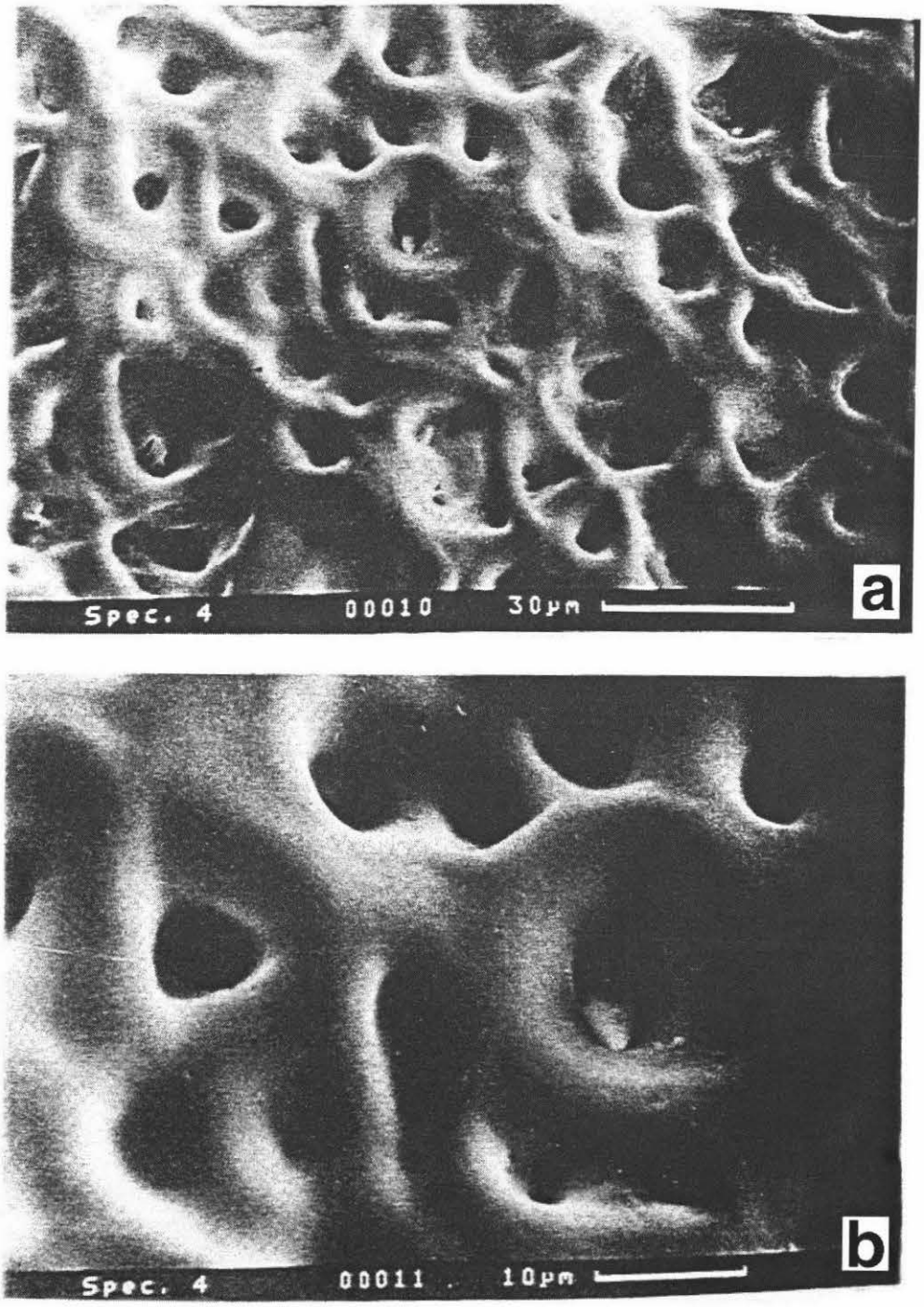

Figure 2.3: (a) and (b). SEM's of whey protein concentrate deposit contacted with 0.1 wt% sodium hydroxide at 50°C for 2 minutes. (after Bird 1997c)

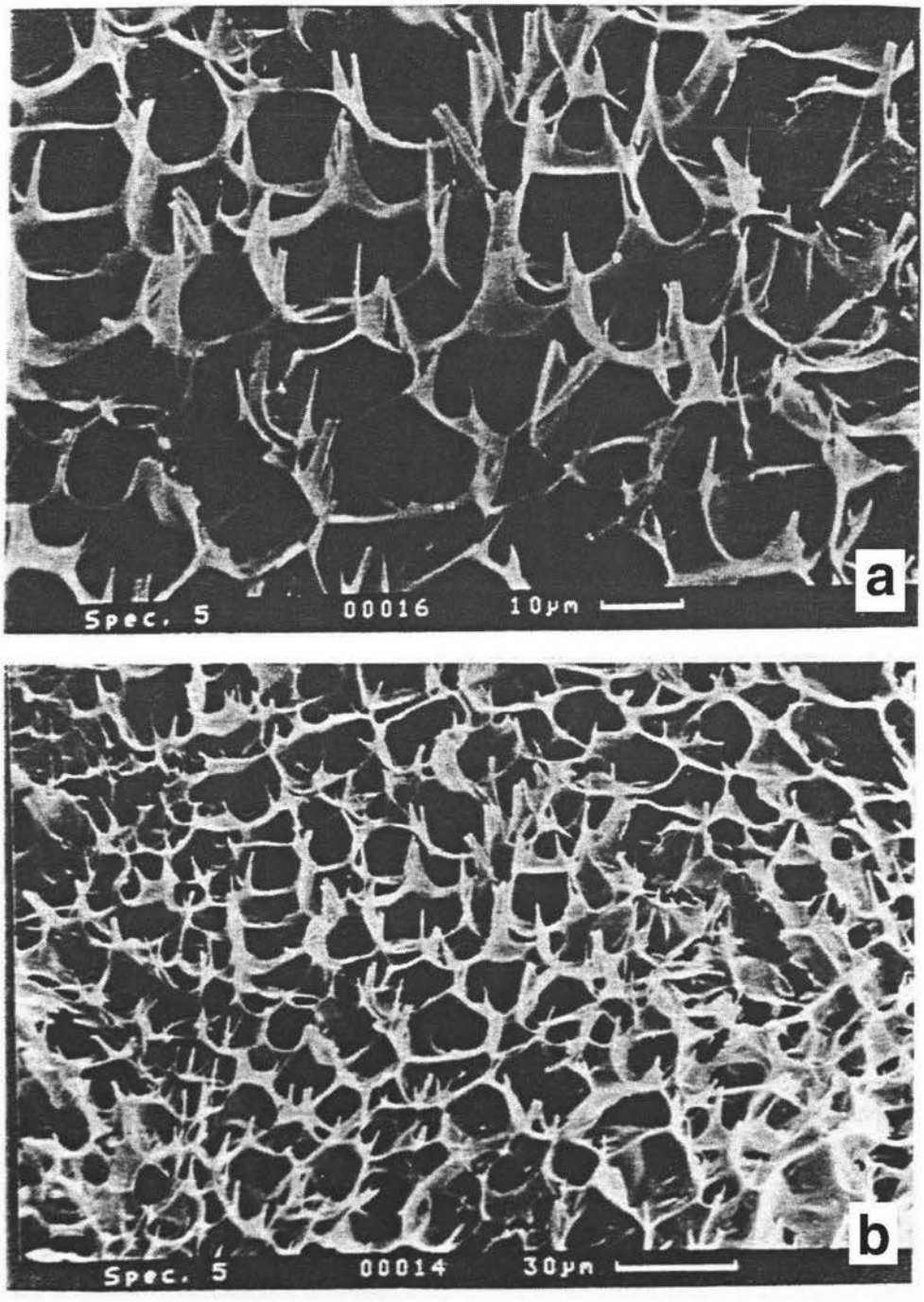

Figure 2.4: (a) and (b). SEM's of whey protein concentrate deposit contacted with 0.5 wt% sodium hydroxide at 50°C for 2 minutes. (after Bird 1997c)

shown in Figure 2.5.
Water serves as (Grasshoff 1997):

- a solvent for the chemicals required for the degradation of the soil
- a transport medium for the soil removed while keeping it suspended
- a transducer of thermal and chemical energy

The mechanical energy of the cleaning fluid required for (Grasshoff 1997):

- Removal of chemically modified soil particles from the solid surface, for example as swollen, electrostatically charged colloids, partially emulsified fat and peptidized protein structures.
- Splitting of larger soil aggregates into smaller units.
- Preventing sedimentation and the re-adherence of already detached soil particles.

Controlling Mechanisms The steps of cleaning are governed by mass transfer by convection and/or diffusion, and reaction and any of these processes could be a limiting one (Fryer and Bird, 1994). Fryer and Belmar-Beiny (1991) suggested four properties or processes that could limit the cleaning rate:

- Mass transfer in low-shear areas, such as points of contact between exchanger plates, will be slow. This will limit both contact and removal.
- Non-wetting surfaces will resist cleaning.
- Cleaning material will diffuse slowly through hard, non-porous deposits, such as those formed by over-cooking.
- Some forms of deposit (e.g. those produced by over-cooking) may be resistant to chemical attack.

The occurrence of the last two points on this list was observed by Jeurnink and Brinkman (1994). In experiments regarding the cleaning of an evaporator it was sometimes found that the evaporator remained fouled after cleaning. Visual inspection showed that the residual deposit had a browned, burned, colour and a rubber-like top layer. They suggested that some sort of chemical reaction had occurred in which the protein had gelled or polymerised in to rubber-like structure. This effect was noticed at a temperature of

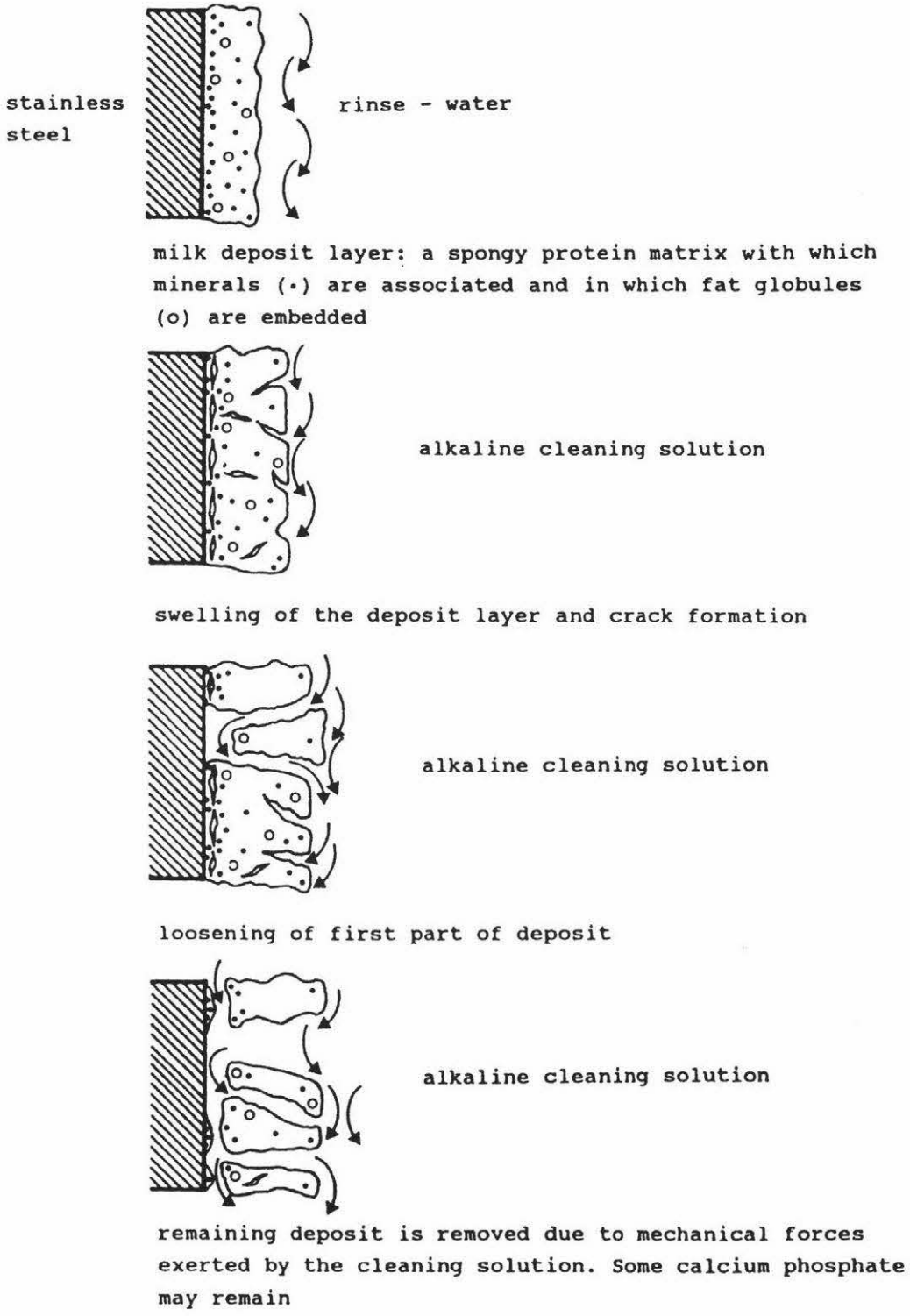

Figure 2.5: Schematic representation of the milk deposit removal during alkaline cleaning. (After Jeurnink and Brinkman, 1994).

70°C. It should be noted that fouling in pasteurisers with cleaning solutions above 80°C does not produce a gelled surface and this indicates that the temperature history of the deposit is an important parameter in the development of a gelled surface. Jeurnink and Brinkman (1994) suggested that if the deposit had already been sufficiently loosed form the wall before gelation of the surface took place there would be no fall in cleaning rate.

Grasshoff (1997) thought that thermodynamic processes at the solid liquid interface, not fluid dynamics, were the controlling process of cleaning.

Optimisation

The effect of temperature Most workers agree that the effect of temperature on cleaning rate can be described using the Arrhenius equation. Jennings (1959) found that a 10°C increase in temperature gave a 1.6 increase in cleaning rate. A similar value of 1.8 was found by Gallot-Lavallee et al. (1984a) . An increase in temperature results in an increase in cleaning rate without an optimum temperature being reached (Schlussler (1970), Jennings (1959), Gallot-Lavallee et al. (1984a), Bird, (1997c)). Gallot-Lavallee et al. (1984a) reported an increase in cleaning rate up a temperature of 90°C, at which point their experiments ended.

Increasing the cleaning solution temperature results in (1) a reduction in the cleaning time, and (2) a higher maximum removal rate at earlier times (Bird, 1997c). An increase in temperature aids deposit removal irrespective of deposit type, cleaning solution composition, concentration, or flowrate.

The effect of detergent concentration It is generally agreed that there is an optimum sodium hydroxide concentration for a cleaning detergent. Fryer and Bird (1994) reported an optimum concentration of 0.5%. Timperley and Smeulders (1988) reported an optimum concentration of 2.5%. However they were using a ready-made cleaning agent, so the alkalinity referred to as pure NaOH should be within the range of approximately 1.0%.

Bird (1997c) found that when the optimum concentration was used (0.5% wt NaOH) the cleaning time was approximately 10 minutes. However when 2.0% sodium hydroxide was used the cleaning time increased to 50 minutes, the same as that for 0.1% sodium hydroxide. When using 2.0% sodium hydroxide the deposit changed rapidly to form a very thick translucent layer which was removed only very slowly, and had a burned brown appearance.

The reason for this optimum can be explained by observing changes in the deposit

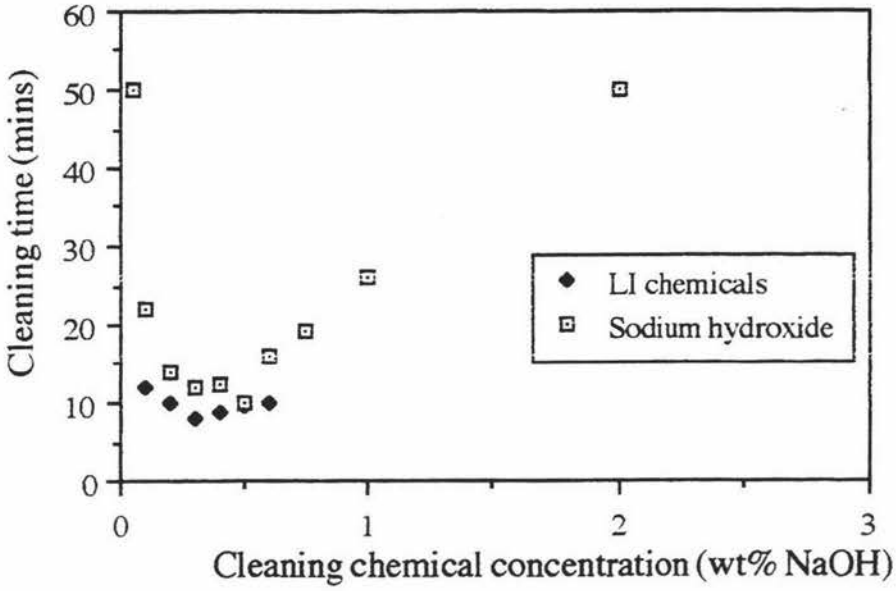

Figure 2.6: Performance comparison of sodium hydroxide and LI chemicals cleaning WPC deposit at 50°C and 0.175 m/s. (After Bird, 1997c).

structure on contact with caustic solutions. When contacted with a 0.1 wt% caustic solution the deposit becomes swollen and has a melted appearance. When the deposit is treated with cleaning solution of the optimum concentration of 0.5%, even greater changes are seen (shown in Figures 2.4). The deposit forms a larger and less dense honeycomb structure (Bird, 1997c). This was estimated by Fryer (1994) to have a voidage of about 0.7.

The effect of additives to the detergent Bird (1997c) also showed that the additives used in industrial detergents, such as sequesterants, significantly improve the performance of a cleaning solution A comparison of the effectiveness of sodium hydroxide vs. Lever Industrial (LI) detergents is shown in Figure 2.6. It can be seen that the industrial detergent performs better than sodium hydroxide when used alone.

The effect of additives has been studied by Grasshoff (a review is given in Grasshoff, 1997). The addition of cleaning agents such as EDTA or nitrilotriacetic acid (NTA) leads to both a significant increase in the cleaning rate and a considerable reduction of soil residues remaining on the test elements at the end of the cleaning process. The addition of a complexing agent allowed the alkalinity of the solution to be reduced without adversely affecting the cleaning rate. Oxidizers were combined with complexing agents which lead to an increasing the cleaning rate by a factor of 10, as compared to the removal by 0.25% NaOH only. Grasshoff (1997) also points out that the extra components of cleaning solutions have

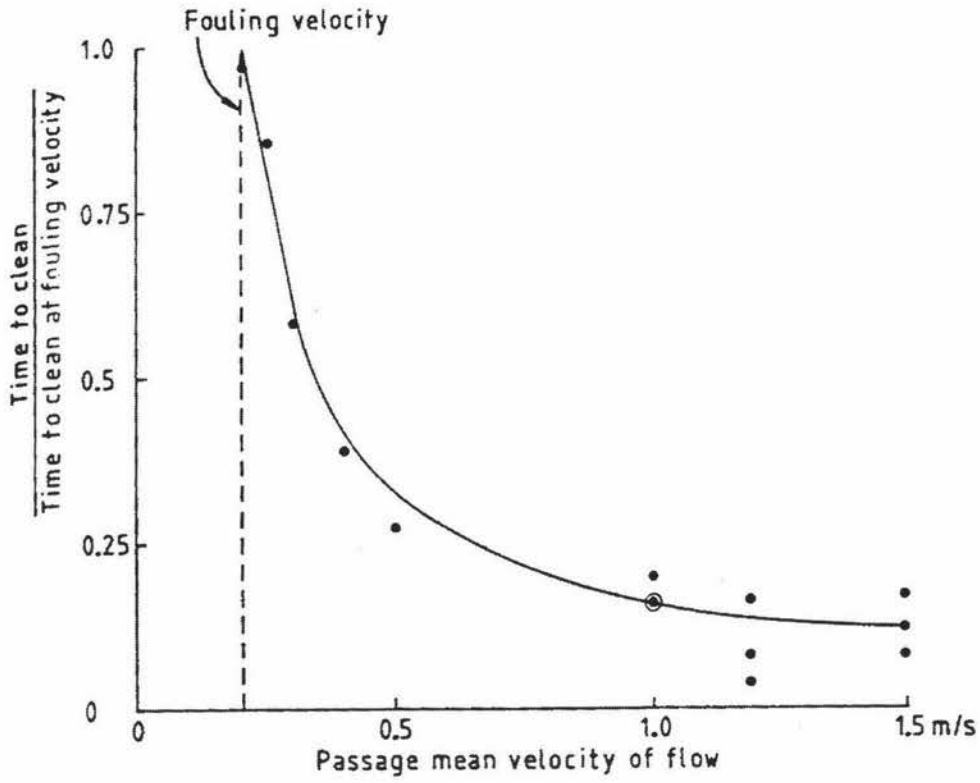

Figure 2.7: Effect of flowrate on cleaning time. (after Timperley and Smeulders, 1988).

a synergistic effect, where the improved performance of a more complex cleaning solution is more than just the sum of the effect of individual components. This suggests that the practice of 'sharpening up' a CIP solution by dosing it with sodium hydroxide may lead to unsatisfactory cleaning results.

The effect of fluid shear / flowrate An increase in cleaning solution velocity has been shown to give an increase the cleaning rate of WPC and whole milk deposits, irrespective of other process conditions (Bird, 1997c, Timperley and Smeulders, 1988). Figure 2.7 shows the effect of flowrate on cleaning time. Bird also showed that there was no minimum flow rate below which, no cleaning occurred.

The effect of CIP cycle design (alkali or acid first?) Despite the fact that the standard order for cleaning in the dairy industry is to pump alkali before acid, several workers have found that the reverse order leads to a shorter and more effective clean (Perlat et al., 1986, Grasshoff, 1993). Perlat et al. (1986) studied the cleaning of a preheater and a UHT pasteurizer using both sequences. Both heat exchangers were cleaned using 2% NaOH

and 2% nitric acid. The degree of cleaning was monitored by measuring the pressure drop across the plate heat exchangers.

Cleaning the preheater When alkali solution was used before acid, all protein and half the minerals were removed during the alkaline cleaning and half the minerals during the acid cleaning. When the sequence was reversed, with acid cleaning first, all the minerals were removed during cleaning and all protein during alkaline cleaning. Cleaning with acid before alkali gave a shorter cleaning time regardless of conditions.

Cleaning the UHT heat exchanger Whatever the cleaning procedure used all the minerals were removed during acid cleaning, not during alkali cleaning. Cleaning with acid before alkali gave satisfactory results: 10% of protein was removed by the acid and the remaining 90% was removed by the alkali. However when an alkaline wash was made before the acid wash unsatisfactory results were obtained. Eighty percent (80%) of the protein was removed by the alkali but only 5% by the following acid cleaning. When the plate heat exchanger was dismantled organic viscous materials were found near the contact points between the plates.

Grasshoff (1997) also obtained similar results showing that using acid before alkali gave a faster and more effective clean. Figure 2.8 shows these results.

Other factors affecting cleaning rate The cleaning process is complex and there is evidence that there are other factors that affect cleaning rate other than the most obvious ones of temperature, flow rate and detergent concentration. Jeurnink and Brinkman (1994) found that the total amount of deposit removed varied from day to day and this is a phenomenon observed by others (Timperley and Smeulders, 1987, Grandison, 1988b, Stemerdink & Brinkman, 1990) and is not yet explained. Fryer and Bird (1994) thought that a multistage cleaning model would be necessary because of the complexity of the process.

2.5 Monitoring CIP processes

2.5.1 Requirements of a CIP monitor

The requirements of a CIP monitor are closely related to those required for a fouling monitor. Fryer and Pritchard (1989) give four requirements for an on-line fouling monitor:

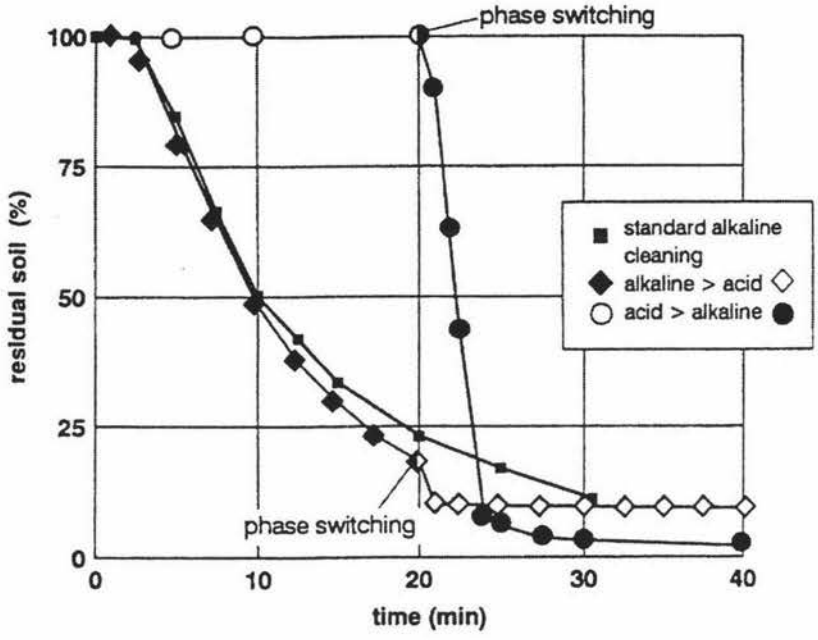

Figure 2.8: Influence of the acid/alkaline sequence on the removal in multiphase cleaning. (After Grasshoff, 1997).

- Size. The monitor should be of modest size so that it can be easily installed, services and replaced. Size is of particular importance to a sensor to be installed in a heat exchanger (especially a plate heat exchanger).

- Cost. It is likely to be some time before the value of using an on-line monitor to measure fouling becomes widely accepted, and therefore the capital cost should be as low as possible. Comparison with corrosion monitors suggests a target figure not much in excess of $NZ 6,000.

- Reliability. The monitor should be robustly constructed, require the minimum of maintenance, and provide reproducible data that is easy to interpret. The probe should also be durable under the various environmental conditions experienced in a milk powder plant. This includes high temperatures, steam and water.

- Relevance. It is important that, within these restrictions, heat transfer and fluid flow conditions in the monitor can be related to those in the plant. It would also be useful if samples of the deposits formed in the monitor could be easily removed for examination.

A useful CIP monitor will also require the following attributes:

- The probe must be in-line and give fouling measurements of the most significant food contact areas of the plant, for example heated surfaces such as evaporators and heat exchangers.
- The signal from the probe should be digital so that it can be recorded on a data logger and be interpreted by a CIP control computer.

2.5.2 Current methods of monitoring CIP

Experimental methods

Heated radial flow cells The heated radial flow cell (RFC) was developed for the study of the adhesion of microorganisms under a range of flow conditions. Duddridge et al. (1982) used the device to study the influence of surface shear stress on the adhesion and removal of bacteria in a flowing liquid. Fryer and Pritchard (1989) used the device to study the fouling from reconstituted skim milk. Figure 2.9 shows a cross-section of the RFC. Milk entering the device flows radially between a pair of parallel disks, both of which can be heated by oil. Because the flow is radial, the velocity decreases as it moved outward, giving a continuous range of decreasing shear stresses.

Thermocouples can be attached to the plate to give on-line measurement of the development of fouling. Several thermocouples spaced radially across the plate give an on-line fouling monitor for a range of shear stresses. Figure 2.10 shows an example of the data and results of a fouling experiment. The photograph also hows the problems inherent with using the RFC to study the heavy fouling produced by milk. The gap between the plates has to be very narrow if the desired range of surface shear stresses is to reproduced, usually less than 2mm (Fryer and Pritchard, 1989). The build up of fouling on the plates will often exceed 2 mm, causing a blockage. In fact, a small build up of fouling will greatly reduce the cross-sectional area of the flow, causing an increase in velocity which accelerated the fouling process. Because the plates can be removed from the device, it is possible to examine the deposit with relative ease after an experiment. Fryer and Pritchard (1989) therefore concluded that the RFC is only suitable for looking at the earliest stages of deposition.

The RFC unlikely to become a useful industrial fouling monitor due to the difficulty in correlating the state of fouling in the device with the state of fouling throughout the rest of the plant.

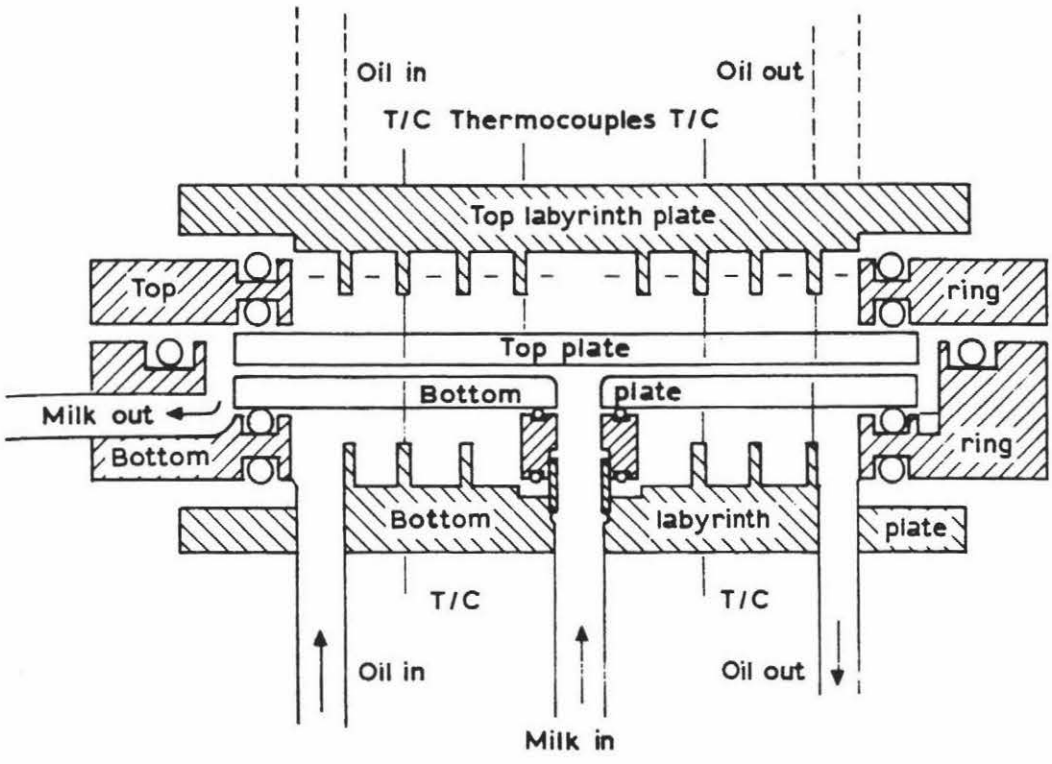

Figure 2.9: Cross-section of the AERE Harwell heated radial flow cell showing the heating oil recirculation system. (After Fryer and Pritchard, 1989).

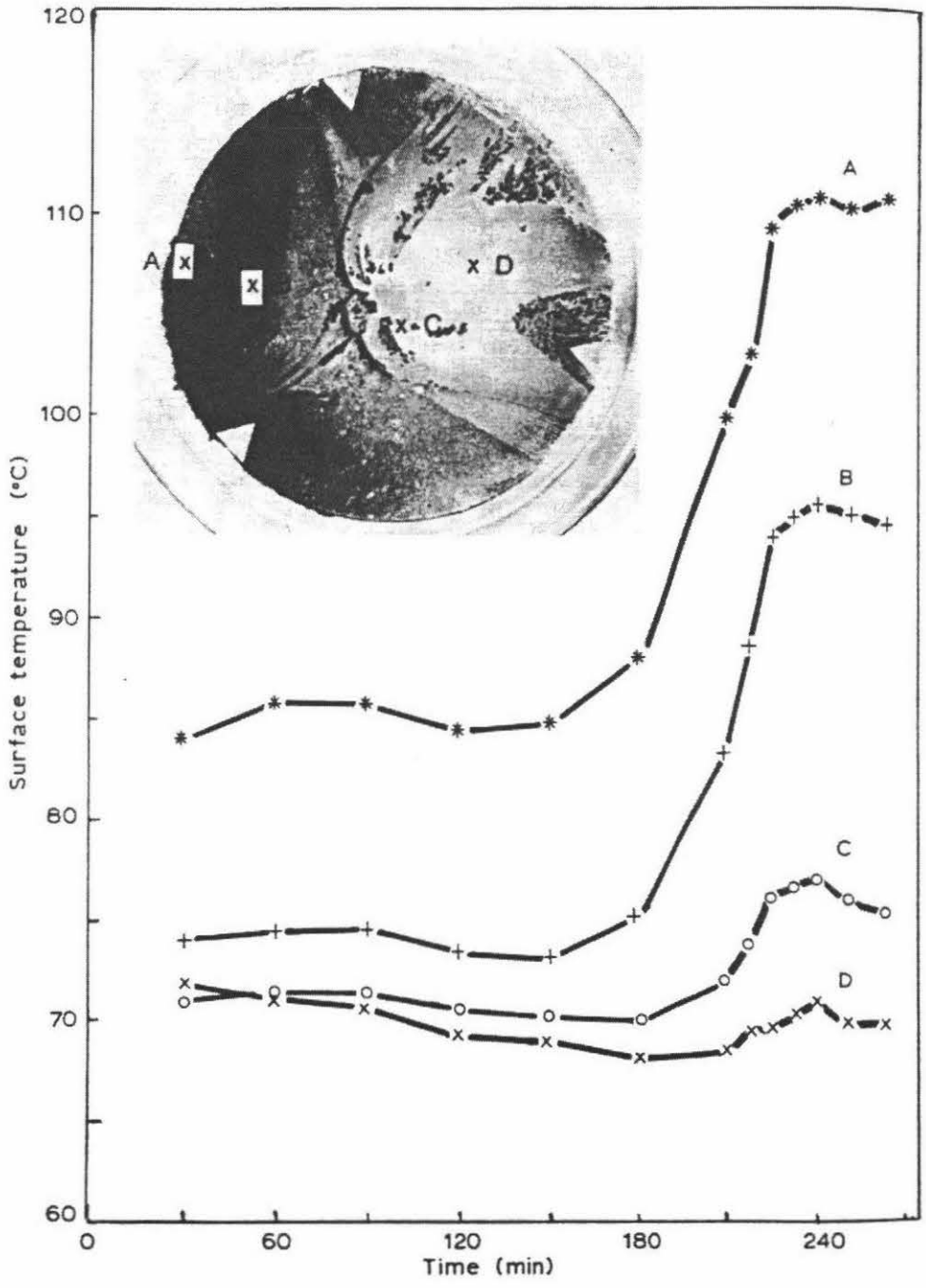

Figure 2.10: Surface temperature variation during the operation of the RFC. The inset shows the fouled plate and positions A, B, C and D (48.5, 28.5, 13.5 and 38.5 mm from the centre, respectively). (After Fryer and Pritchard, 1989)

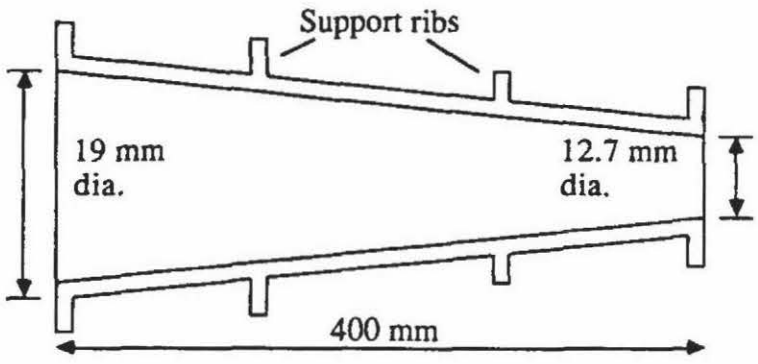

Figure 2.11: Schematic diagram of the tapered tube. (After Fryer and Pritchard, 1989).

Tapered tubes A diagram of a tapered tube is shown in Figure 2.11. Because the diameter of the monitor is much larger than that of the RFC is does not suffer the same blockage problems. A range of shear stresses is again produced due to the variation in diameter along the length of the device. Thermocouples can be attached to the wall of the monitor to give on-line measurements of fouling. But a disadvantage of the system is that the device cannot be broken apart in order to study the fouling layer developed in detail.

In terms of industrial use, the tapered tube is unlikely to become a commercial fouling monitor due to the same problems that are inherent in the Radial Flow Cell: The state of fouling in the device would be hard to correlate with the state of fouling throughout the rest of the plant.

Ultrasonic sensors

Pulse-echo technique The pulse-echo technique uses a single transducer attached to the side of a pipe to project ultrasound into the pipe. The same transducer is then used to detect any echoed signals (Withers, 1996). A reflection or echo will result from the sound wave striking a boundary or interface between different materials or phases. The aim of using the pulse-echo technique for measuring fouling is to detect the reflections from the metal/deposit and deposit/fluid interfaces. The time interval between the detection of these two echos can be used to determine the thickness of the fouling deposit. However this approach requires that the velocity of sound in the deposit and cleaning solution to be known (Withers, 1996). Furthermore, the surface of the deposit will be uneven, resulting in a very weak echo that will be difficult to detect. This situation will be made worse by

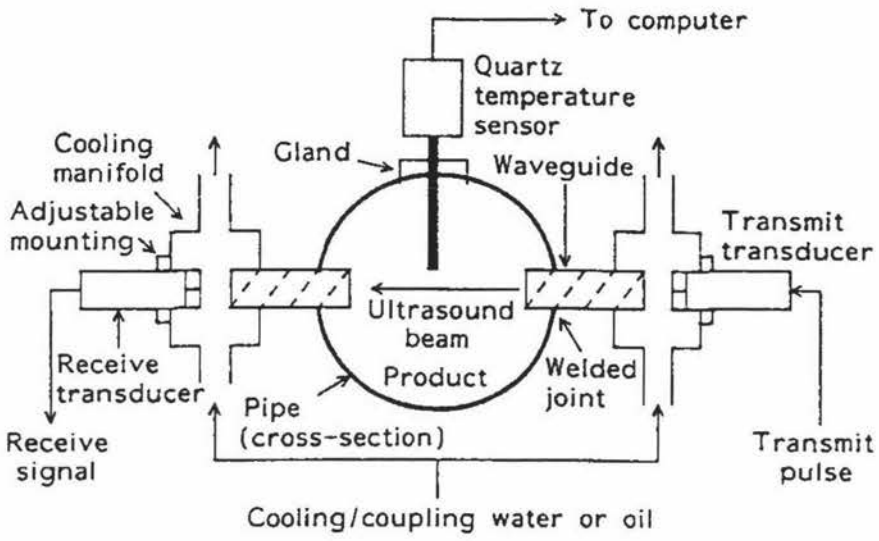

Figure 2.12: An ultrasonic transmission system for detecting a fouling deposit. (After Withers, 1996).

the mismatch between the acoustic properties of the pipe wall and the fouling layer, which will result in a large reflection form the pipe-product boundary, tending to drown out the fouling reflection signal. For these reasons the pulse-echo technique is not very suitable for the measurement of the thickness of a fouling layer.

Transmission technique The transmission technique requires two transducers: one attached to one side of the pipe emitting ultrasound into the pipe, and the other directly opposite the first transducer, detecting the arriving sound waves (Withers, 1996). The time required for a sound wave to traverse the distance between one transducer and the other is dependent on the thickness and speed of sound on each substance that the wave travels through. Figure 2.12 shows a diagram of this device.

The amplitude of the wave before and after it traverses the pipe can also be used to provide information about the thickness of the fouling layer. However for this method to work, it is necessary for the properties of the pipe walls, product and transducers to constant with time, and this is not likely to be the case (Withers 1996). Although it may be possible, with careful mechanical design, to minimize the influence of the transducers and the pipe walls on the signal, compensation for variations in the product would be more difficult to achieve (Withers, 1996). Figure 2.13 shows a typical graph of the change in

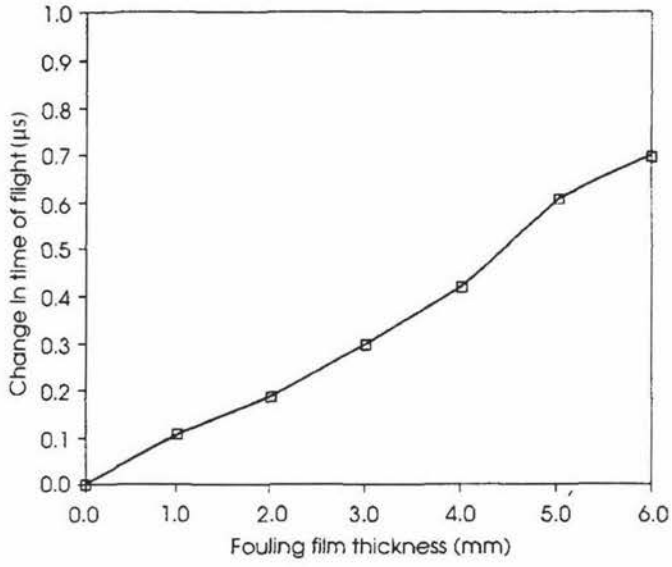

Figure 2.13: Change in time of flight of the ultrasonic signal against fouling film thickness for a artificial fouling film (layers of adhesive film) in a water filled pipe. (after Withers, 1996).

time required for a wave to traverse the pipe against the thickness of the fouling layer. The results were obtained with an artificial layer created with an adhesive film. Water was used as the process fluid in place of milk. These changes made the system significantly simpler than a milk fouling process. A milk deposit will not be smooth like adhesive tape, and this will result in the scattering of echos from the deposit / liquid interface, weakening the signal. Water is also a pure substance containing no particulates or component phase, whereas milk is a fluid containing fat globules, making the movement of sound through that much more complicated. The presence of bubbles in the stream or a high flow velocity would also create more reflections, further complicating interpretation of data (Withers 1996). The speed of sound through the food would also be dependent on temperature but the relationship between temperature and sound properties of milk have been published (in Kaye, G.W.C. and Laby, T.H. (1986), Tables of Physical and Chemical Constants (16th edn), Longman, Harlow, UK.)

The applicability of ultrasonic sensors to industry Both types of ultrasonic sensors face a particular difficulty if they are to be applied to an industrial dairy setting. To date ultrasonic sensors have only been used to study fouling on a straight section of pipe. In industry the point of critical measurement, (that is, where fouling is likely to greatest and the most difficult to completely remove), is unlikely to be a straight piece of pipe. It is

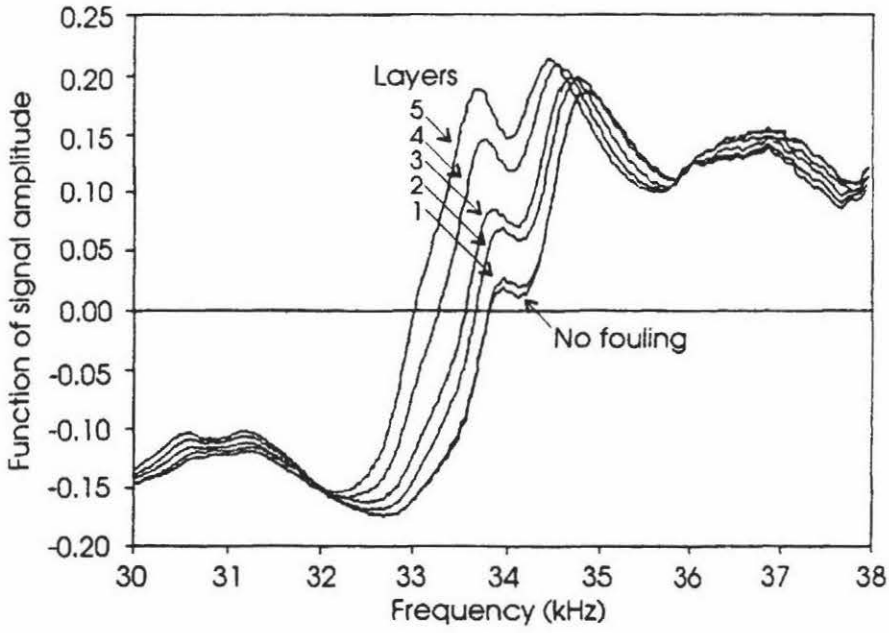

Figure 2.14: Frequency response of the vibration sensor plotted against a function of signal amplitude for cleaned and fouled states. (after Withers, 1996).

more likely to be within a plate heat exchanger or in an evaporator, which does not have simple geometry. Geometry is crucial to the successful use of an ultrasonic sensor as it affects the shape and speed of an echos wave front. The more complex the geometry of the system, the more complex the signals coming from and already noisy system. For this reason it would be difficult to design a relatively cheap fouling sensor for the dairy industry in the near future.

Acoustic vibration sensors

The transducer, a piezo-electric crystal-based device, is made to vibrate over a range of frequencies that encompass its own natural frequency (Withers, 1996). The build up of fouling on the device has two effects. First it reduces the amplitude of the vibrations experienced by the probe. Secondly it shifts the natural frequency of the probe, to a degree dependant on the thickness of the fouling layer. Figure 2.14 shows an example of experimental results for the shift in natural frequency as the fouling layer thickness is increased.

Because the device is very small, it can be installed between the plates of a plate heat exchanger. This is very important, as fouling is most serious on heated surfaces such

as those in a heat exchanger. It is important that the design of the sensor be optimised to ensure that is fouls in the same way as the remainder of the plate pack and that it can be cleaned during the cleaning-in-place operation (Withers 1996).

Testing of the prototype sensor demonstrated that it was able to detect relatively small masses of fouling, equivalent to a film thickness of 0.1mm, and could measure film thicknesses up to a maximum of 0.4mm (Withers, 1996). As milk deposits will easily grow to a thickness of 2 mm, the acoustic vibration sensor would only be useful for measuring the initial stages of fouling development. The sensor is able to operate under realistic temperatures and pressure; 1-2 x 10^5 Pa, 5-140°C.

The applicability of acoustic vibration sensors to industry The small size of this sensor gives it a significant advantage over other sensors, with the exception of the heat flux probe which is equally small and thin. The ability to install the probe in a cramped space such as those found in plate heat exchanger are likely to be a key factor in determining what is a viable fouling monitor or the dairy industry.

The difficulty in developing this probe for use in the dairy industry would be the interpretation of noisy signals. Although the signals may be useful in a laboratory setting, interpreting signals from a noisy milk powder plant would greatly increase the difficulty of using this probe.

Optical sensors

The principle of operation relies on the fact that the light-reflectance characteristics of the boundary between the transparent sight glass and the product will change in the presence of a fouling film (Withers, 1996). The system requires that a sight glass be installed in a section of the pipe as, obviously, an optical system will not work through a stainless steel pipe. This raises the issue of whether fouling occurs at an identical rate on glass as it does on stainless steel. For an optical sensor to be used, this data would have to be measured.

Initial trials showed that the amount of reflected light changed with increasing fouling in terms of mass per unit area for very thin films. Sensor output was also found to be dependent on processing conditions, including flowrate and temperature. The lower limit of sensitivity in terms of film thickness was in the order of 0.10 mm. Figure 2.15 shows an example of the typical output from the sensor for various fouling thicknesses.

Optical sensors can also be used to measure the turbidity of the solution passing

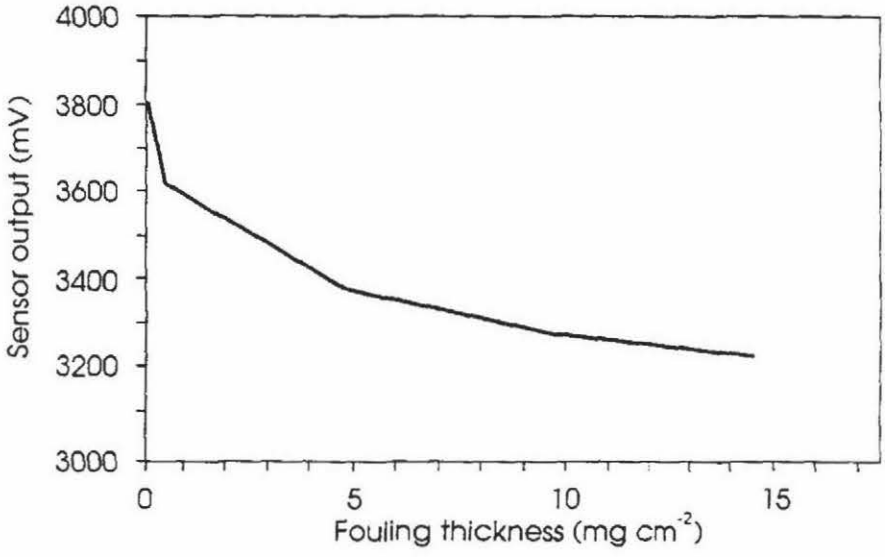

Figure 2.15: Output from the optical sensor (in millivolts) against fouling film thickness (expressed in terms of mass per unit area). The product used was skim milk. (Withers, 1996).

through a pipe if two transducers are used. As with the ultrasound transmission technique the two transducers are set up directly opposite one another across the pipe. A glass wall is also required to allow the light to move through the pipe. Gallot- Lavallee et al. (1982 & 1984a) used such a device to study the cleaning kinetics of milk deposits. They related the turbidity of the flow leaving the fouled equipment to the flux of milk deposit moving through the pipe in solution. Integrating this flux gave the total amount of deposit removed from the fouled tube. The sensor was found to measure concentration to an accuracy of 4%.

The applicability of optical sensors to industry Optical sensors, like ultrasonic sensors, are impossible to mount on a structure such as a plate heat exchanger. This would mean that an optical sensor would not be mountable on the most critical pieces of processing equipment (from the fouling point of view). Laboratory studies so far have only attempted to mount the optical sensor on a straight pipe, which as has been previously mentioned, is unlikely to be critical area of the plant in terms of fouling and cleaning.

Optical sensors also require transparent materials and stainless steel is not such a material. The use of an optical sensor therefore require glass inserts on equipment. Glass also has different fouling properties than stainless steel so there is a problem of correlating

data collected.

The optical sensor is unlikely to be a viable dairy industry fouling monitor in the foreseeable future.

Heat flux sensors (refer to Chapter 2.6 "Heat flux sensors")

2.5.3 Industrial methods

Commercial CIP systems currently in use do not directly measure the cleanliness of the surfaces being cleaned. Instead indirect measurements are made of a broad section of the plant, for example measuring the pressure drop across a heat exchanger in order to infer the progress made during cleaning. Comparisons of the pressure drop with the values obtained from clean equipment give an indication whether the flow paths are free of soil. But thin films of soil in local areas may not be detectable by such broad measurements (Grasshoff, 1997).

Despite the lack of a direct control of the cleaning performance, the effectiveness of the cleaning process can be ensured if external process parameters are monitored (Grasshoff, 1997). However, because no direct measurement of deposit remaining can be made, excess cleaning time is almost always used to provide a safety margin (Gallot-Lavallee et al., 1982).

A commonly used measurement for the assessment of cleaning effectiveness is the conductivity of the returning cleaning solution. This provides an indirect measurement of the concentration of the solution. Caution is necessary because it is known that the total salt load in the measuring fluid is indicated by the conductivity only in so far as it influences the ionic product. The character of the cleaning solution, whether acid or alkaline, also cannot be distinguished by measuring conductivity (Grasshoff, 1997).

Grasshoff (1997) recommends the use of a pH probe. At neutral pH small amounts of alkali or acids, which are not detectable sensorically, cause a considerable shift in pH. This shift can be measured with great reliability by a pH probe before health risks are incurred through the carry over of cleaning solution residues into the product. However Grasshoff also points out the reason pH probes have not been popular to date: unlike maintenance free conductivity sensors, pH probes must be checked and calibrated at regular intervals.

2.6 Heat flux sensors

2.6.1 Thermocouples

Thermocouples use a principle known as the Seebeck effect. If two pieces of wire, each being made of different metals, are joined together at the ends and one end is heated then a very small current flows in the circuit (Carstens, 1983). This is shown in Figure 2.16. The figure shows that when heat is applied to junction 1 (J1) a small net EMF can be measured by the millivoltmeter.

The Seebeck effects results from the difference of the density of free electrons in various metals. The density of free electrons can be further varied by altering the temperature of the metal. The difference of free electron densities across a junction causes an EMF across the junction. If the junction at the other end is at the same temperature an equal and opposite EMF will act on the circuit and there will be no net current flow. But if, for example, J_1 is at a different temperature from J_2 as shown in the figure there will be a net EMF across the circuit and a current will flow. If the temperature at J_2 (T_2) is a constant reference temperature then the temperature of J_1 can be determined using the net EMF across the circuit (Carstens, 1993).

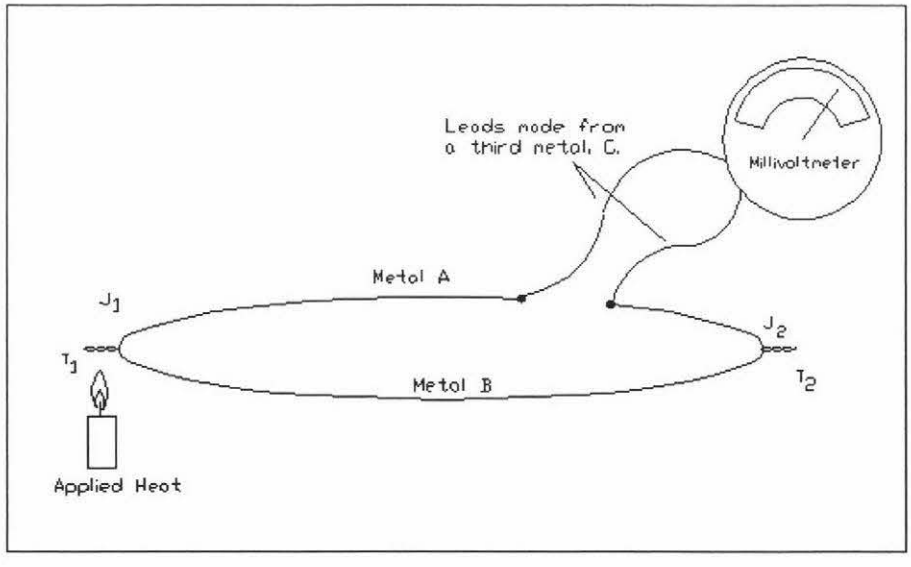

Figure 2.16: The Seebeck effect. (after Carstens 1993)

2.6.2 Thick film heat flux sensors

A heat flux meter is a thermal sensor that measures a heat flow in terms of temperature differences. The heat flux passing through a solid layer induces a temperature difference, due to the thermal resistance of the material. The resulting temperature difference can be measured and related to the heat flux. The thermal resistance of the sensor may affect locally the original heat flow to be measured. Therefore a low thermal resistance for the sensor configuration is recommended (Smetana, 1994). A heat flux through a thin layer causes a temperature difference ΔT according to equation 2.1.

$$q = \frac{\lambda_p}{L_p}\Delta T \tag{2.1}$$

Where: q = heat flux (W/m^2)

λ_p = thermal conductivity of the layer in the probe (W/mK)

L_p = thickness of the layer (m)

ΔT = temperature difference across the layer (K)

Because the layer is thin (to prevent the probe becoming an insulator) the temperature difference across it is small. Therefore the temperature difference can only be accurately measured by a number of thermocouples connected in series (Smetana, 1994). Figure 2.17 shows a schematic diagram of a micro-foil heat flux sensor.

For a pipe containing milk the heat flow through the wall of the pipe can be described as follows. The heat transfer through the pipe is:

$$q = U.\Delta T \tag{2.2}$$

Where: q = heat transfer rate per area (W/m^2)

U = overall heat transfer coefficient (W/m^{2}K)

ΔT = temperature difference across pipe wall (K)

The total resistance to heat transfer, R_t, between the milk inside the pipe and the ambient atmosphere is expressed as the inverse of the overall heat transfer coefficient $R_t = 1/U$. It is made up of several components (Truong et al. 1998):

$$R_t = R_o + R_{ss} + R_f + R_m \tag{2.3}$$

Where: R_o = heat transfer resistance of ambient air (m^{2}K/W)

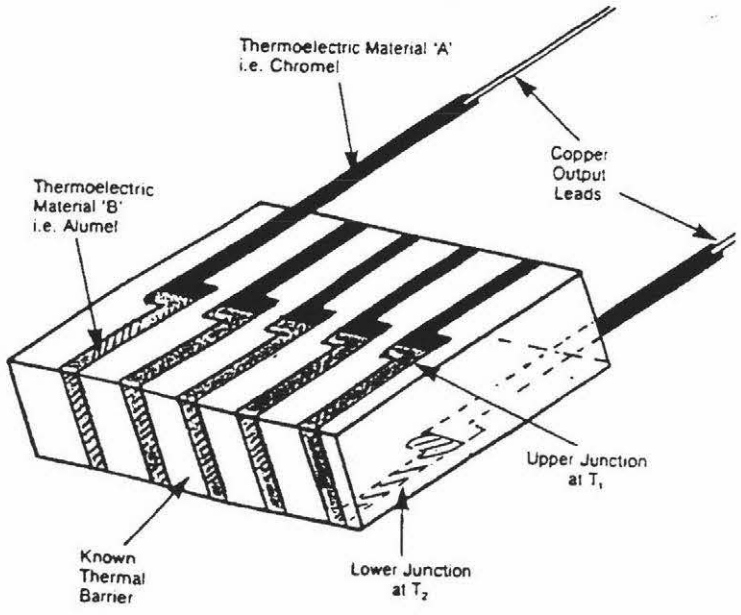

Figure 2.17: Diagram of a heat flux sensor. (after Rhopoint Ltd.)

R_{ss} = heat transfer resistance of stainless steel wall (m^2K/W)
R_f = heat transfer resistance of fouling layer (m^2K/W)
R_m = heat transfer resistance of milk inside pipe (m^2K/W)

Before the production run when the pipes are clean $R_f = 0$ and therefore the resistance at time zero is:

$$R_{t,t=0} = \frac{1}{U_0} = R_0 + R_{ss} + R_m \tag{2.4}$$

Where: U_0 = initial heat transfer coefficient

2.6.3 Previous studies using heat flux probes

Jones, Ward, Schreier and Fryer (1996)

Three studies of the use a heat flux sensor to measure fouling have been made, beginning with Jones et al. (1996). Figure 2.18 shows the sensor apparatus they used.

The experiments used a protein solution made from whey protein concentrate (WPC) powder. The temperature difference was measured by (1) keeping the heated block

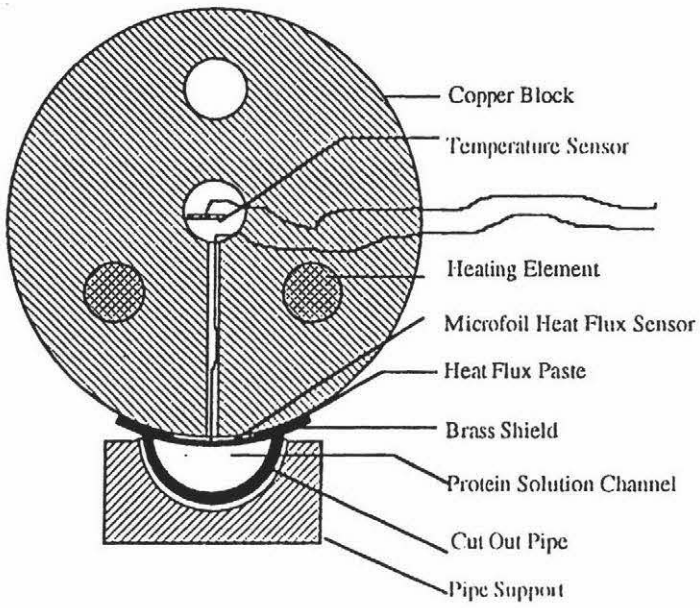

Figure 2.18: Cross section through the heated block and cut-out pipe arrangement. (after Jones et al., 1996).

at a constant temperature using electric cartridge heaters and a temperature controller, and (2) measuring the liquid temperature.

Since both heat and mass transfer coefficients are a function of the mean fluid velocity and the nature of the flow (i.e. turbulent, laminar or transition), there will be some small variations in the conditions of the system. The effects of these variations were minimised by taking time averaged recordings of heat flux. This allowed longer term effects to show through.

The aim of this study was to demonstrate the suitability of the sensor for commercial use in turbulent flows. According to Jones et al. results from the sensor match those of established theory and observation of milk protein fouling.

Truong, Anema, Kirkpatrick and Trinh (1998)

Truong et al. (1998) made a further study using a heat flux probe to measure fouling. Measurements were made at or near the direct steam injection unit in two commercial milk powder plants. Up to six sensors were used for each trial. The sensors were attached to the outside of the unheated pipes.

Heat flux sensors in this study were not covered in a large thermal mass such as the copper block used in the previous study (Jones et al., 1996). This lead to a great deal

of noise in signals from the sensor due to changes in the ambient environment affecting heat flow through the piping. The experimental plant was located in a room at the bottom of the evaporator system, with two access doors. The traffic through these doors can set up draft currents which alter the external heat transfer resistance. When access to this room was restricted the overall heat transfer coefficient became much more stable. However, restriction of access to work areas is not practical as it is disruptive to plant operations.

A solution to this problem was to monitor the temperature of the external pipe wall. This allows the calculation of the internal overall heat transfer coefficient and the internal resistance.

Results from this study showed that the geometry of the plant has a significant impact on fouling rates. When a sensor was placed 26 pipe diameters from the DSI exit fouling was found to be negligible. But when the horizontal test piece was replaced, in the same location, with a sudden 12/25 mm expansion, the change in geometry was sufficient to induce fouling which was measured to be almost 2 mm thick at the end of the run.

Davies, Henstridge, Gillham and Wilson (1997)

This study used a movable heat flux sensor to study the thermal conductivity of milk fouling along a straight section of oil heated pipe. The pipe was fouled before the measurements with the heat flux sensors were taken. After a fouling layer had developed, water at 18°C was flushed at a constant flowrate through the pipe. The heat flux sensor was mounted in a brass block that was held at a constant temperature of 50°C. Measurement of the heat flux from the brass block to the cool water through the heat flux sensor was used to calculate the thermal conductivity of the fouling layer. The mass of deposit on each section of the pipe was determined by cutting up the tube and measuring mass gravimetrically.

Figure 2.19 shows the device used by Davies et al. (1997) . Retaining screws clamped the block around the fouled tube and held the sensor flush against the tube surface. High thermal conductivity paste was used to ensure minimal thermal resistance between the pipe and the sensor. The block was maintained at a near constant temperature using water circulated through the block at 50±1°C and the actual temperature measured using a thermocouple.

The results of all the thermal resistance measurements on fouled tubes are presented as fouling resistances in Figure 2.20. It can be seen that there is significant scatter where the thickness of the fouling is high. The regressed gradient of Figure 2.20 gives a value of $\rho_f \lambda_f$ for the deposit of 470 Wkg m^4 K^{-1}, which is less than that of water (602

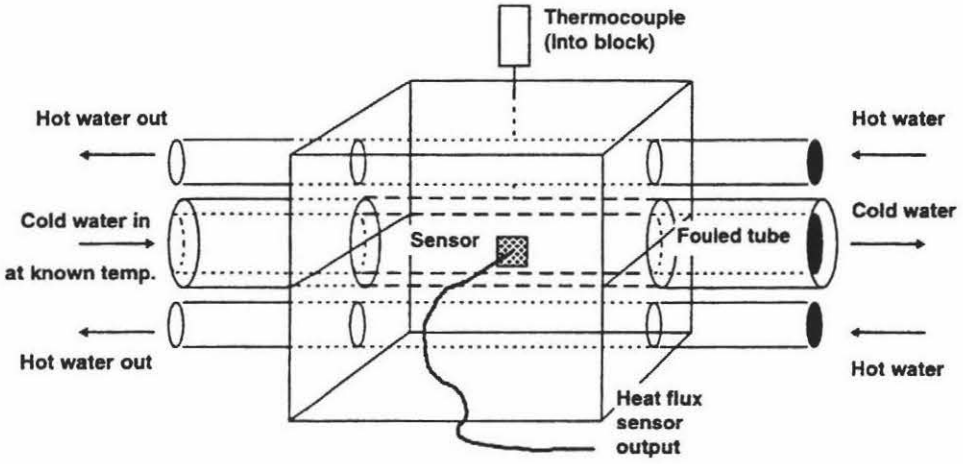

Figure 2.19: Schematic diagram of thermal resistance measurement cell. (after Davies et al. 1997)

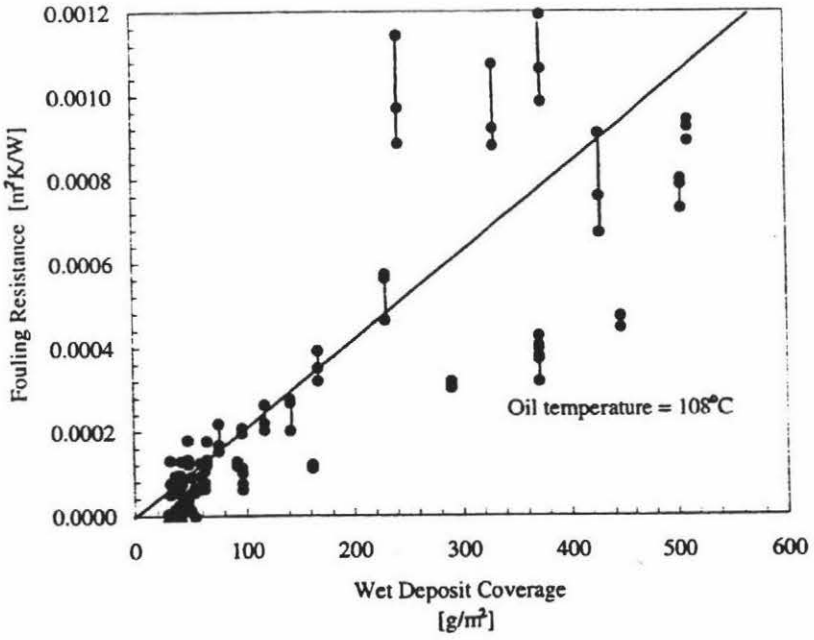

Figure 2.20: Plot of corrected fouling resistance against wet deposit coverage. (After Davies et al., 1997).

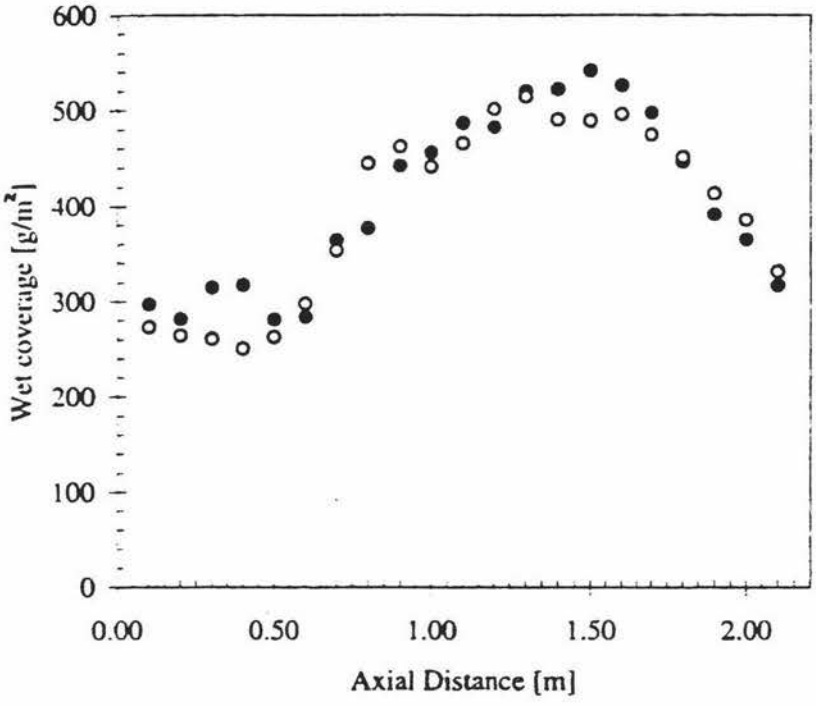

Figure 2.21: Variation of deposition along heat exchanger. Re = 5000; oil temperature = 97°C, solid circles–run 1; open circles–run 2. (After Davies et al., 1997).

Wkg m^4 K^{-1} at 20°C).

Figure 2.21 shows the variation of deposition along the heated pipe. The variation in deposit weight illustrates the effect of a change of fouling control mechanisms along the pipe. The wall temperature is greater than 75°C throughout the tube whereas the bulk fluid temperature exceeds this value at an intermediate location (around 0.5 m). When the bulk temperature is lower than 75°C the reaction rate is controlled by surface reactions, and can be seen to be relatively slow. Where bulk temperature is above 75°C the fouling rate is controlled by bulk reaction rates and is more rapid. The decrease in coverage towards the tube exit was thought, by Davies et al., to arise from exhaustion of whey protein.

2.7 Conclusions.

Knowledge of the cleaning process used in dairy factories is still in its early stages. A theoretical understanding of the cleaning process is yet to develop. The effect of some factors such as temperature and flowrate are quite well understood. Knowledge about other factors such as caustic concentration is quite incomplete. It is generally agreed that there

is an optimum caustic concentration but the precise value is uncertain. The effects of other factors such as local geometry, fouling age or history have yet to be studied.

Research has been hindered by the lack of an effective method for measuring the amount of fouling present on a surface in real-time during CIP. None of the local measurement methods used to measure fouling tested in the laboratory have yet been taken up by industry. The most common techniques for measuring fouling mass present have been based on the effect of fouling on the heat flux through a fouled wall. The use of heat flux sensors has proved promising both in the laboratory and in industry although it has not yet been used for the measurement of CIP.

Chapter 3

Theory

The operating principle of the CIP monitor is based on the relationship between the heat transfer resistance of the flow system and the amount of fouling present on the wall. A diagram of the flow system is shown in Figure 3.1. The heat flux moving through the heat flux (HF) sensor is given by the equation:

$$q = U.\Delta\theta \tag{3.1}$$

Where: q = heat flux (W/m^2)

U = Overall heat transfer coefficient between θ_p and θ_s (W/m^2K)

$\Delta\theta = \theta_s - \theta_p$, the temperature difference between the heat flux sensor (θ_s) and the CIP solution (process fluid, θ_p). (K)

The heat transfer coefficient can thus be calculated from three experimental measurements:

- The heat flux (HF, W/m^2) moving through the plate as measured by the heat flux sensor (HF sensor).
- The temperature of the surface of the heat flux sensor farthest from the plate. This was measured by a thermocouple on-board the heat flux sensor.
- The temperature of the process fluid moving past the opposite side of the plate from the HF sensor. This was initially measured by an RTD shielded by a stainless steel sheath. In later experiments an unshielded thermocouple was used as it had better performance characteristics.

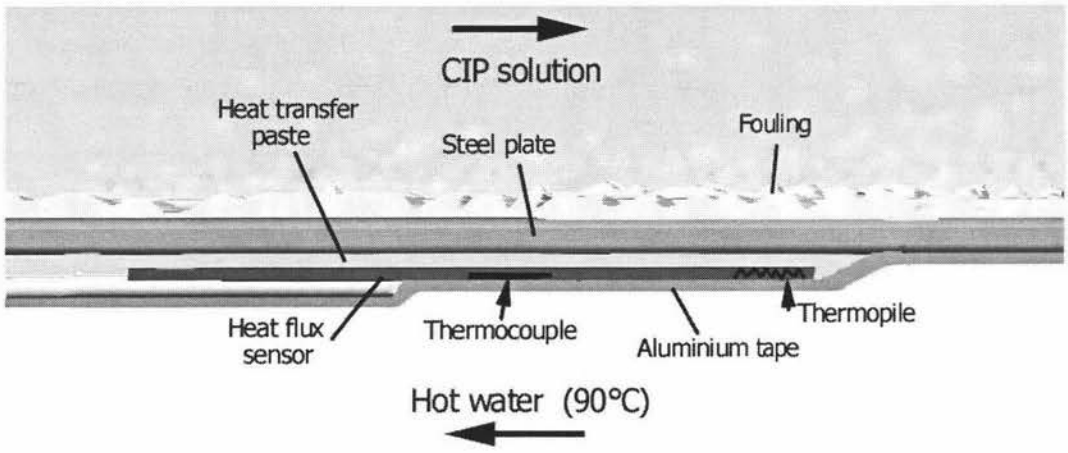

Figure 3.1: Diagram of the experimental system showing the sensor setup on a fouled wall.

$$U = \frac{q}{\theta_s - \theta_p} \tag{3.2}$$

The total resistance to heat transfer from the hot side of the HF sensor to the bulk of the CIP (process) fluid is the sum of following series of resistances:

$$R_{\mathrm{T}} = R_s + R_{\mathrm{HTP}} + R_{\mathrm{wall}} + R_p + R_f \tag{3.3}$$

Where: R_{T} = total heat transfer resistance ($\mathrm{m^2K/W}$)

R_s = heat transfer resistance of the HF sensor ($\mathrm{m^2K/W}$)

R_{HTP} = heat transfer resistance of the heat transfer paste or cement ($\mathrm{m^2K/W}$)

R_{wall} = heat transfer resistance of the wall ($\mathrm{m^2K/W}$)

R_p = heat transfer resistance of the CIP fluids ($\mathrm{m^2K/W}$)

R_f = heat transfer resistance of the fouling ($\mathrm{m^2K/W}$)

These individual resistances are shown in Figure 3.2. The main parameter of interest is the heat transfer resistance contributed by the fouling deposit, R_f.

$$R_f = R_{\mathrm{T}} - R_s - R_{\mathrm{HTP}} - R_{\mathrm{wall}} - R_p \tag{3.4}$$

In fouling studies (Chen, 1997, Truong et.al., 1998) the sum of resistances, R_{T}, minus the fouling resistance, R_f, would be obtained experimentally from the initial heat transfer coefficient (HTC) at the beginning of the run, before fouling had developed.

$$\frac{1}{U_0} = \Sigma R = R_s + R_{\mathrm{wall}} + R_{\mathrm{milk}} \tag{3.5}$$

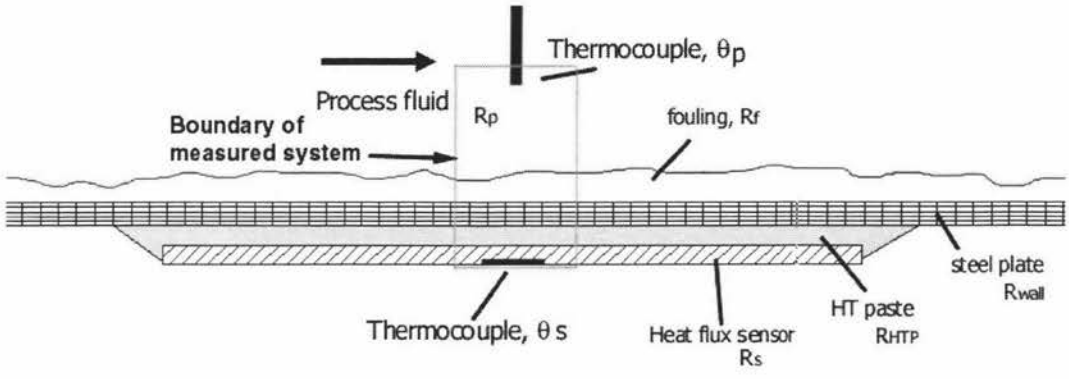

Figure 3.2: Schematic diagram of the heat transfer system showing the individual heat transfer resistances.

Where: U_0 = Overall heat transfer coefficient at time zero. (W/m^2K)

ΣR = Total HT resistance of the system at time zero. (m^2K/W)

During CIP the resistance of the CIP process fluids (R_p) would not be constant, unlike the fouling process fluid, milk (R_{milk}), which would remain constant during the run. The convection resistance of the CIP solution (R_p) may change with its thermophysical properties. Since there are several fluids used during a CIP cycle (water, caustic and nitric acid) and since the fouling deposit will contaminate the CIP solutions as cleaning progresses some compensation technique had to be developed to account for these changes.

Chapter 4

Materials and Methods

4.1 Introduction.

This chapter first lists the materials used then discusses the equipment built for this research. An overview of the entire pilot plant is presented then design considerations are discussed for key elements of the plant. A generic procedure for plant operation is described followed finally by the specific methodology for running the different experiments performed in this research.

4.2 Materials.

4.2.1 Milk.

Standardised pasteurised and homogenised whole milk (3.3% fat, 3.2% protein approximately) was purchased in 800 litre units from Kiwi Coop. Dairies Ltd's Longburn site. The milk was stored in a refrigerated milk vat until, and during, experimentation.

4.2.2 CIP solutions.

- Caustic soda. 50% (765g/L) in a 200L drum supplied by Orica Chemnet Ltd, Tauranga.
- Nitric acid. 68% (970g/L) in a 200L drum supplied by Orica Chemnet Ltd, Tauranga.

4.2.3 Steam.

Steam (2 Bar) generated by the Riddet Building at Massey University used as a heating medium within the Pilot Plant.

4.2.4 Water.

Water from the high pressure water circuit was used to clean the plant and as a cooling medium.

4.2.5 Concentrated soiled caustic (Retentate).

This was the retentate of a separation process used to recover caustic from used cleaning-in-place solutions in a dairy factory. Two 20 litre containers of retentate were obtained from New Zealand Dairy Group's Te Rapa site (supplied by Orica Chemnet Ltd). The retentate was from a single batch of used caustic that had been used to clean a cream plant.

4.2.6 Heat transfer paste.

- Silicone Heat Transfer Compound - Electrolube HTS35SL
- Heat Transfer Compound - Electrolube HTC103 was initially used but was found to be too sensitive to heating.

4.2.7 Adhesive tape.

Aluminium adhesive tape, 3M Scotch 425, was used to press and hold the HF sensor to the stainless steel test plates.

4.3 Design and construction of the pilot plant.

In order to develop the CIP monitor it was necessary to conduct experiments using a heat flux (HF) sensor in a controlled situation where the measured fouling surfaces could easily be inspected and process variables altered to suit experimentation. For these reasons it was decided to construct a pilot plant that could replicate the pre-heating and fouling of a milk powder plant. The plant would also have a cleaning-in-place (CIP) system that would clean the plant in a manner as similar as possible to that used in the dairy industry.

4.3.1 Objectives.

The design of the pilot plant was based on the following objectives:

- To replicate the processes found in a milk powder plant up to and including the evaporator.
- To provide a system for developing milk fouling layers on specified surfaces within the plant.
- To minimise undesired fouling on surfaces such as the plate heat exchanger.
- To provide plant run times of more than 10 hours with continuous milk supply at 50L/hr.
- To include special fouling surfaces within the plant that would aid the inspection and measurement of fouling during processing or cleaning.
- To incorporate a clean-in-place (CIP) cleaning system for the plant. The CIP system was designed to be as similar to CIP systems used in the dairy industry as possible.

4.3.2 Overview of the Pilot Plant.

Figure 4.1 shows a process flow diagram of the Pilot Plant for the milk processing operation. The process involved a series of heating operations directed at producing fouling on target surfaces. It began with the milk being heated from 4°C to either 55°C or 80°C in the plate heat exchanger. Then if further heating was required a Direct Steam Injection unit could be used to lift the milk to the desired temperature.

The aim of this pre-heating section was to heat the milk to temperatures above 70°C so that when the milk came into contact with a heated surface it would foul on that surface. Therefore following the first heating section were the two types of target fouling surfaces; the fouling modules and the fouling tubes. The fouling modules were an array of mini plate heat exchangers (MPHE) that could be easily dismantled during processing for inspection. The fouling tubes were double pipe heat exchangers (DPHE) from which the inner tube could be removed and inspected at the end of milk run.

Following the fouling tubes were pre-heating units for conditioning the milk for evaporation in the falling film evaporator. This included another pair of Direct Steam Injection units (DSI 2) and two holding tubes. From the holding tubes the milk would enter the falling film evaporator which was the last processing step of the pilot plant.

Milk Powder Pilot Plant: Milk processing.

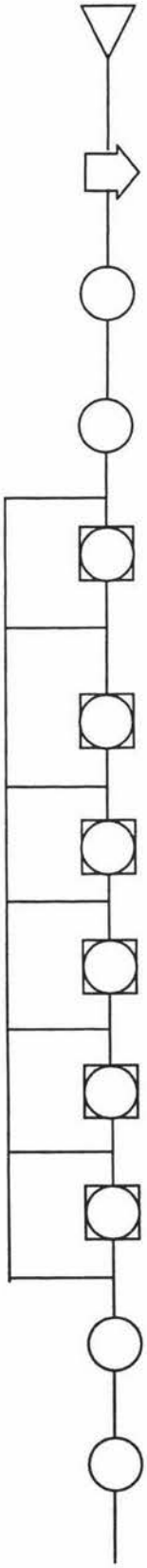

Milk vat, 850 litres with refrigeration. Milk stored at 4°C

Milk pumped to plate heat exchanger at 50L/hr.
Ebara centrifugal pump CDX 70/05.

Plate heat exchanger. Milk heated to 55 or 80°C. Hot water on non-process side of PHE. Alfa Laval U265R.

Direct steam injection (DSI). Two DSI units arranged in parallel. 20°C may be added to the temperature of the milk flow if necessary.

Fouling module 1. Single flat plate heat exchanger. HF sensor attached to the hot water side of the plate. Module can be isolated from the running process flow and the plate removed for inspection. Milk is not significantly heated in each of the fouling modules.

Fouling module 2

Fouling module 3

Fouling module 4

Fouling module 5

Fouling module 6

Fouling Tubes. Either two or six double tube heat exchangers. Milk is heated by 10°C if two tubes are used.

Direct steam injection. Two DSI units in parallel. May be used to increase the temperature of the milk flow by 20°C.

Figure 4.1: Process flow diagram for milk processing on the Pilot Plant.

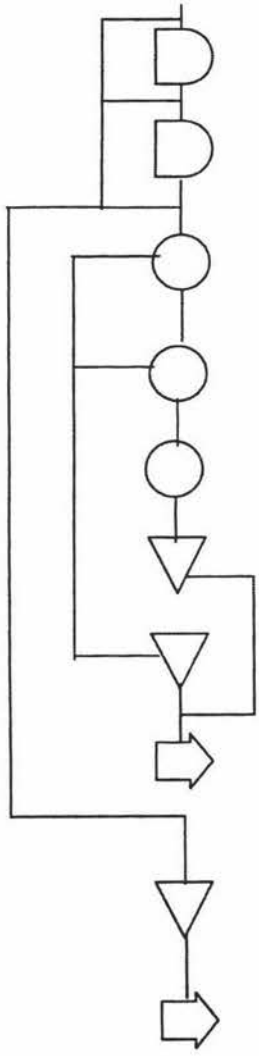

Holding tube. 50 seconds. @45L/hr

Holding tube. 25 seconds @45L/hr.

Falling film evaporator. Single evaporative plate. 1.3 m tall. Vacuum of 0.4 bar.

Separator.

Condenser.

Condensate collection vessel.

Product collection vessel.

Pump to drain. Mono-pump.

Collection tank (Tank 1). 500L.

Processed milk pumped to drain at the end of the run mixed with water and caustic from the Clean-in-place (CIP). Fristram centrifugal pump FP712KF 1.1kW

Figure 4.2: Photo of the Pilot Plant.

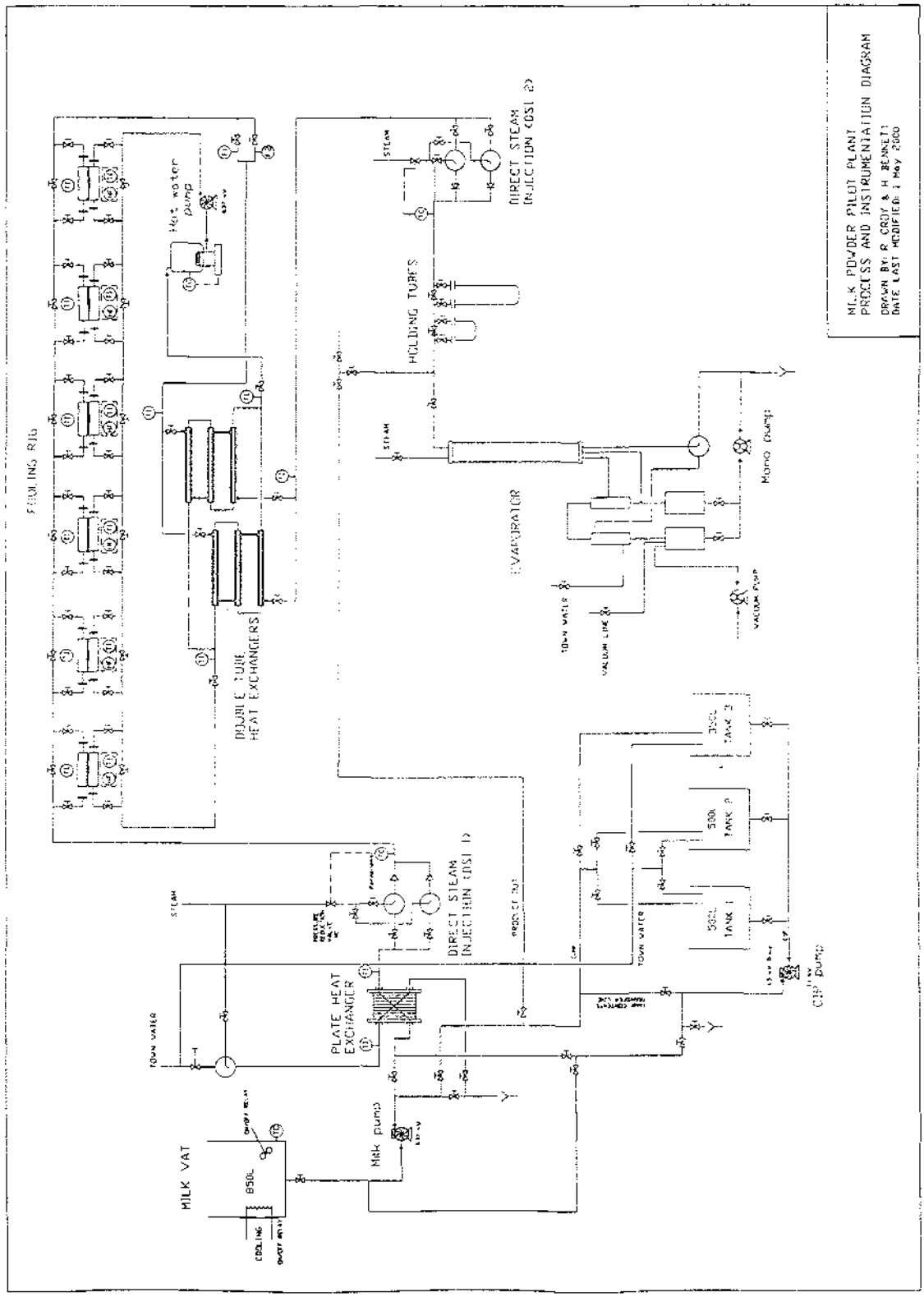

Figure 4.3: Process and Instrumentation Diagram of the Pilot Plant.

Figure 4.3 shows a Process and Instrumentation Diagram (P&ID) of the the pilot plant. The diagram represents the plant as it was at the end of the experimentation period after all modifications to the plant had been made. The only significant differences between this figure and the plant as it was at the beginning of experimentation was the addition of four extra double tube heat exchangers (Fouling tubes) and the addition of another flowmeter (F2) in parallel with flowmeter F1.

Cleaning-in-place (CIP).

Figure 4.4 shows a process flow diagram of the CIP process for the Pilot Plant. Figure 4.5 shows the Process and Instrumentation diagram of the plant with the path of the caustic fluids marked with a bold line. The path of the process fluid flow through the plant is similar to that during milk processing except at the beginning and the end. The CIP solutions began in either Tank 2 or Tank 3. They would then be pumped by both the CIP pump and the milk pump into the plate heat exchanger and on through the plant taking the same path as the milk flow. After the holding tubes the CIP solutions would either return to the CIP tanks via the CIP return line or enter the evaporator where it would exit to drain. Caustic solutions were usually recycled through the plant by returning the fluid back to Tank 2 where it began.

Pilot plant group members.

Responsibility for the design and construction of various parts of the pilot plant were shared across the group members involved in building it.

Hayden Bennett	Fouling Rig, Falling Film Evaporator, wiring conduits .
Richard Croy	CIP System, milk vat and plate heat exchanger, RTDs
Mark Dorsey	Control Cabinet, PLC, micro-computer and control systems.
Andrew Hinton	Direct Steam Injection units, Fouling tubes, Holding Tubes and Hot water circuit.

4.3.3 Design or selection of major items.

Custom fouling modules.

Custom fouling modules were designed for the pilot plant to provide a suitable surface for the study of fouling during milk processing and cleaning. Six fouling modules were built into an array so that a number of fouled surfaces could be studied in any one run.

Milk Powder Pilot Plant: Cleaning-in-place (CIP)

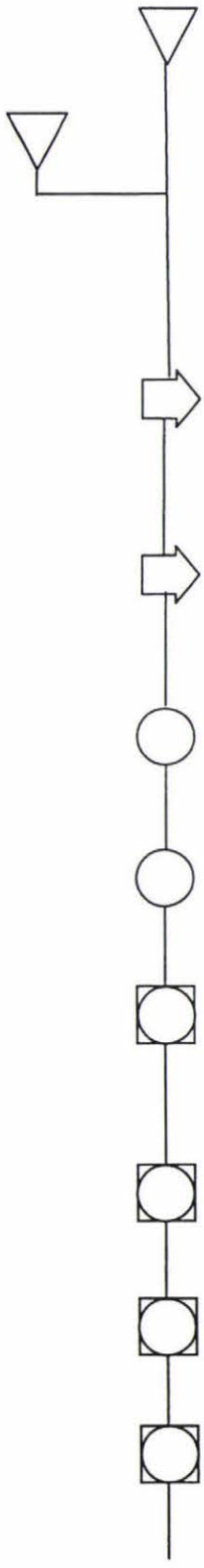

Water tank (Tank 3). 350L of tap water held for rinsing.

Caustic/Nitric tank (Tank 2), 500L. Holds approximately 350L of 1.0% caustic at 75°C. If a nitric clean was undertaken after the caustic wash then Tank 2 would be rinsed at filled with 350L of a 0.5% hot nitric solution.

CIP solution pumped to milk pump at 1.4m^3/hr. Fristram centrifugal pump FP712KF 1.1kW.

Milk pump used to boost the pressure of the CIP solution and increase flowrate. Ebara centrifugal pump CDX 70/05.

Plate heat exchanger. Alfa Laval U265R. Water rinse: water heated from 20 to 35°C. Steam only applied to utility side of PHE.
Caustic/ Nitric wash: No heat applied to PHE.

Direct steam injection (DSI). Not used during CIP. Both DSI units opened to the CIP flow.

Fouling module 1. Single flat plate heat exchanger. HF sensor attached to the hot water side of the plate. Module can be isolated from the running process flow and the plate removed for inspection.

Fouling module 2

Fouling module 3

Fouling module 4

Figure 4.4: Process flow diagram for clean-in-place system of the Pilot Plant.

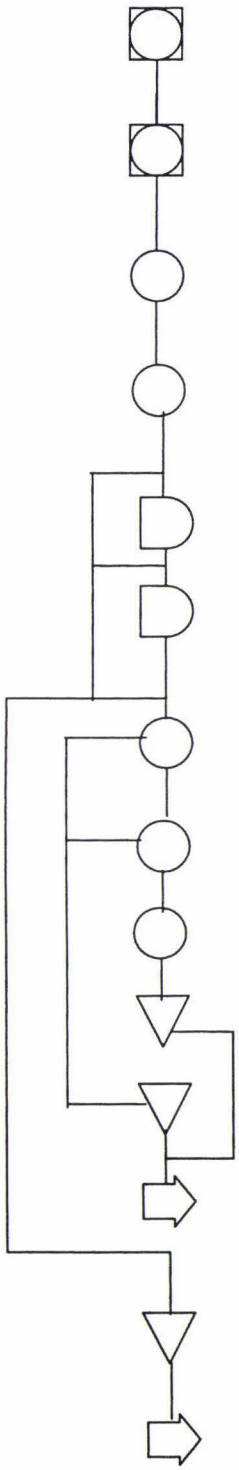

Fouling module 5

Fouling module 6

Fouling Tubes. Usually two double tube heat exchangers in parallel. Sometimes six fouling tubes were used (but not during experiments for this project).

Direct steam injection. Not used during CIP.

Holding tube. 60 seconds.

Holding tube. 30 seconds.

Falling film evaporator. Single evaporative plate. 1.3 m tall. Vacuum of 0.4 bar.

Separator.

Condenser.

Condensate collection vessel.

Product collection vessel.

Pump to drain. Mono-pump.

Collection tank (Tank 1). 500L.

Processed milk pumped to drain at the end of the run mixed with water and caustic from the Clean-in-place (CIP). Fristram centrifugal pump FP712KF 1.1kW

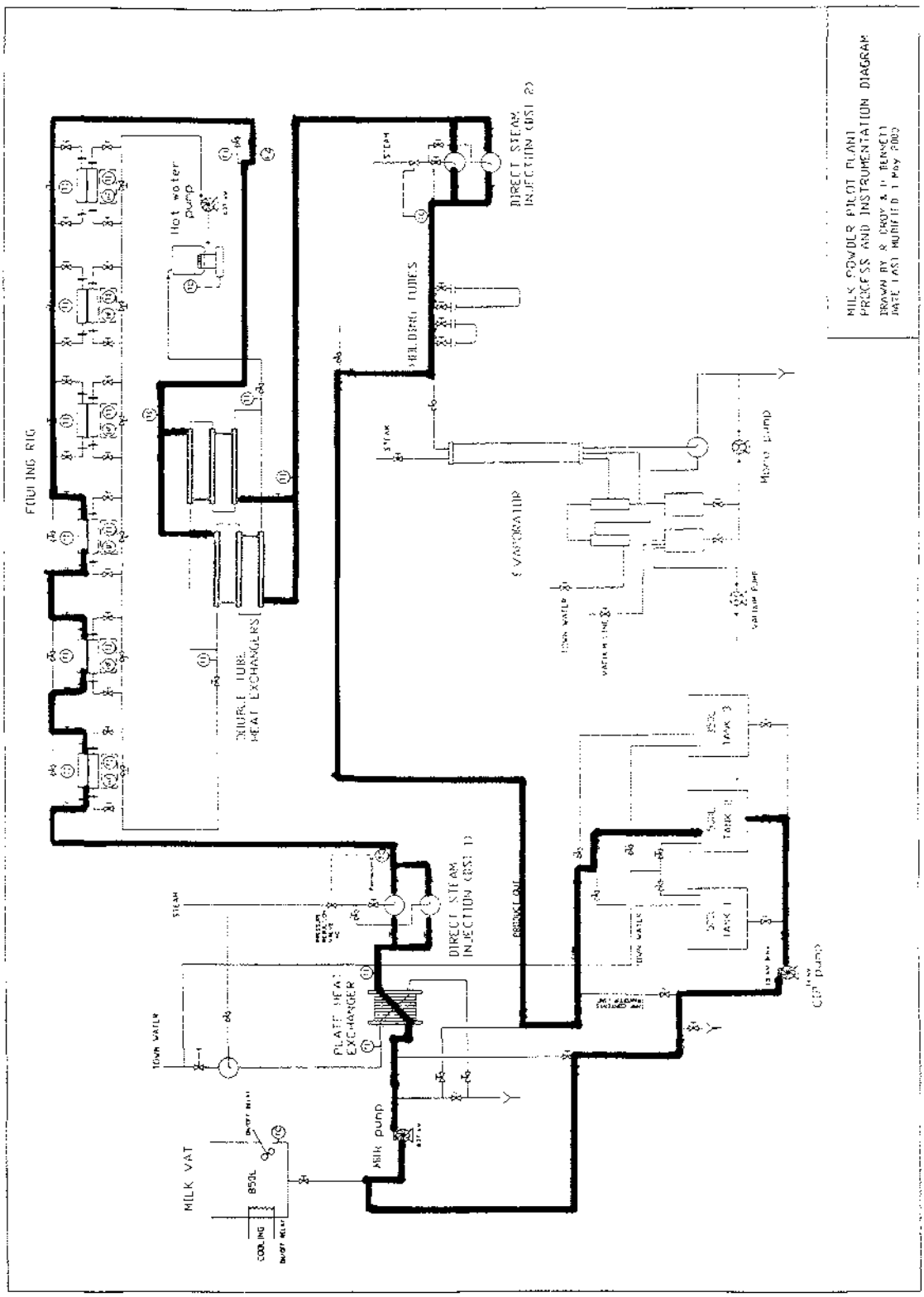

Figure 4.5: Process and Instrumentation diagram of the pilot plant with the flow path of CIP solutions marked in bold.

Fouling module requirements.

- The first requirement of the fouling modules was that they should provide an easily accessible fouling surface which could be inspected at any stage during the operation of the plant. The surface also had to be removable so that that fouling could be photographed or examined under such equipment as a microscope.

- The fouling surfaces needed to be subject to relatively high and stable heat fluxes. This meant that a liquid to liquid heat transfer situation with the two fluids separated by a wall similar to that found in a plate heat exchanger was preferable to liquid to air heat transfer.

- The heat flux sensor needed to be easily installed and removed from the fouling surface. Each heat flux sensor had to be re-attached to a new fouling surface for each experiment as this would allow different types of stainless steel surfaces to be used for experimentation. Disposable plates also allowed fouling layers to be kept after development for cleaning at a later date.

- Each fouling module needed to be isolatable from the plant flow at any time during processing so that the fouling surface could be inspected without stopping the milk processing.

- Each module should not significantly increase the temperature of the fluid moving through the process side. The objective was to have the temperature profile across the fouling module array as uniform as possible so that fouling modules would be comparable in terms of process fluid temperature.

Figure 4.6 shows a 3-dimensional model of the fouling module developed. The fouling module was a very small single plate heat exchanger that could be easily dismantled. It consisted of two stainless steel chambers separated by a thin removable stainless steel plate. The process fluid (milk or CIP fluids) flowed through one side of the module and hot water (the utility fluid) passed through the other side. To create a tight seal between the three parts a silicone sheet gasket (thickness 2.35mm) was inserted between each of the chamber flanges and the removable plate. The fouling module pack was held together using a bolt and wing-nut at each of the four corners of the module flange.

Six fouling modules were built and connected to one another in series. A diagram of the fouling module array is shown in Figure 4.7 and a photo in Figure 4.8. Piping for

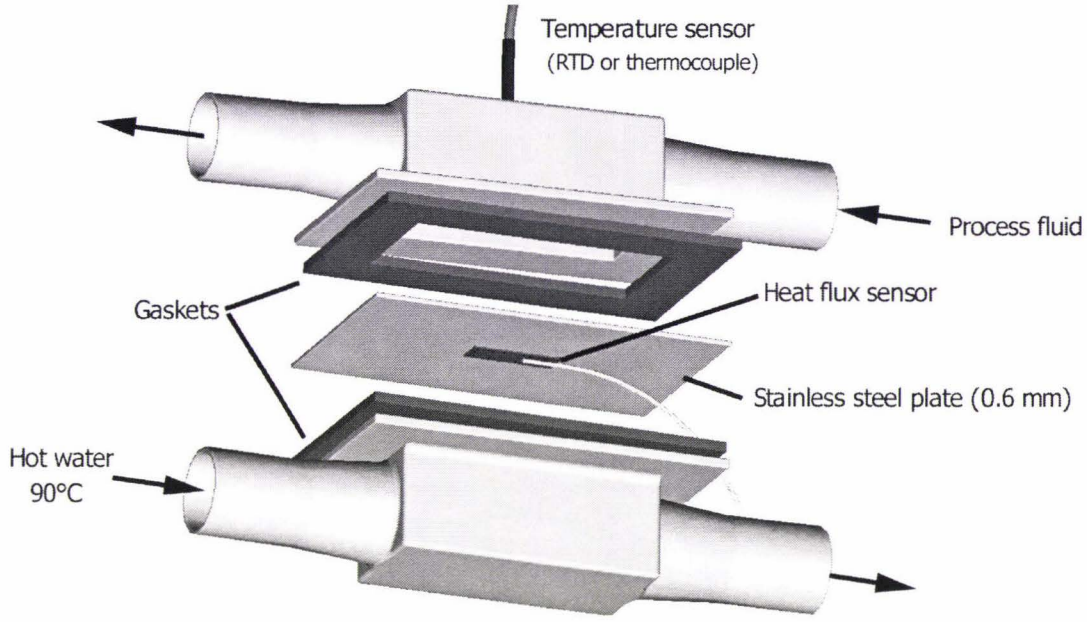

Figure 4.6: A 3D model of the fouling module developed for the study of fouling and CIP cleaning.

the array was built using 19 mm stainless tube with 12.7 mm fittings. This allowed fouling on the plates to be inspected at any time during processing.

Initially the process fluid side of the fouling module array (known as the fouling rig) was at the bottom so that milk would flow on the underside of the plates. This orientation was chosen as fouling has been shown to develop faster on downward facing surfaces (Ma and Trinh, 1999). A problem with this orientation was encountered however. Air entrained and released in the milk flow was found to collect on the milk side of the plates which both prevented fouling and interfered with heat transfer through the plates. To solve this problem the fouling rig was inverted so that the process fluid side was positioned at the top. In this orientation milk flowed down onto the fouling module plates and pockets of air would not develop. Pockets of air did not build up on the utility side of the fouling modules because the flowrate of the hot water was higher than the milk flow.

The utility side fouling module chambers were connected to the fouling rig using flexible plastic hose fittings. This allowed the hot water chambers some movement when the wing-nuts were removed from the fouling modules so that the plates could be either installed or removed.

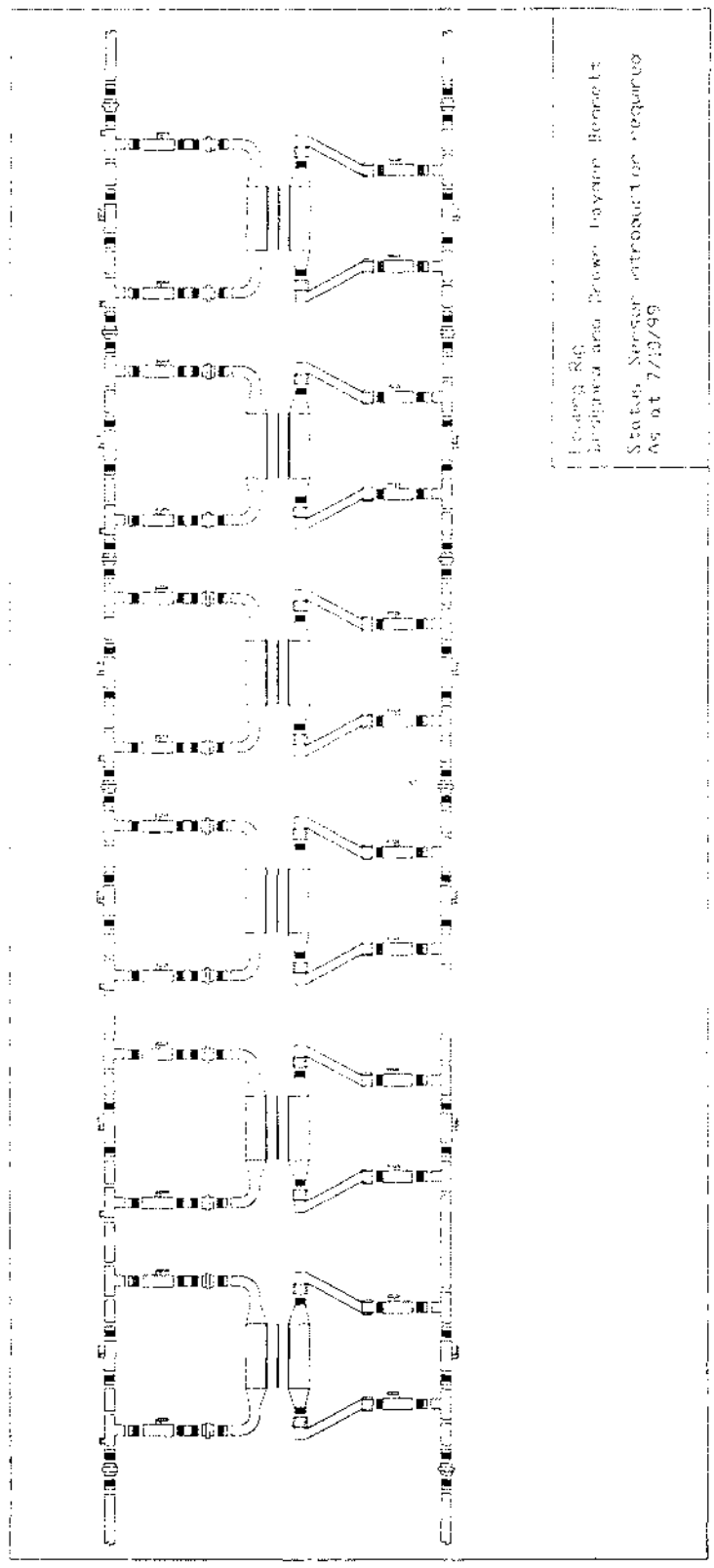

Figure 4.7: The array of the six fouling modules. Each module has six valves that allow it to be isolated from the main flow at any time without disturbing the other modules. (Drawing by H. Bennett.)

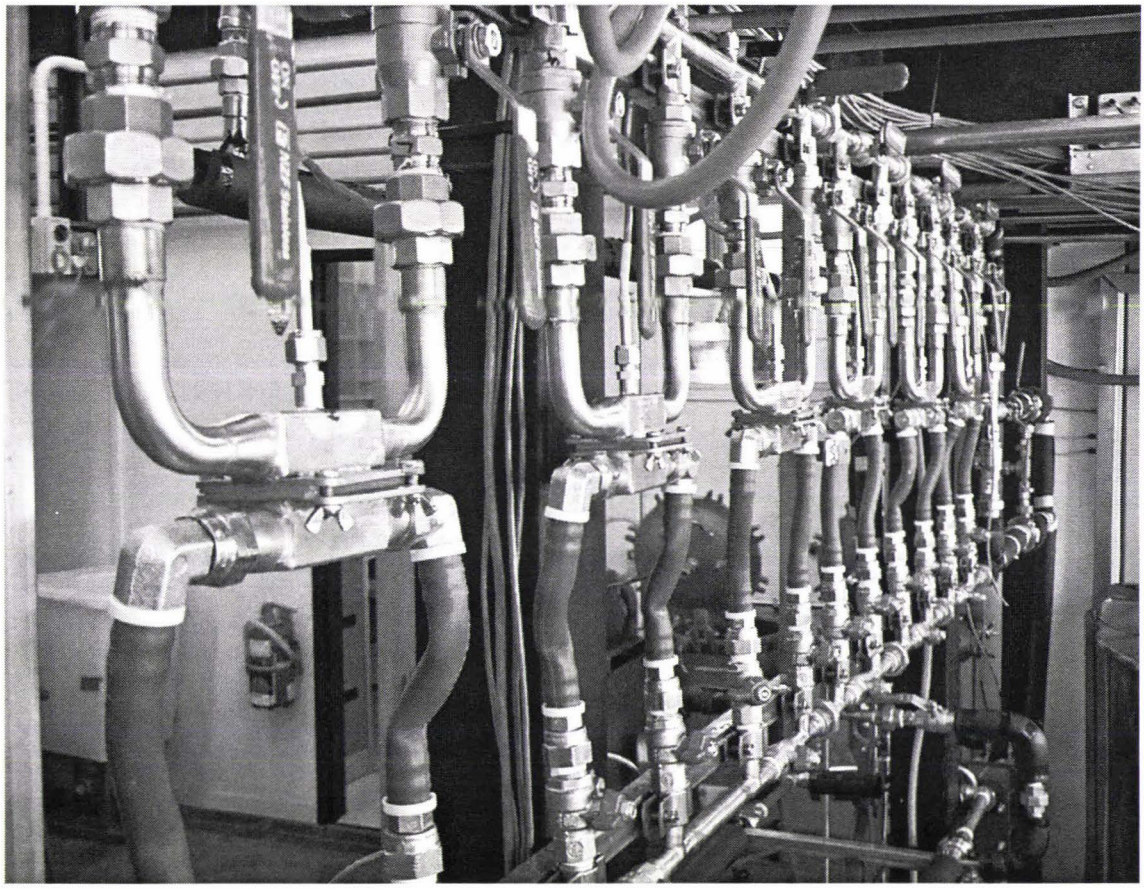

Figure 4.8: Photograph of the fouling rig containing the six fouling modules.

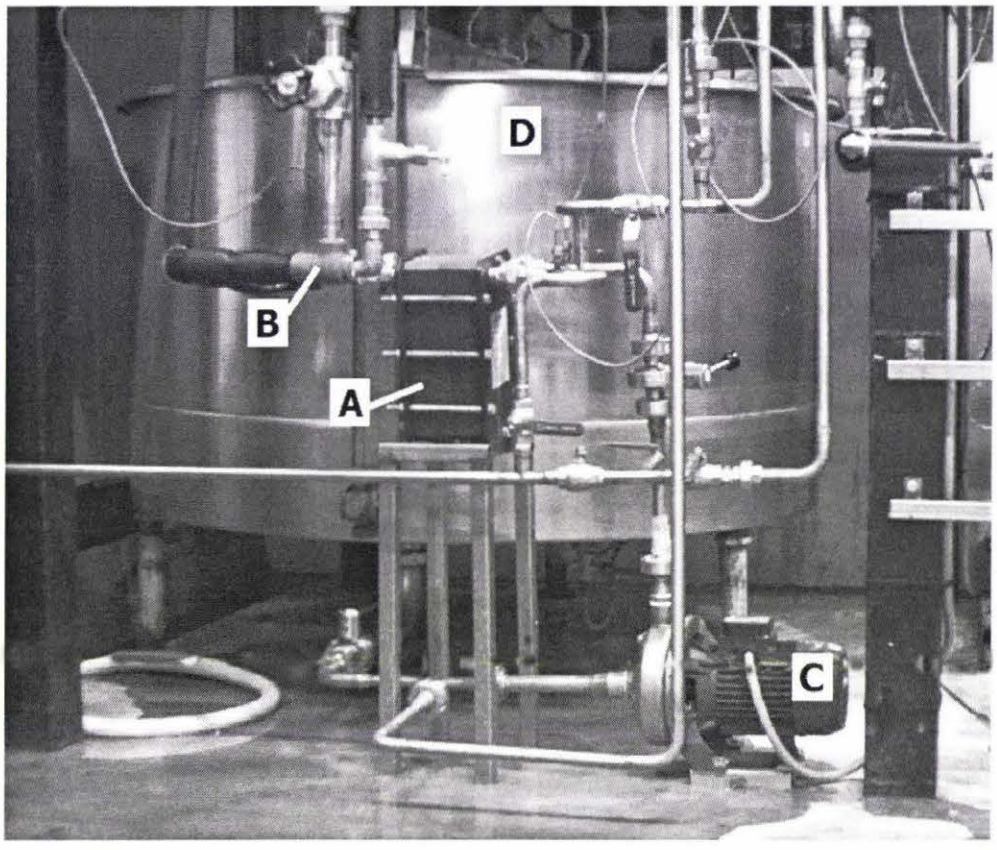

Figure 4.9: Photo of the Plate Heat Exchanger (PHE) and surrounding equipment. [A] Plate Heat Exchanger. [B] DSI that provided hot water to the PHE. [C] Milk pump. [D] Milk vat.

Plate Heat Exchanger.

The plate heat exchanger (Alfa Laval Type U-265-R) was used to pre-heat chilled milk before it entered the first Direct Steam Injection unit (DSI 1). Figure 4.9 shows a photo of the plate heat exchanger and surrounding plant equipment. Because the DSI was found to give an unstable milk flowrate it was not used during most milk runs. In this case the plate heat exchanger (PHE) was the only pre-heating step before the fouling modules. Therefore during milk runs the plate heat exchanger was used in one of two ways:

- If the Direct Steam Injection Unit 1 was being used then the PHE was used to heat chilled milk from the milk vat (4°C) to 55°C.
- If the DSI was not being used (almost all cases) then the PHE was used to heat the chilled milk from 4°C to 75°C.

During cleaning-in-place (CIP) the plate heat exchanger was used to heat the cold rinse water. At the relatively high flowrate of 1.4m^3/hr the PHE could heat the cold tap water from around 18°C to 35°C. During caustic or nitric washes the PHE was not used as the caustic and nitric solutions were pre-heated to 75°C and recycled through the plant.

Hot water/steam supply to PHE. The utility fluid for the PHE was either hot water or steam. Both were supplied using a direct steam injection unit that mixed cold tap water with 200kPa.g steam. Temperature of the hot water supply from the PHE DSI was controlled by altering the flowrate of cold water into the DSI. When the utility fluid for the PHE was to be steam the cold water supply to the DSI would simply be turned off. This was the configuration used to heat rinse water during CIP.

Tanks.

The milk vat. A stainless steel milk vat of 850 litre capacity (diameter 1.4m, depth 0.61 m) was used to store fresh milk. The tank held enough milk for about one week of experimentation. Figure 4.10 shows the interior of the milk vat. The stainless steel column marked [B] contained an RTD temperature sensor positioned close to the bottom of the tank to measure the temperature of the milk. The column was filled with heat transfer oil (Mobiltherm 603) to improve thermal conductivity between the milk and the RTD. An agitator paddle and motor were purchased second hand from NDA Engineering Ltd.

Refrigeration. The milk vat had refrigeration heat exchange tubes built into its base but did not have a refrigeration unit attached. A second hand 1.1 kW refrigeration unit was therefore purchased from NDA Engineering Ltd.

Figure 4.11 shows a photo of the refrigeration unit mounted to the outside wall of the pilot plant. The unit was mounted on the wall with two brackets and covered with a galvanised iron shroud to protect it. The milk vat was directly opposite the refrigeration unit on the other side of the wall.

Filling the milk vat. A 2.5 inch stainless steel tube built through the outside wall was used to transport milk from outside into the milk vat. This is shown (marked [B]) in Figure 4.11. A rotary lobe pump and flexible plastic hosing was used to pump milk from the delivery truck to the 2.5 inch pipe where it would flow into the milk vat.

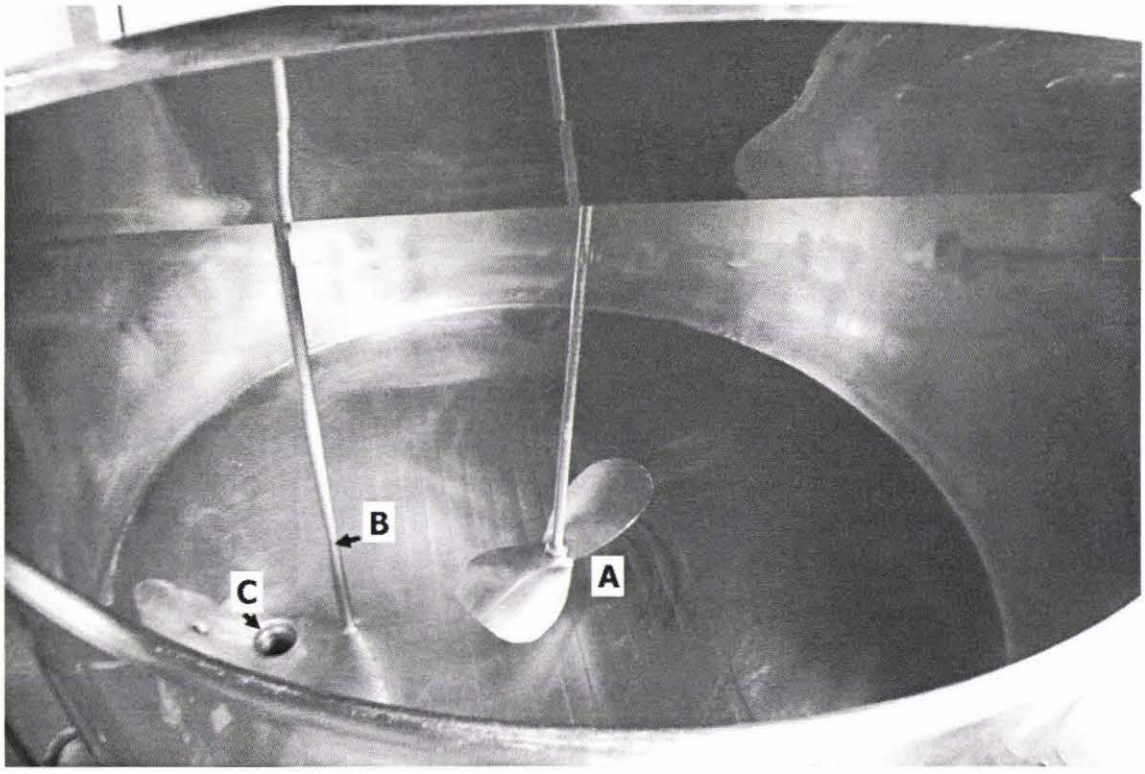

Figure 4.10: Photo of the inside of the milk vat. [A] Agitator paddle. [B] Temperature sensor column (filled with heat transfer oil and an RTD). [C] Tank outlet to plant.

Figure 4.11: Photo of the refrigeration unit for the milk vat. [A] Refrigeration unit with shroud. [B] Exterior pipe to milk vat. Used to fill the milk vat from a truck parked outside.

CIP tanks. Three stainless steel tanks were used to hold fluids for the CIP system. Tank 1 and 2 were 500 litre tanks and Tank 3 had a capacity of 350 litres. Initially the Tanks 1, 2, and 3 were to hold dilute caustic, dilute nitric and rinsing water respectively. However because nitric acid was not often used to clean the plant Tank 1 was used to collect spent CIP solution as well as the milk from milk processing. This allowed used milk, rinse water and caustic to be mixed and pumped at a relatively high flowrate to the the drain. This method was used to reduce the build up of milk within the drains.

Tank 2 was used to hold dilute caustic or nitric acid solutions. Tank 3 was used to hold the rinsing water. Each tank had the same piping configuration such that each tank had:

- A supply of high pressure cold water.
- A connection to the CIP return line - the line coming from the process line at a junction before the evaporator.
- An outlet to the CIP pump.
- A line to drain (through the CIP pump).
- A line to any of the other CIP tanks (through the CIP pump).

All three tanks were purchased second hand from MacDonalds Machinery (Auckland). Stainless steel lids for each of the tanks were fabricated by Mike Christie Sheet Metals Ltd (Palmerston North).

Pumps.

Four pumps were required to move fluids through the pilot plant. The pumps required are listed below.

- Milk pump. For moving milk from the milk vat to the evaporator or the collection tank (Tank 1). This pump was also used as a CIP booster pump.
- CIP pump. Pumped water, nitric acid or caustic solution through to the milk pump and on back to the CIP tanks. The CIP pump was also used to empty the CIP tanks to the drain.
- Hot water pump. Provided circulation of water from the hot water tank through the fouling rig and fouling tubes and back to the hot water tank.

- Evaporator pump (Mono-pump). Used to pump fluids from the evaporators separator collection tank and condenser collection tank to drain. This pump was not used for cleaning-in-place experiments. Details can be found in Bennett (2000).

The positions of these pumps within the pilot plant are shown in Figure 4.3 (pg. 54). The Ebara CDX 70/05 (centrifugal, 0.37kW) model was chosen for both the milk pump and the hot water pump. A Fristam Type FP712KF (centrifugal, 1.1kW) was used for the CIP pump. Allen Bradley 60-BA04NSF1 drive controllers (1.5kW) were used to control the speed of the milk pump and the CIP pump.

Centrifugal pumps were chosen for the milk, CIP and hot water pump, as they are the most common pump type used in the dairy industry. Centrifugal pumps were also significantly cheaper than the positive displacement pumps considered.

Direct Steam Injection Units.

Two pairs of direct steam injection units were used in the plant. Following the plate heat exchanger there was a pair of direct steam injection units arranged in parallel to heat milk coming from the plate heat exchanger by 20°C before it entered the fouling modules. Another pair of DSI units was located before the holding tubes and the evaporator.

Two direct steam injection units were built so that during very long runs (longer than 6 hours) the milk flow could be switched from one DSI to the other when the build up of fouling severely affected the performance of the DSI in use.

Each DSI consisted of a plastic fitting contained within a stainless steel pipe of diameter 35 mm. When assembled the DSI had an outer chamber filled with steam. Milk travelled through a narrow tube through the central axis of the DSI. Four 1 mm holes connected the steam chamber with the the stream of milk. The flowrate of steam entering the milk was controlled using a pneumatic control valve (W Arthur Fisher V201 BUE) located on the steam supply pipe to both DSI units.

Holding Tubes.

Two holding tubes, in series, were installed after the 2nd Direct Steam Injection Unit and before the evaporator. These were used for pre-conditioning whey proteins in the milk before entry into the evaporator. The first tube had a holding time of 50 seconds at a flowrate of 45L/hr. The second tube had a holding time of 25 seconds at 45L/hr.

Figure 4.12 show a photograph of the holding tubes. The holding tubes consisted of U shaped 1 inch stainless steel tube with plastic foam insulation (Centurylon AP-701).

Figure 4.12: Photo of the holding tubes before the evaporator. [A] Holding tube 1, 50 seconds. [B] Holding tube two, 25 seconds.

Each holding tube had three butterfly valves (SPEC) to control whether flow entered the holding tube or bypassed it.

Hot water circuit for the fouling modules and fouling tubes.

Circulated hot water at 90°C was used to provide heating to the fouling modules and the fouling tubes. A 130L stainless steel tank (diameter 0.28m, depth 0.45m) with a 3kW element (Eutron Type Fold) was used to hold and heat the water. A centrifugal pump (Ebara 0.37kW CDX 70/05) was used to circulate the hot water first through the fouling rig and then through the fouling tubes and back to the hot water tank.

Figure 4.13 shows a photo of the hot water circuit. The path of the hot water through the plant is shown as a white line on the photo. The hot water flowed counter current to the process flow.

Falling film evaporator.

The falling film evaporator was not used for CIP experiments in this project. A discussion of the design and construction of the falling film evaporator is given in Bennett (2000).

4.4 Process control and instrumentation.

4.4.1 Process control computers.

A micro-computer and a Modular Programmable Logic Controller (Allen Bradley SLC 500) were used to control the pilot plant and display and log experimental data.

Programmable Logic Controller.

The Programmable Logic Controller (PLC) was a modular system containing a Central Processing Unit (CPU model SLC 5/03) and 12 input/output modules. Table 4.1 shows the layout of the PLC in terms of the module type in each chassis slot. Figure 4.14 shows a photo of the PLC. The PLC managed all of the sensor inputs and control outputs for the plant. PID control calculations were not handled by the PLC (although it was capable) but were instead managed by the micro-computer. This allowed easy and quick reprogramming of the control loops.

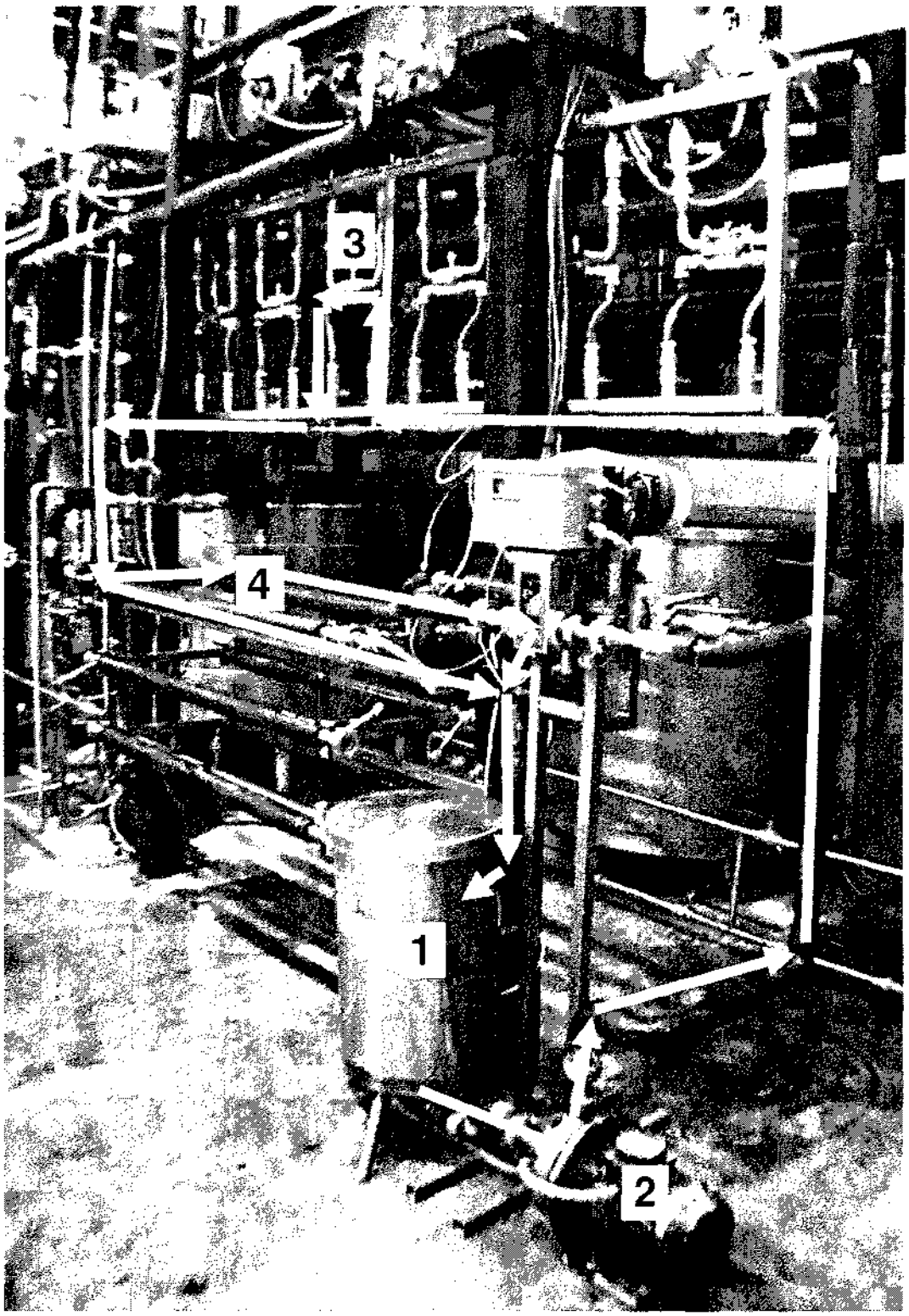

Figure 4.13: Photo of the pilot plant with the hot water circuit marked in white. [1] Hot water heater. [2] Hot water pump. [3] Fouling rig. [4] Fouling tubes.

Table 4.1: Modules within the Allen Bradley Programmable Logic Controller.

Chassis Module Slot	Module Type	No. of channels
1	CPU	-
2	Thermocouple/mV input	4
3	Thermocouple/mV input	4
4	Thermocouple/mV input	4
5	RTD input	4
6	RTD input	4
7	RTD input	4
8	Analog input	4
9	RTD input	4
10	Digital input (not used)	16
11	RTD input	4
12	Relay output	8

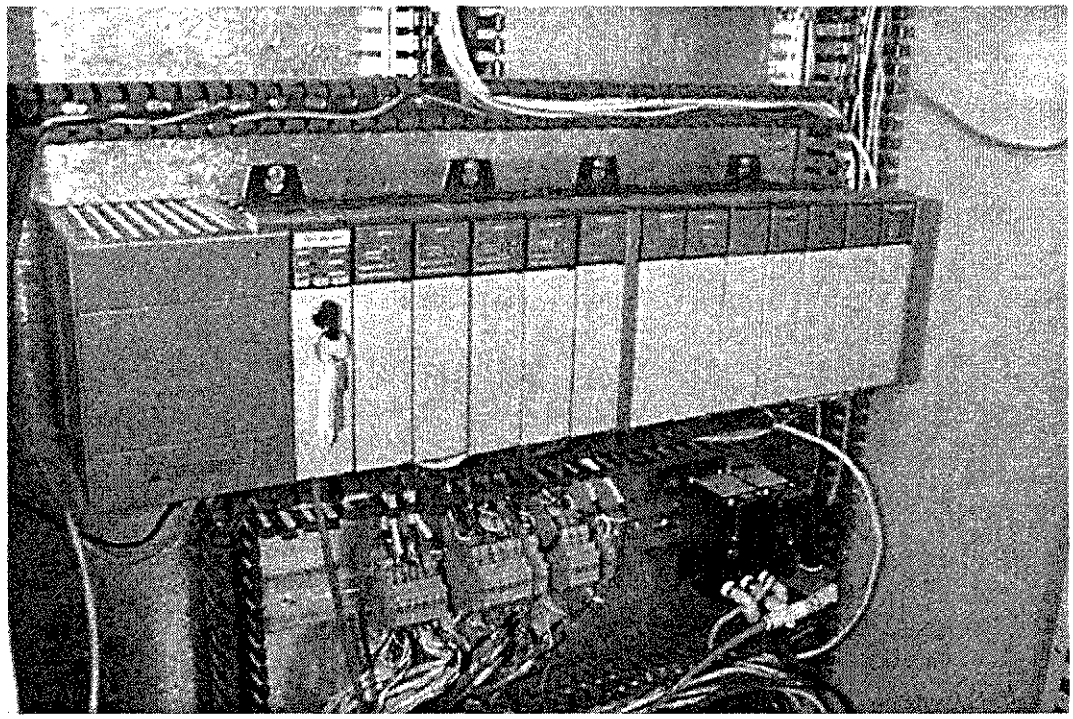

Figure 4.14: Photo of the Allen Bradley Programmable Logic Controller (PLC).

Table 4.2: Variables controlled using the micro-computer.

Plant item	Control type	Automatic control	Auto Cntl using
Milk pump	speed control	yes	milk flowmeter
CIP pump	speed control	yes	CIP flowmeter
Hot water pump	on/off	no	
Agitator - milk vat	on/off	no	
Refrigeration unit	on/off	yes	RTD 6 (milk vat)
DSI 1	% open	yes	RTD 10 (DSI 1 outlet)
DSI 2	% open	yes	RTD 11 (DSI 2 outlet)
Hot water heater	on/off	yes	RTD 7 (oil heater)
Vacuum pump	on/off	yes	Evaporator vacuum sensor

Micro-computer.

A micro-computer (Intel Celeron processor running Windows NT 4.0) was used to display and log data from the PLC and also to provide PID feed back control to the pilot plant via the PLC. The Intellution FIX DMACS 7.0 software package was used to display, log and control the plant data.

Plant monitoring and control. Although the process fluid flow path was directed using manual control valves most other variables of the plant operation were controlled using the micro-computer. Table 4.2 shows a list of the variables controlled using the micro-computer.

Variable monitoring and data logging. All sensor measurements were available to the plant operator via the control screens used to control the plant. Figure 4.15 shows a screen shot of one of the data monitoring and control screens. Real time trending of variables could be viewed using the Historical Display software which also ran while the plant was in operation. An example of a trend graph display is shown in Figure 4.16.

Data collection.

All data managed by the micro-computer was logged to disk automatically. A sample of each sensor measurement was logged to disk every 1 second. Control variables such as pump speeds were logged to disk every 30 seconds. Data required for further analysis would be exported from the FIX DMACS software into comma-delimited text files so that it could be manipulated as a spreadsheet in Microsoft Excel.

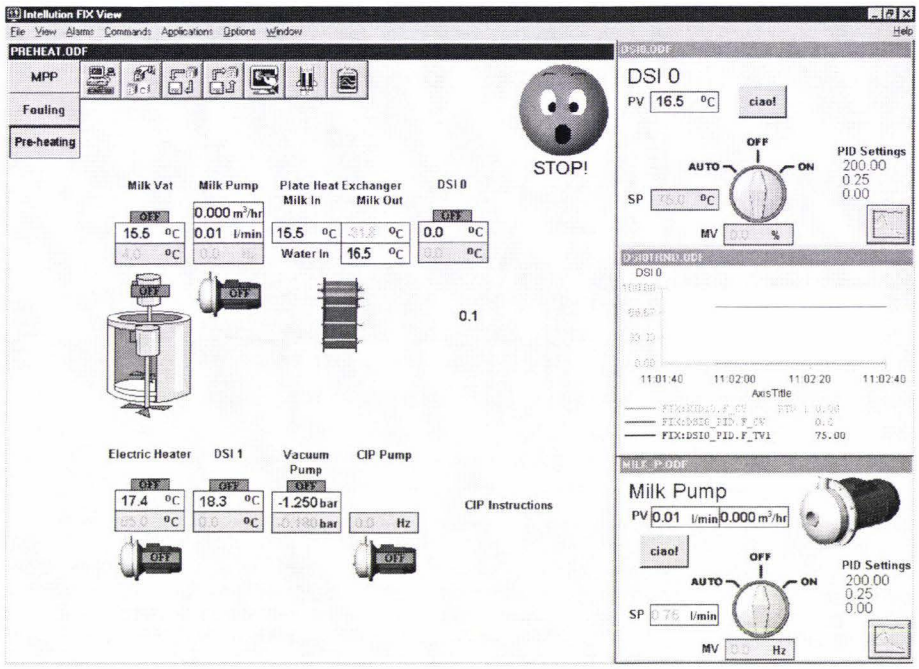

Figure 4.15: Screen shot of one of the control screens on the micro-computer used to monitor plant data and control the plant.

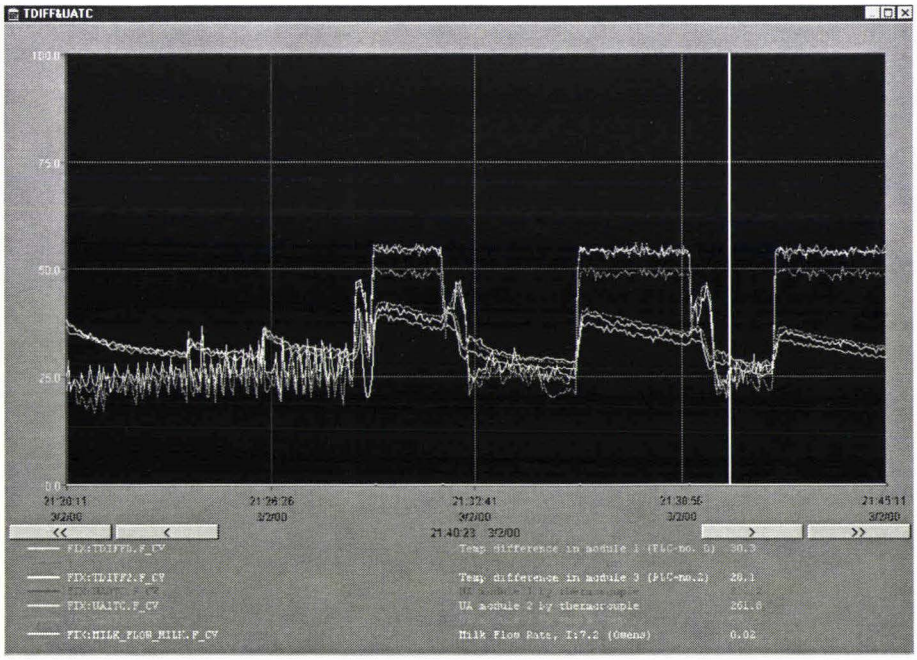

Figure 4.16: Screen shot of one of the historical trend graphs on the micro-computer.

4.4.2 Flowmeters.

Two flowmeters were used to measure the process fluid flow. The two flowmeters were arranged in parallel following the fouling module rig and before the fouling tubes. Manually controlled valves located before each of the flowmeters were used to control the flow of the process fluid through one or other of the sensors. Two flowmeters were installed because of the large difference in the flowrate used for milk processing and cleaning-in-place.

CIP flowmeter.

Endress-Hauser Promag 30FT25-AA1AA11A2113.

- Used to control the process fluid flowrate of Clean-in-place fluids if the CIP and milk pumps were not set to full speed. In this case the flowmeter would be linked to the milk pump with a PID control loop in the FIX DMACS software.
- Always used to measured the process fluid flowrate during CIP experimentation.

Milk flowmeter.

Endress-Hauser Picomag 11 PM16533. Used to monitor control the process fluid (milk) flowrate during milk processing runs. The milk flowmeter was linked to the milk pump with a PID control loop in the FIX DMACS software.

4.4.3 Temperature sensors.

Resistance temperature detectors (RTDs) shielded in stainless steel sheaths manufactured in-house were initially used for all of the temperature sensors within the plant. The 6 RTDs measuring the process flow temperature in the fouling modules were later replaced with commercial sensors and then removed altogether.

Building the RTD temperature sensors.

- The two leads of the RTD were soldered to three signal wires. The two connections were insulated from one another by applying heat-shrink tube to one of the leads.
- A 10 cm length of stainless steel tube (0.25 inch outer diameter) was cut and one end welded into a closed dome.
- The RTD and lead wires were inserted down to the end of stainless steel sheath.

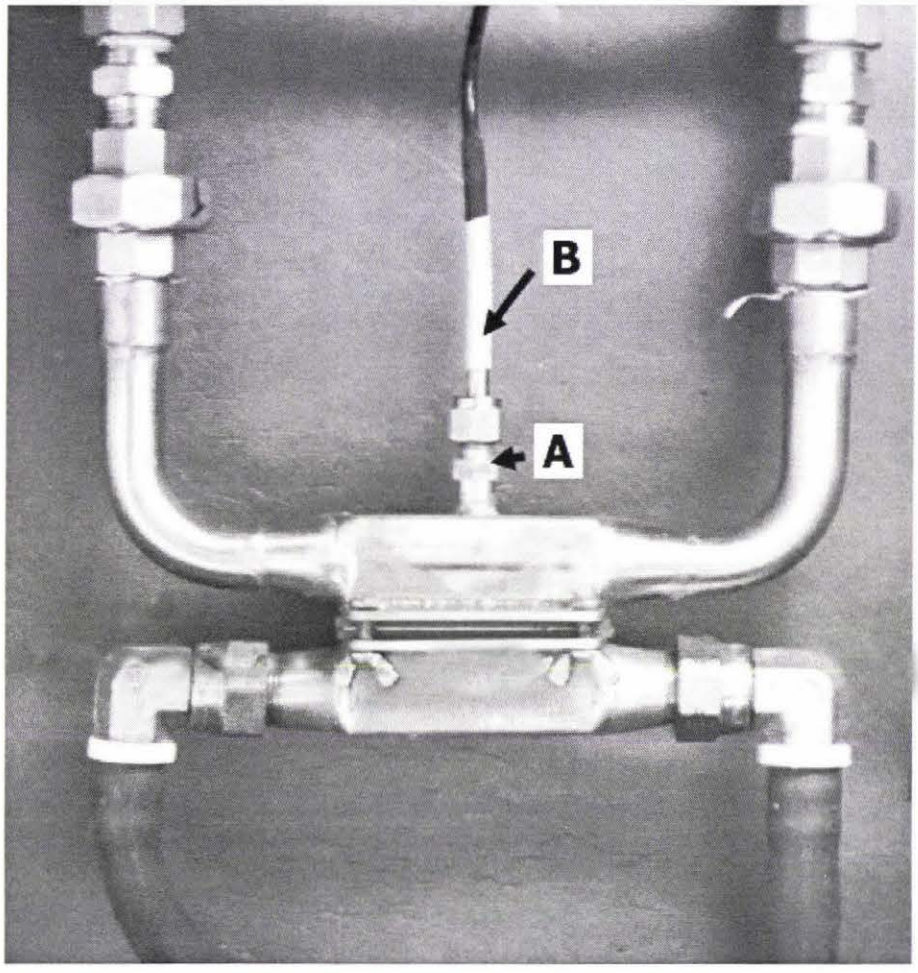

Figure 4.17: Photo of a RTD temperature sensor mounted in a fouling module. The RTD is measuring the process fluid chamber. [A] Swagelok fitting welded to the fouling module holds the RTD. [B] The shaft of the RTD and the sensor wire.

- Heat transfer oil (Mobiltherm 603) was used to fill the sheath to improve heat transfer between the sheath and the RTD.
- Shelleys Super Strength Araldite epoxy resin was used to seal the end of the sheath and hold the sensor wires in place. Heat shrink tube was used to provide a flush join between the sheath and the sensor wires.

RTD sensors were inserted in piping through Swagelok fittings welded to the piping. Figure 4.17 shows a photo of a RTD mounted in a fouling module.

Fouling module temperature sensors.

Initially the process fluid temperature sensors in the fouling modules were found to be subject to unexpected deviations in temperature. This was believed to be due to poor contact between the the RTD transducer and the stainless steel sheath. Therefore because the accuracy of these sensors were critical to experimentation they were replaced with commercially available sensors.

Thermocouples. The unexpected deviations continued and further investigation revealed the cause to be the connection between the RTD sheath and the Swagelok fitting. Details of this finding are given in section 5.5 (pg. 130). Because of the poor performance of the RTD sensors thermocouples were later used in place of them for measuring process fluid temperature in the fouling modules. Small rubber bungs were inserted into the Swagelok fittings and the thermocouples were inserted through a hole in the rubber bungs and into the fouling module.

A photo showing the three types of temperature sensor used are given in Figure 4.18.

Temperature sensor locations.

- RTD = Resistance temperature detector.
- TC = Thermocouple (T type).

The locations of the temperature sensors initially used during experimentation are given in Table 4.4.3.

The changes made to the locations of temperature sensors after the RTD sensors were no longer used to measure the process fluid temperatures in the fouling modules are given in Table 4.4.3.

Temperature sensor calibration.

The six RTD temperature sensors in the fouling modules and the thermocouples on board the Heat Flux sensors were calibrated using boiling water and an ice water slurry as references points of 100°C and 0°C respectively. The temperature sensors were first placed in the ice water slurry and their output temperatures on the FIX DMACS computer software recorded for two minutes. Then the sensors were placed in the centre of a boiling kettle and the measured temperatures recorded for a further two minutes. A linear regression of the

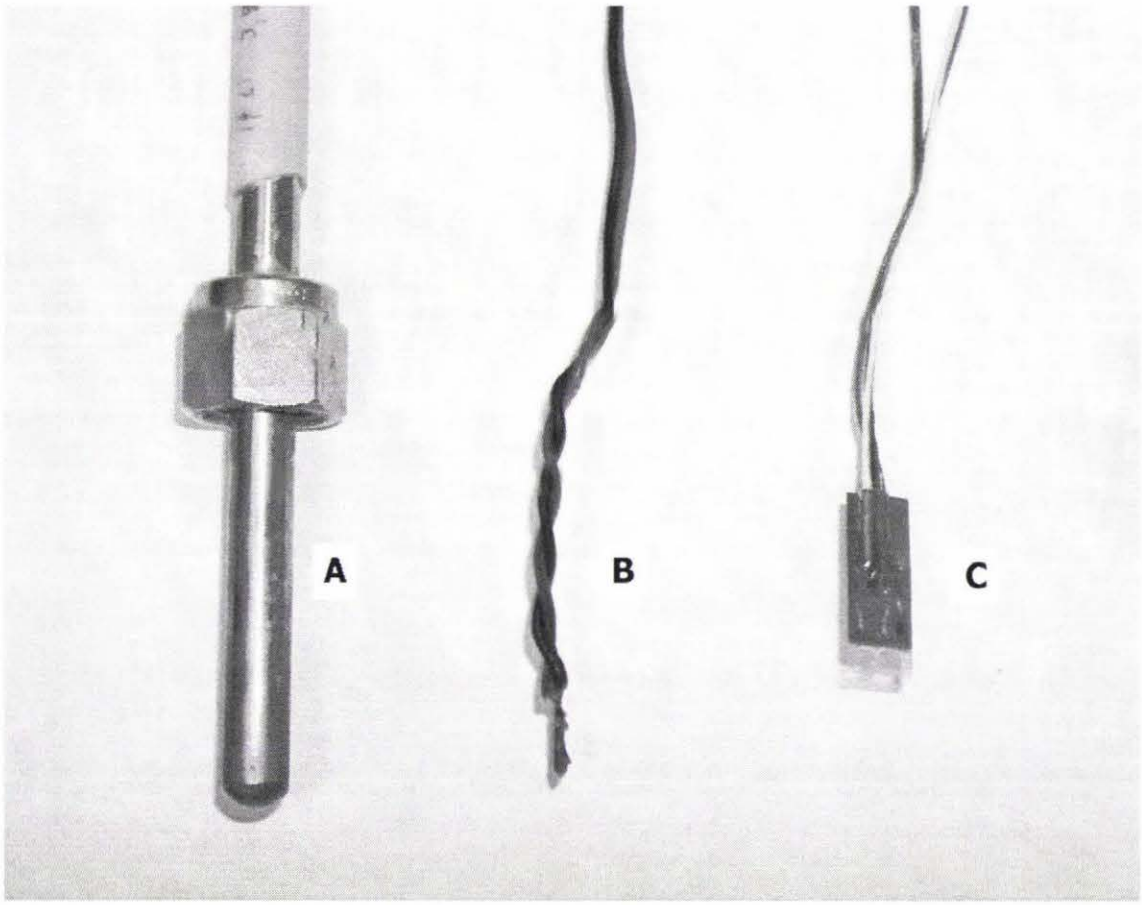

Figure 4.18: Photo of the three types of temperature sensors used. [A] RTD. [B] thermocouple. [C] Heat flux sensor, containing a thermocouple on-board.

Table 4.3: Initial temperature sensor locations.

Temperature sensor	Location
RTD 0	Fouling module 1 - process fluid temp.
RTD 1	Fouling module 2 - process fluid temp.
RTD 2	Fouling module 3 - process fluid temp.
RTD 3	Fouling module 4 - process fluid temp.
RTD 4	Fouling module 5 - process fluid temp.
RTD 5	Fouling module 6 - process fluid temp.
RTD 6	Milk in milk vat
RTD 7	Water in hot water heater
RTD 8	Plate heat exchanger - process fluid outlet
RTD 9	Plate heat exchanger - hot water inlet
RTD 10	DSI unit 1 - outlet temp.
RTD 11	DSI unit 2 - outlet temp.
RTD 12	Fouling tubes - process fluid inlet temp.
RTD 13	Fouling tubes - process fluid outlet temp.
RTD 14	Fouling tubes - hot water inlet temp.
RTD 15	Fouling tubes - hot water outlet temp.
TC 0	TC on Heat flux sensor 1
TC 1	TC on Heat flux sensor 2
TC 2	TC on Heat flux sensor 3
TC 3	TC on Heat flux sensor 4
TC 4	TC on Heat flux sensor 5
TC 5	TC on Heat flux sensor 6

Table 4.4: Changes made to the locations of temperature sensors.

Temperature sensor	New Location
TC 3	Fouling module 1 - process fluid temperature
TC 4	Fouling module 2 - process fluid temperature
TC 5	Fouling module 3 - process fluid temperature
RTD 0	No longer used
RTD 1	No longer used
RTD 2	No longer used
RTD 3	No longer used
RTD 4	No longer used
RTD 5	No longer used

two reported values for each sensor was done to provide a calibration for the temperature sensors.

$$a = \frac{100}{\theta_{100} - \theta_0} \tag{4.1}$$

Where: a = regression coefficient

θ_{100} = reported temperature at 100°C.

θ_0 = reported temperature at 0°C.

$$b = -a\theta_0 \tag{4.2}$$

To obtain a calibrated temperature reading the raw value reported by the PLC would be manipulated using a linear equation:

$$\theta_{\text{calibrated}} = a\theta + b \tag{4.3}$$

Fouling module RTD calibration values.

Table 4.5: Calibration data for fouling module RTD sensors.

	Reported temperature at 0°C	Reported temperature at 100°C	Linear regression a	b
RTD 0	0.5	98.3	1.02246	-0.484
RTD 1	-0.3	99.5	1.00201	0.253
RTD 2	0.2	99.8	1.00200	0.253
RTD 3	0.0	99.5	1.00488	0.015
RTD 4	1.0	100.7	1.00275	-1.003
RTD 5	-0.1	99.3	1.00601	0.101

Heat flux sensor thermocouple calibration values.

Table 4.6: Calibration data for heat flux sensor thermocouples.

	Reported temperature at 0°C	Reported temperature at 100°C	Linear regression a	b
TC 0	1.1	100.7	1.00411	-1.133
TC 1	1.4	100.7	1.00609	-1.362
TC 2	1.1	100.8	1.00371	-1.139
TC 3	1.0	100.6	1.00349	-0.963
TC 4	0.8	100.5	1.00233	-0.757
TC 5	0.8	100.6	1.00197	-0.791

When the RTDs in the fouling modules were removed and replaced with 3 thermocouples it was initially assumed that calibration values for the thermocouples taken when the thermocouples were connected to another computer could be used. After experimentation this was realised to be incorrect as some of the error being calibrated for was due to drifts and offsets in the the Analog to Digital equipment connected to the thermocouple (i.e. variations between the individual channels on the PLC). At this point the three thermocouples had been unplugged from the plant so it was not known which thermocouple had been used in each of the three relevant thermocouple channels on the PLC. Therefore each of the three thermocouples were calibrated in the three relevant PLC channels (TC3, TC4, TC5) and the results assessed to determine whether the three thermocouples differed significantly from one another or whether calibration was necessary mainly to compensate for offsets in the individual mV channels of the PLC. The results are presented in Table 4.7.

Table 4.7: Calibration data for thermocouples used to measure the process fluid temperature in fouling modules 1, 2 & 3.

PLC channel	TC3	TC4	TC5	TC3	TC4	TC5
Thermocouple arrangement	Reported temp. at 100°C			Reported temp. at 0°C		
1-2-3	100.5	100.3	100.3	1.0	0.8	0.9
3-1-2	100.3	100.2	100.3	1.1	0.8	0.9
2-3-1	100.5	100.2	100.4	1.0	0.9	0.8

It can be seen from the data in Table 4.7 that variation between the three thermocouples in a channel was not more than 0.1°C except for one data point. This showed that variation between the three thermocouples was small. Therefore the three values for each channel were averaged to provide a linear calibration for each channel (TC3, TC4 and TC5). These results are shown in Table 4.8.

Table 4.8: Calibration results for TC3, TC4 and TC5 with thermocouples for measuring process fluid temperature in fouling modules 1, 2 & 3.

	TC3	TC4	TC5
mean temp at 100°C	100.42	100.24	100.33
mean temp at 0°C	1.05	0.80	0.88
a	1.006339	1.005631	1.005530
b	-1.057	-0.805	-0.885

4.4.4 Heat flux sensors.

Six heat flux sensors (RDF Corp. Model 27036-3) were used to measure heat flux moving through the removable plates of the six fouling modules. The dimensions of the HF sensors were 16 mm by 6 mm by 0.3 mm with four thin sensor wires leading from one end of the sensor.

The heat flux sensors were not independently calibrated due to the difficulty in building calibration equipment for heat flux. Constructing such equipment was considered beyond the scope of this Masters project. Therefore the individual calibration for each HF sensor provided by the manufacturer was used.

Heat flux sensor	1	2	3	4	5	6
Output (μV/BTU/ft^{2}hr)	1.32	1.29	1.31	1.29	1.31	1.29
Output SI units (μV/Wm^{-2})	0.4184	0.4089	0.4153	0.4089	0.4153	0.4089

The HF sensors were connected to thermocouple/mV modules within the Allen Bradley PLC. Millivolt channels connected to HF sensors were programmed to measure the voltage across the sensors within a range of ±50mV and to convert (digitise) the voltages to a signed integer between -32,767 and 32,768. These digital values were retrieved by the FIX DMACS software running on the micro-computer every second and stored under variable names HF0 to HF5. Conversion of these digital values to heat flux values in SI units was done in real-time using the FIX DMACS software.

First the HF value that corresponded to a voltage of 50mV was calculated for each probe using the manufacturers calibration. For heat flux sensor HF1:

$$\phi_{50\text{mV}} = \frac{50,000\mu\text{V}}{output(\mu\text{V/Wm}^{-2})} = 119502.87\text{W/m}^2 \tag{4.4}$$

Then a factor for converting the signed integer (±32,767) to a real HF value was calculated.

$$\text{MF} = \frac{\phi_{50\text{mV}}}{32,767} = \frac{119502.87}{32767} = 3.64705\text{W/m}^2 \tag{4.5}$$

Heat flux sensor	1	2	3	4	5	6
$\phi_{50\text{mV}}$	119502.87	122279.29	120394.90	122279.29	120394.90	122279.29
MF	3.64705	3.73178	3.67427	3.73178	3.67427	3.73178

All HF sensors also came with a standard temperature correction curve that related HF sensor temperature to a Temperature Multiplication Factor (TMF) that was applied to the calibration factor. The FIX DMACS control software was used to apply the TMF to each HF data point in real time. A 3rd order polynomial equation was fitted to the the supplied data and this equation

$$TMF = 1.02258 - 1.2735\text{x}10^{-3}\theta + 6.08438\text{x}10^{-6}\theta^2 - 1.080556\text{x}10^{-8}\theta^3 \tag{4.6}$$

Therefore the complete calculation to convert the raw HF value from the PLC (e.g. HF) to the calibrated value (HFQ) was:

$$HFQ = \frac{(HF)(\text{MF})}{TMF} \tag{4.7}$$

All these calculations were performed by the FIX DMACS software in real-time so that calibrated values for the HF sensor were logged to disk immediately.

The application of a heat flux sensor to a fouling module plate.

Ideally a heat flux sensor would be permanently fixed to a surface using an adhesive with high thermal conductivity. This would ensure a consistent and uniform contact of the HF sensor with the measured surface which would ensure a consistent and reliable measurement of heat flux. For the purposes of these experiments the HF sensor could not however be permanently glued to fouling module plates as new plates were used every day and the six HF sensors would have to be re-applied each day to a new plate. Therefore a method had to be developed that would provide an attachment that was as consistent and stable as possible during long experimental runs.

The basic method for attaching a HF sensor to a plate in a non-permanent manner was developed during the preliminary fouling trials very early on in the project. That basic method was improved upon several times during the duration of experimentation to provide more consistent and stable contact between the HF sensor and the fouling module plate.

The material used to attach the heat flux sensor to the plate was aluminium adhesive tape which had the following advantageous properties:

- It was tough and quite rigid. Once pressed on the plate it held its form providing a flush cover to the HF sensor.
- Its adhesive was quite strong and would remain strong when heated to 90°C.
- It was a satisfactory thermal conductor as it consisted of thin plastic and aluminium layers.

The other material required was silicone heat transfer paste (HTP) to ensure good thermal conductivity between the fouling plate and the HF sensor. The final method used to apply the HF sensor to the plate is listed below:

Method.

- A square of aluminium adhesive tape would be cut large enough to cover the entire surface of the plate.
- The correct position for the HF sensor would be marked on the tape using a ruler and a ball point pen. This position would result in the HF sensor being in the centre of the plate when the tape was applied.
- The HF sensor was placed on the adhesive side of the tape in the marked position.
- A small amount of silicone heat transfer paste would be applied to the HF sensor covering its entire surface but not surrounding areas.
- The tape (with HF sensor) was applied to the plate with one corner of the tape being set flush with the edge of the plate to guarantee the correct positioning of the HF sensor. Tape surface would be rubbed down to remove any creases.

This method of attachment usually worked very well during CIP runs as the run times were relatively short, being only 1 to 2 hours long. Difficulties more often arose when run times were long, such as milk runs. It was found that the application of too much heat transfer paste would lead to blistering of the tape during long runs. Figure 4.19 shows a photo of a HF sensor applied to a block of Perspex using the standard attachment technique. The layout of heat transfer paste under the HF sensor can be seen in the photo and it can be seen that it extends beyond the boundary of the HF sensor. The adhesive of the aluminium tape remained strong when heated (in fact it seemed to strengthen) but it seemed to loose its strength in the presence of excessive HTP. Heating of the plate would

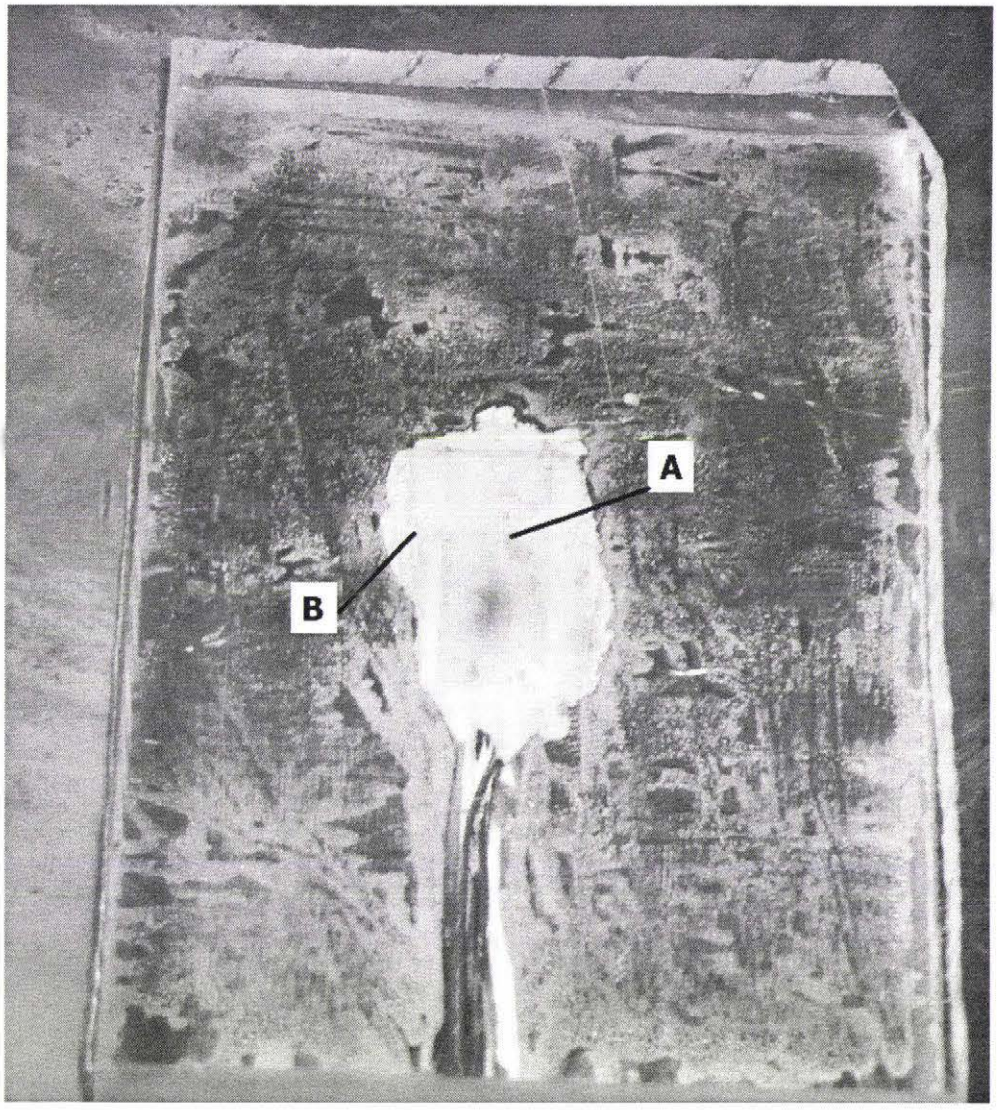

Figure 4.19: Photo of a HF sensor applied to a block of Perspex using the standard application technique. [A] HF sensor (outline can just be seen). [B] Heat transfer paste between the HF sensor and the Perspex.

lead to an increase in pressure under the tape and the presence of too much HTP would allow the tape to come free from the plate and form a blister, lifting the HF sensor from the surface of the plate in the process. Therefore care was taken to only apply enough HTP to cover the surface of the HF sensor and not the surrounding tape when setting up a plate.

4.5 Experimental techniques.

The development of the CIP monitor involved three major experimental processes:

- Generation of whole milk fouling on stainless steel surfaces fouled with milk.
- Cleaning of the fouled surfaces using a Clean-in-place (CIP) process and monitoring of the cleaning process using a heat flux sensor. This was carried out to investigate the sensitivity of the heat flux sensor to the presence of fouling during cleaning.
- Measurement of the effect of changing process fluid properties on the overall heat transfer coefficient of heat exchange surfaces.

These experiments were performed with thin stainless steel plates installed into the custom fouling modules. These plates were small (47 mm by 74 mm) and only 0.6 mm thick. Because the plates were thin the build up of even a thin layer of fouling would result in a significant relative reduction of heat flux moving through the wall which could be measured. The plates could be removed from the fouling modules at any time for inspection by adjusting valves surrounding the module to isolate it from the flow and then unpacking the module.

Fouled plates were made during fouling experiments performed by Hayden Bennett and Carol Ma for research not directly part of this project. These fouled plates would be removed from the fouling modules at the end of the milk run and inspected and sometimes photographed while the CIP solutions were prepared.

When the CIP system had been prepared for cleaning and the fouled plates had been inspected chosen plates would be loaded back into the fouling modules. CIP cleaning experiments could then be performed either during the cleaning of the plant or during a second clean run just for the purposes of experimentation.

4.5.1 Instrumentation used.

Measurement of the fouling modules with the CIP monitor system involved the use of the following instruments:

Heat flux sensor.

Heat flux through the fouling module plate was measured using a heat flux (HF) sensor attached to the hot water side of a fouling module plate (RDF Corp. Model 27036-3).

The HF sensor was a thin wafer of dimensions 16mm x 6mm x 0.3mm. A photo of a HF sensor of the type used is shown in Figure 4.20. It consists of a thermopile at the tip of the wafer that measures the heat flux through the local area surrounding the thermopile. This measured area for heat flux is very small. The surface area of the thermopile was approximately 2mm by 4 mm for the model of HF sensor used in this project. Four signal wires (3m long) came from one end of the HF sensor.

Aluminium tape was used to hold the the HF sensor firmly to the surface of the plate. In initial experiments only a small piece of aluminium tape was used to hold the HF sensor to the plate. This lead to the seepage of water along the HF sensors wires under the tape towards the HF sensor causing the tape to lift a little at one end and altering the heat transfer through the HF sensor. To avoid this problem the layer of aluminium tape was applied to the entire plate surface. Water could not then reach the edge of the tape layer as the edge was protected by the gasket.

A consistent contact between the HF sensor and the plate was ensured by applying heat transfer paste to the contact side of the HF sensor before applying it to the plate surface. A non-silicon based heat transfer paste was initially used but it was found to dry excessively temperatures of 90°C which was the temperature it was subject to for several hours at a time. This was not expected as the specifications of the paste reported that the paste was suitable for temperatures up to 130°C. To improve this situation a silicon based heat transfer paste was used which was more stable at higher temperatures. This paste performed well and would only dry a little during long experimentation becoming more somewhat more viscous but not dry.

Temperature of the hot water side of the HF sensor.

A T-type thermocouple was built on board the HF sensor. It was used to measure the temperature of the hot water in contact with the HF sensor. The thermocouple was located in the centre of the wafer towards the upper surface of the probe. It is important to note that the temperature measured by the thermocouple is not necessarily that of the thermopile as the two transducers are separated by a distance of 3 mm.

Flowrate.

The flowrate of the CIP system was measured using the high flowrate flowmeter located after the fouling modules. When a specified flowrate was required, such as during the thermophysical properties compensation experiments the flowmeter would be coupled

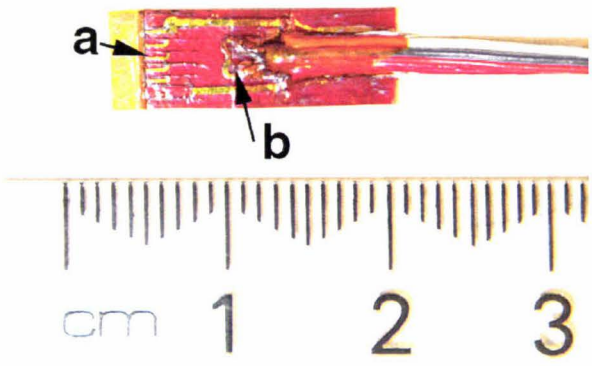

Figure 4.20: Photo of a heat flux (HF) sensor of the type used in all experimentation. The sensor contains a thermopile [a] that measures the HF at the tip and an thermocouple [b] in the centre of the probe to measure the probe temperature.

to the milk pump with a PID control loop to provide automatic flow control. During normal CIP cleaning experiments, however, the flowmeter was not coupled to the pump as both pumps were run at full speed to provide the maximum flowrate.

During milk fouling runs the flowrate was measured using the smaller milk flowmeter installed in parallel with the large flowmeter. The process fluid was routed through the correct flowmeter using a couple of isolating valves positioned before the flowmeters. The small flowmeter was used for milk as the flow was so small as to be unsuitable for measurement using the large CIP flowmeter. The milk flowmeter was usually coupled to the milk pump with a PID control loop to provide automatic control of the milk flow during fouling experiments.

4.5.2 Methods of plant operation.

Generation of fouled plates.

For fouling development milk was run through the modules at a temperature of 75 to 85°C and at a flowrate of 0.75L/min. The hot water circuit was set to 90°C to maintain a hot surface to the steel surface in contact with the milk and constant temperature difference across the plate. Fresh pasteurised milk with 3.3% fat was always used.

All milk runs on the pilot plant for plates used for CIP experimentation were made with a one-pass flow configuration i.e. there was no recycling of the milk. Fouling runs were typically 4 hours long. Rapid fouling was encouraged by carefully controlling the startup

procedure of the milk run. It was found that pre-heating the dry plates to 90°C with the hot water circuit before applying milk to the plate surface caused a 'burn on' effect that produced a fouling substrate in less than 2 minutes. This substrate would continue to foul well over the period of the next four hours.

The thickness of the fouling was usually limited to approximately 1 mm high but a milk run of longer than 4 hours would produce a fouling layer than was less porous than a younger one. The structure of the fouling layer was cratered. At first large craters would form but fouling from long runs would have fouling layers where the large craters would contain smaller craters hence becoming more dense.

Milk processing procedure.

Several configurations of the plant could be used for milk processing but one configuration was used for the majority of fouling experiments from which fouled plates were taken for use in cleaning-in-place experiments. The procedure for running the plant in this configuration is listed below.

Plant startup.

- Hot water heat turned on and set to 90°C. The milk flow would not be turned on until the water had reached the set temperature.
- Test plates would be loaded in to the fouling modules.
- Flow path set as described in Figure 4.21. Fouling modules would however be closed to the flow (isolated).
- Outlet valve to tank 1 (the last valve on the line) partly closed to increase to increase back pressure on the milk pump. This allowed the milk pump to be run at a higher speed to protect against overheating.
- Hot water pump started and fouling modules opened to the hot water flow.
- Milk pump started and set to automatic control at 45 L/hr.
- Opening of the fouling modules to the milk flow was delayed while water remaining in the plant was flushed out by the on-coming milk.
- When milk could be seen flowing into the collection tank at the end of the process line (Tank 1) then the fouling modules would be opened to the process flow.

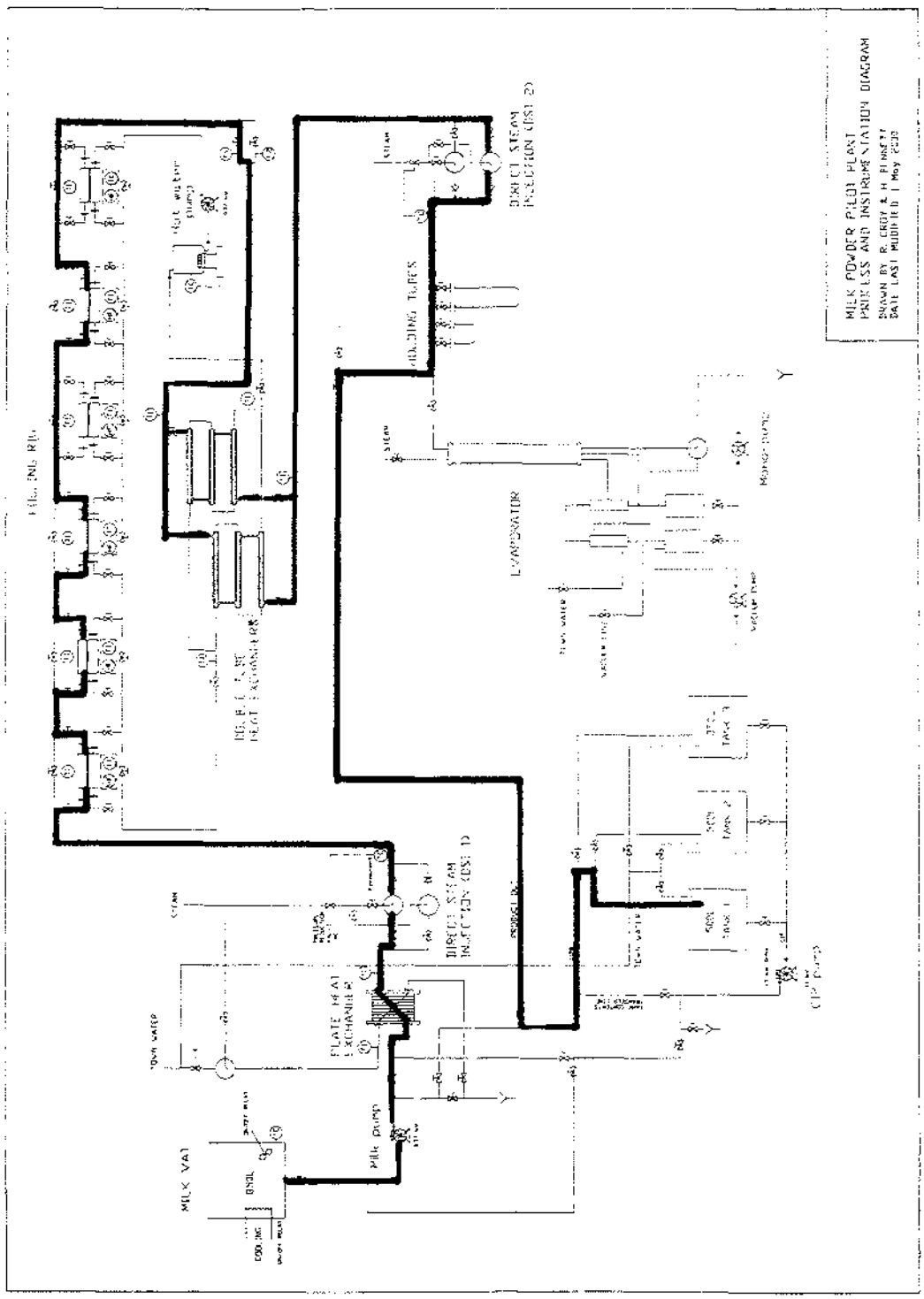

Figure 4.21: P&ID diagram of the pilot plant showing the path taken by milk during milk processing.

Removing plates from fouling modules during processing.

This simply involved isolating fouling module from both the process flow and the hot water flow. Other parameters of the plant did not have to be altered to do this. Then the plate could be removed from the fouling module and inspected. If a plate was removed more than two hours before the end of a milk run then a new clean plate could be installed in the fouling module to develop another fouling layer.

Shutting down milk processing.

- Milk pump and hot water pump stopped.
- If the Direct Steam Injection unit 1 was being used then the control valve would be closed.
- Steam supply to plate heat exchanger turned off. Cold water left running through the PHE.
- The valve at the outlet of the milk vat would be closed.
- Plates remaining in the fouling modules would be removed.

4.5.3 Cleaning-in-place procedure.

Preparing for cleaning-in-place (CIP).

After a fouling run the plates would be removed from each of the fouling modules inspected and sometimes photographed. During this time the hot caustic solution for CIP would be prepared. The pipe feeding hot water into the plate heat exchanger would be disconnected and attached to a hose which would be placed in Tank 2. Steam and water would be mixed using the plate heat exchangers DSI to provide water at 85°C to Tank 2. When Tank 2 contained approximately 300L of hot water the hose would be removed and the depth of the water measured to determine its exact volume. This volume would then be used to calculate the amount of concentrated caustic soda required to provide a solution of predetermined caustic concentration (usually 1.0% w/w). The caustic used to dose the water was of 50% concentration (765g NaOH/L) supplied by Orica Chemnet. Tank 3 would be filled with cold water giving 350L of rinse water. The hot water supply to the PHE would then be reconnected and the hose put away.

Selected fouled plates would be prepared by reapplying a heat flux sensor if necessary.

CIP cleaning steps.

The cleaning process involved two general sections; the caustic clean and the nitric clean. Each section would have a water rinse before and after the wash.

The caustic clean.

Preparation of the caustic was discussed in section 4.5.3 (p. 92). Following the caustic preparation Tank 2 would contain 350L of 1.0% w/w caustic at 75°C. Tank 3 would contain 350L of cold water.

- The fouled plates with heat flux sensors attached would be installed in the fouling modules. The control computer would then be examined to determine if the HF sensors and process temperature sensors in the fouling modules were functioning properly.
- Control flow valves throughout the plant would be set for CIP. The path of the CIP solutions through the plant are shown in Figure 4.5. Initially the tank supplying the CIP pump would be Tank 3; the rinse water tank.
- *Pre-caustic rinse - Rinse 1.* Both the CIP pump and the milk pump were set manually to their maximum speed of 50Hz and then switched on. The flowrate monitored to ensure that a flow developed.
- Then the steam supply to the plate heat exchanger would be fully opened to provide heating of the rinse water from room temperature to 35-40°C. A check would then be made to ensure that the rinse water was flowing into tank 1.
- The rinse would last until approximately 200L of water had passed through the plant. This was about half of the water in Tank 3 and provided a rinse time of around 4 minutes.
- *Caustic wash.* When the rinse was finished the flow being feed to the CIP pump would be switched from the Tank 3 to the hot caustic in Tank 2. The steam supply to the PHE would then be turned off and the CIP return valves set to return the hot caustic to Tank 2 so that it would be recycled.

- Recycling of the caustic solution would continue for approximately 15 minutes or until the measured overall heat transfer coefficient in the fouling modules had levelled out. The temperature of the caustic solution would remain constant during the clean as heat lost through the piping would be made up with the heat gained by the caustic solution in the fouling tubes.

- If the water level in Tank 3 was too low for the up-coming rinse or a longer post-caustic rinse was required additional water could be added to the tank during the caustic wash.

- *Post caustic rinse - Rinse 2a.* To put the system back on to water rinse the fluid supply to the CIP pump was switched from the caustic in Tank 2 back to the rinse water in Tank 3. The steam supply to the plate heat exchanger would be fully opened to provide heating for the rinse water. The rinse would end when the supply of water in Tank 3 was exhausted.

The nitric clean.

- *Preparation of the nitric solution.* At this point the cleaning process would be stopped while hot nitric acid was prepared in Tank 2. Tank 2 would be rinsed to remove any remaining caustic and then the hot water supply would be disconnected from the PHE and connected to a hose .

- Tank 2 would be re-filled with about 300 litres of hot water and the water depth measured so that the amount of concentrated nitric acid required could be calculated. The concentration of nitric acid used for the nitric washes was 0.5% w/w. The necessary quantity of concentrated nitric acid would be added to the Tank 2 and the mixture manually stirred to ensure good mixing.

- Tank 3 would be re-filled with cold tap water.

- *Pre-nitric rinse - Rinse 2b.* From this point the nitric clean would be a repeat of the method used for the caustic clean. Another rinse would initially done for a further minute so that the change from water to nitric acid could be accomplished with a continuous flowrate.

- *Nitric wash.* The hot nitric solution would be recycled through the plant for about 10 minutes.

- *Final rinse - Rinse 3.* Supply to CIP pump switched from nitric (Tank 2) to rinse water (Tank 3). Rinse for 5 minutes.

- Following this the fouling modules could be unpacked and the plates inspected.

4.5.4 Effect of process fluid thermophysical properties.

All of the thermophysical properties experiments were performed using a similar experimental procedure.

- Before the experiment the plant would be cleaned if it was not already so. Then a clean plate would be installed in fouling module 2 with a heat flux sensor attached.

- The solution being tested would be prepared in Tank 3 at room temperature and well mixed in the tank by hand.

- The hot water tank would be set to 90°C and then and the circulation started.

- Flow direction of the process fluid would be set as for cleaning-in-place with supply to the CIP pump coming from Tank 3 and the CIP return line pointing back to Tank 3. Therefore the process fluid would be recycled through the plant.

- The CIP pump would be set to a speed setting of 86% of its maximum speed. (This was known from experience to be suitable). The milk pump would be set to automatic control at a process fluid flowrate of 1.0 m^3/hr.

- The fouling module containing the test plate would then be open to both the process fluid flow and the hot water flow.

- The temperature of the hot water entering the plate heat exchanger would then be set to approximately 60°C such that the temperature of the process fluid leaving the PHE was at 45°C. Because the warm water was being pumped back into Tank 3 the temperature of the fluid in that tank would rise resulting in an increasing temperature of the process fluid entering and then leaving the plate heat exchanger.

- The temperature of the process fluid would increase at about 1°C per minute. The temperature of the process fluid would be allowed to rise until it reached 85°C at which point the small temperature difference of across the plate would lead to increasing noise in the data.

- Upon reaching 85°C the steam applied to the hot water supply of the PHE would be turned off so that 25°C water would be passing though its utility side.
- This cooling process would be continued until the temperature of the process fluid in tank 3 was less than 40°C. At this point the composition of the CIP fluid could be adjusted, usually by adding caustic, nitric or soil, to increase the concentration of the CIP solution. Then the process would be repeated with the new process fluid composition.

4.5.5 Details of experimental procedures

Effect of nitric concentration

- Run number 3
- HF sensor installed in fouling module 2.
- Water circulated. Water heated to 85°C then cooled back to < 40°C.
- 2% w/w nitric solution circulated. Solution heated to 85°C then cooled back to 40°C.
- 6% w/w nitric solution circulated. Solution heated to 85°C then cooled back to < 40°C.

Effect of caustic concentration

- Run number 38.
- Water circulated. Water heated to 85°C then cooled back to < 45°C.
- 2% w/w caustic solution circulated. Solution heated to 85°C then cooled back to < 45°C.
- Data for lower temperatures was quite curved which was not expected. This may possibly have been due to the mixing of caustic with rinse water remaining in the plant at the beginning of the run. The solution was cooled back to 45°C and heated to 55°C.
- 4% w/w caustic solution circulated. Solution heated to 85°C then cooled back to < 40°C.
- 6% w/w caustic solution circulated. Solution heated to 85°C then cooled back to < 40°C.

Effect of soil concentration

- Run number 32.
- Monitored plates installed in fouling modules 1-3. Fouling modules 1 and 2 contained HF sensors 1 and 2 respectively (as normal). Fouling module 3 contained HF sensor 5.
- Water circulated. Water heated to 85^{o}C then cooled back to $< 40^o$C.
- Six (6) litres of soil retentate added to 117 litres of water in Tank 3. Solution heated to 85^{o}C then cooled back to $< 40^o$C.
- A further 6 litres of soil retentate added to Tank 3. Solution heated to 85^{o}C then cooled back to $< 40^o$C.
- Put about 200 litres of water in Tank 2. Water circulated through plant until the temperature reached 85^{o}C. This was done to check the data from the first water run.
- A further 6 litres of soil retentate added to Tank 3. Solution heated to 85^{o}C then cooled back to $< 40^o$C.

Video of cleaning-in-place.

- Special process fluid fouling module chamber with a perspex window on the upper side was put in place of the standard process fluid fouling module chamber for module 6.
- A 3Com WebCam digital camera was positioned above the fouling module looking down into the process fluid chamber. The WebCam was connected to a laptop micro-computer. A light was positioned above the fouling module to light the fouled plate.
- A photo of the fouled plate chosen for the experiment was taken using the digital camera (Kodak DC290).
- A fouled plate with a HF sensor attached was installed in the fouling modules using the normal procedure.
- Tank 3 was filled with tap water. Tank 2 was filled with about 300 litres of hot caustic (1.0% at 65°C).

- The CIP cycle would then be performed using essentially the same method described in section 4.5.3. Modifications to the general procedure are listed below.
  - Only a caustic wash was performed. The total cleaning cycle was kept to within 10 minutes so that the digital video file would not become unmanageably large.
  - The water rinse 1 was set to be 2 minutes long.
  - The caustic wash was 6 minutes long.
  - The water rinse 2 was about 2 minutes long.
  - A process flows (water rinses and caustic) were once-through only, i.e. no recycling.
  - The rinse was begun with the fouling module opened up to the process flow. The beginning of the water rinse was therefore marked by the starting of the CIP pump and the milk pump.

Chemical Analysis.

A chemical analysis was made of the concentrated retentate to determine its protein, fat and caustic content.

Protein analysis. The Kjeldahl method was used to determine the protein content of the retentate. A 1 g sample of retentate was used for each test. Details of this procedure are given in appendix D.2.

Fat analysis. The Mojonnier method was used determine the fat content of the retentate. 5 g samples were used to for each of the tests. Details of the procedure used are given in appendix D.1.

Caustic content. The caustic concentration of the retentate was determined by titrating a sample against 0.1M HCl with bromothymal blue as an indicator. Details of the procedure and results are given in appendix D.2.6.

Chapter 5

Results and Discussion

5.1 Mathematical Analysis

5.1.1 Heat transfer coefficient normalisation.

Heat transfer coefficient data was normalised so that comparisons could be made between HTC traces of plates measured in different modules. It was not possible to obtain reproducible probe attachments for experimentation. Each experimental plate would have a different HTC for a given set of process conditions due to variations in the following parameters.

- Variation in the thickness (x_{HTP}) of the layer of heat transfer paste (HTP) between the HF sensor and the plate. Each time a HF sensor was attached to a plate a layer of aluminium tape would be applied on top of the HF sensor to hold it to the plate. Variations in the pressure that the tape applied to the HF sensor would cause variations in the thickness of the layer of heat transfer paste. This would alter the resistance of the heat transfer paste layer, R_{HTP}:

$$R_{\mathrm{HTP}} = \frac{x_{\mathrm{HTP}}}{\lambda_{\mathrm{HTP}}} \tag{5.1}$$

  Where: x_{HTP} = thickness of the heat transfer paste layer (m)

  λ_{HTP} = thermal conductivity of the heat transfer paste (W/mK)

- Variation in the position of the HF sensor within the fouling module. This could affect the process fluid convection resistance (R_p) due to entrance effects in the short

fouling module.

- Variation in the resistances of the different HF sensors (R_s). HF sensor resistance would remain constant over time but individual probes may have different heat transfer resistances.

The HTC traces were normalised by first taking the value of the HTC (U) at the end of the post-cleaning rinse. If only a caustic wash was performed then this would be the value of HTC at the end of the post-caustic rinse (Rinse 2). If a complete cleaning cycle was performed the value of the HTC would be taken at end of the post-nitric rinse (Rinse 3). This final HTC was defined as U_{inf}. It was assumed that the plate was clean at this point and therefore the HTC is that of the clean plate only with no fouling resistance:

$$\frac{1}{U_{\text{inf}}} = R_s + R_{\text{HTP}} + R_{\text{wall}} + R_p \tag{5.2}$$

Where: U_{inf} = heat transfer coefficient of the flow system at the end of the final water rinse. ($\text{W/m}^2\text{K}$)

Each value of U during the run would then be divided by this final HTC:

$$U_n = \frac{U}{U_{\text{inf}}} \tag{5.3}$$

Where: U_n = Normalised overall heat transfer coefficient.

The assumption that there is no fouling remaining on the plate during the final rinse was found not always to be true. Section 5.4.4 (pg. 128) discusses this.

5.1.2 Temperature compensation of traces

To provide a temperature correction process that could be applied to all fouling modules, data from water runs on a clean plate were analysed using linear regression. Figure 5.1 shows a plot of the data used. For each clean plate the HTC was measured for water at over a temperature range of 40 to 80°C at a constant flowrate of $1.0\text{m}^3/\text{s}$. Details of the experimental method used are given in section 4.5.4. Before the regression analysis was done each of the data sets were normalised so that U would be equal to 1.0 at 60°C.

$$U_{nt} = \frac{U}{U_{60}} \tag{5.4}$$

Where: U_{nt} = HTC normalised to 60°C

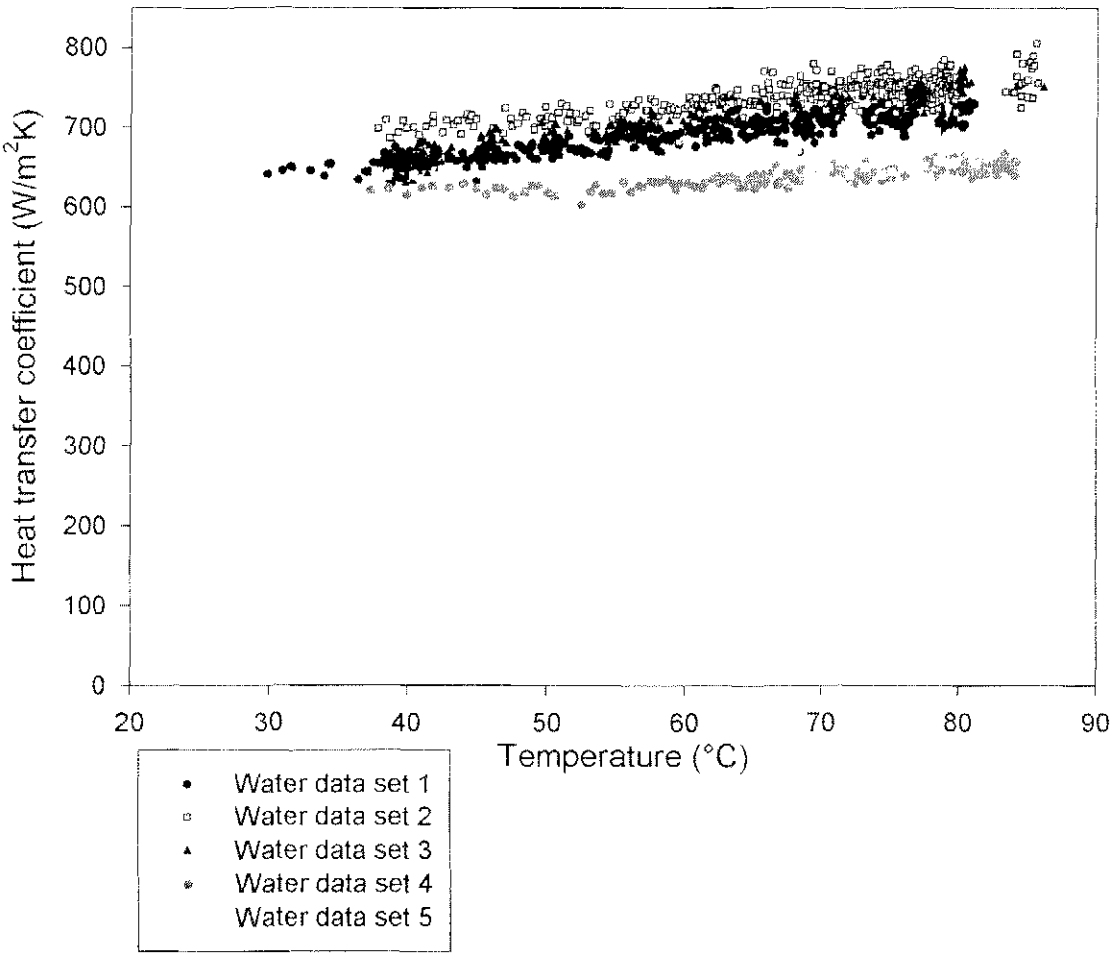

Figure 5.1: Plot of HTC against temperature for water moving across a clean plate. The data is from five separate runs.

U = heat transfer coefficient (W/m^2K)
U_{60} = HTC at 60°C. (W/m^2K)

Because the response of the HTC to temperature is approximately linear between 30 and 90°C a linear regression was made on each of the normalised data sets.

Run number	Gradient	Intercept
1	0.002376	0.841
2	0.001980	0.881
3	0.003408	0.798
4	0.001393	0.919
5	0.001190	0.918

The mean of the the five gradients and the five intercepts were then calculated. The resulting mean coefficient and intercept provided a correlation for a temperature correction factor (TCF):

$$\text{TCF} = 0.002069.\theta_p + 0.8713 \tag{5.5}$$

A temperature corrected HTC value (U_{tc}) could then obtained by dividing each HTC data point by its respective TCF:

$$U_{tc} = \frac{U}{\text{TCF}} \tag{5.6}$$

Figure 5.2 shows an example of a fouled plate trace with and without the temperature correction factor (TCF). The initial rapid increase in both traces is due to the removal of fouling from the plate. After the 6th minute the black trace (no temperature compensation) is almost level during each subsequent phase of the cleaning process with step changes due to temperature changes as the process fluid is changed (caustic at 70°C, water at 33°C, nitric acid at 65°C and water at 33°C).

The grey trace (with temperature compensation) shows no step changes between phases of the cleaning process. Equation 5.5 provides a convenient empirical approximate method for temperature compensation. This is not fully accurate because it is based an assumption that will not always be true. For a temperature range of 30 to 90°C is assumed that the only the process fluid HT resistance (R_p) is affected by temperature and that other resistances (except R_f) do not change between runs. Because it was not possible attach a HF sensor to a plate in a reproducible manner the resistance of the HT paste (R_{HTP}) would vary between runs. If the resistance of the HTP changed with temperature then the total resistance R_T would involve at least two variables R_p and R_{HTP} and equation 5.5 would not adequately compensate for both.

A more rigorous method for compensating for temperature was not developed as it would have involved measuring the value of R_p and the sum of R_s, R_{HTP} and R_{wall} (defined as R_c).

$$R_c = \frac{1}{U_c} = R_s + R_{\text{HTP}} + R_{\text{wall}} \tag{5.7}$$

A method for estimating R_c is given in section 5.2.1 but it was not directly measured.

5.2 Effect of changing properties of the process fluid on the heat transfer coefficient trace.

The effect of changing fluid thermophysical properties in the CIP stream was investigated in order to determine whether compensations to the HTC trace would be required to account for changes in the thermophysical properties of CIP fluids during cleaning.

5.2.1 Effect of process fluid temperature

The experimental data in Figure 5.1 was compared with calculations from heat transfer theory. An equation for calculating the heat transfer coefficient (HTC) within a circular duct under turbulent forced convection was used to calculate the process fluid HTC (h_p) (Perry and Green, 1984).

$$Nu = 0.036 Re^{0.8} Pr^{\frac{1}{3}} (L/D_H)^{-0.054} \tag{5.8}$$

Where: Nu = Nusselt number (dimensionless)
Re = Reynolds number (dimensionless)
Pr = Prandtl number (dimensionless)
L = Length of the duct (m)
D_H = Hydraulic diameter of the duct (m)

U_c is then defined as the the sum of all the HT resistances that are assumed to remain constant during an experimental run:

$$\frac{1}{U_c} = R_s + R_{\text{HTP}} + R_{\text{wall}} \tag{5.9}$$

The total resistance to heat transfer is therefore:

$$\frac{1}{U} = \frac{1}{U_c} + \frac{1}{h_p} \tag{5.10}$$

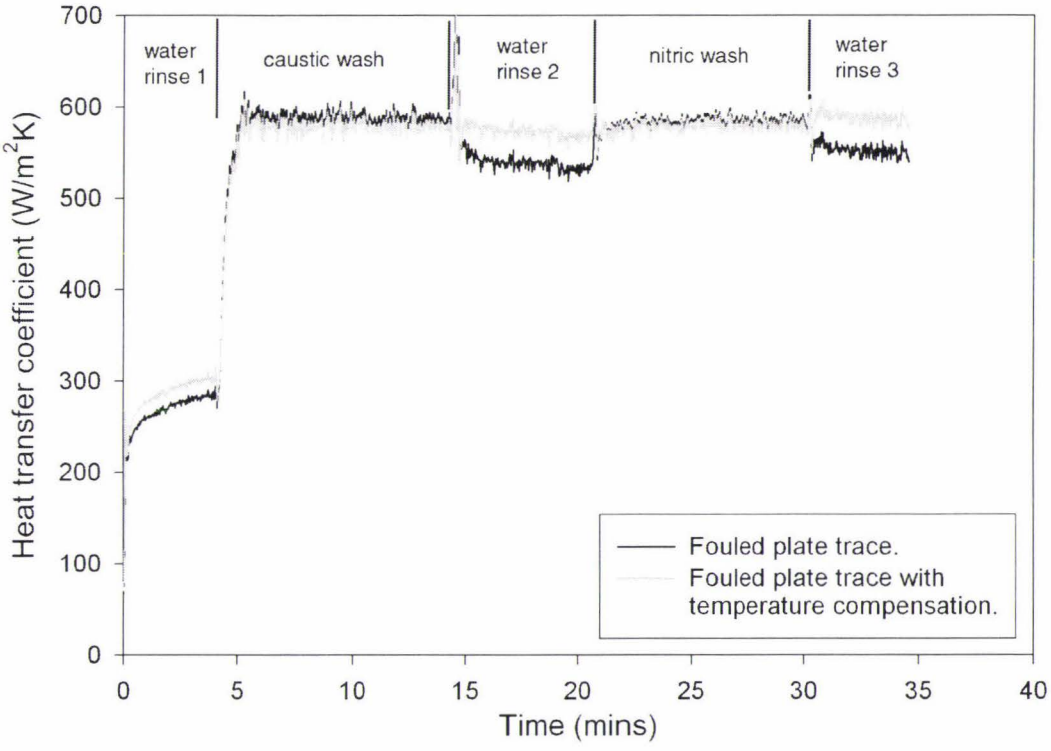

Figure 5.2: Comparison of two CIP monitor traces (Module 1, Run 30) with and without the temperature correction factor (TCF). (A) Traces without temperature correction. (B) Traces with TCF.

and

$$\frac{1}{U_c} = \frac{1}{U} - \frac{1}{h_p} \tag{5.11}$$

A sample calculation of the HTC is given in appendix B.1. The value of U_c was calculated using the experimental measurement of U at 60°C and an estimate of h_p from equation 5.8. For example if $U = 696$ at 60°C then U_c will be:

$$\frac{1}{U_c} = \frac{1}{696} - \frac{1}{2245.5} = \frac{1}{1008} \tag{5.12}$$

If it is assumed that the value of U_c remains constant for a temperature range of between 30 and 90°C then the response of the total heat transfer coefficient (U) to temperature changes can be calculated using theoretical values of h_p at different temperatures. Values of h_p for water at temperatures of 30, 40, 50, 60, 70, 80 and 90°C were calculated using eqn. 5.8.

Table 5.1: Table of calculated h_p values for temperatures from 20 to 90°C.

Temperature °C	20	30	40	50	60	70	80	90
Viscosity Pa.s	1.00E-03	7.98E-04	6.54E-04	5.48E-04	4.67E-04	4.05E-04	3.55E-04	3.16E-04
Density kg/m^3	998	996	992	998	983.3	997	971	965
Cp J/Kg.K	4182	4179	4179	4181	4185	4191	4198	4207
k W/mK	0.603	0.618	0.632	0.643	0.653	0.662	0.67	0.676
Re	11,526	14,443	17,552	21,074	24,365	28,487	31,651	35,338
Pr	6.95	5.40	4.32	3.56	2.99	2.56	2.22	1.97
L/D^-0.054	0.963988	0.96399	0.96399	0.96399	0.96399	0.96399	0.96399	0.96399
Nu	117.5848	129.458	140.547	152.52	161.619	173.937	180.477	189.179
hp	**1508.588**	**1702.24**	**1889.91**	**2086.6**	**2245.47**	**2449.93**	**2572.75**	**2720.96**

The results calculated are shown in Figure 5.3. The gradient of the predicted data matches closely the measured data. This shows that the estimation of U_c is quite accurate and that heat transfer theory predicts the effect of process fluid temperature changes of the HTC well.

The results show that the overall heat transfer coefficient is significantly affected by changes in the temperature of the process flow. The overall HTC increases by about 15% from a temperature of 30°C to 85°C. This caused step changes in the measured HTC during CIP experiments as the temperature of the rinse water was typically 35°C lower than the caustic and nitric wash fluids.

Note that the simpler temperature compensation from equation 5.6 was used in Figure 5.2 and proved adequate. As discussed in section 5.1.2 a simpler approximate correlation for temperature, equation 5.5 was developed for compensation of HTC during

operation.

5.2.2 Effect of soil concentration in the caustic solution.

Soiled caustic solutions were passed over a clean plate installed in fouling module 2 to determine the effect of soil on the heat transfer coefficient (HTC). The soil used was the retentate of a separation process used to recover caustic from used CIP caustic solutions. The retentate contained a mixture of water, milk fouling soil and caustic soda. The composition of the retentate was 10.6% protein, 0.96% caustic and 0.74% fat (all by weight). Details of this chemical analysis are given in appendices D.1.5, D.2.5 and D.2.6.

The retentate was used to dose water in tank 3 with soil to create three solutions with increasing concentrations of soil and caustic. Table 5.2 shows the composition of each of the soiled solutions used in this experiment.

Table 5.2: The composition of the soiled solutions used in the Soil Effect experiments

Name	Protein content (%)	Fat content (%)	Caustic content (%)
Soil level 1	0.52%	0.036%	0.05%
Soil level 2	0.99%	0.069%	0.09%
Soil level 3	1.41%	0.099%	0.13%

Figure 5.4 (Run 32) shows a plot of the HTC of each of the three soiled solutions and water over a temperature range of 40 to 85°C. The figure provides a comparison of three soiled solutions against water. The HTC traces of the soiled solutions vary slightly from that of water at lower temperatures (lower than 50°C) but this difference is very small. At temperatures above 50°C where CIP cleaning usually occurs there is no significant difference between the heat transfer coefficients of the soiled caustic solutions and water.

This result suggests that the inclusion of milk solids in the caustic cleaning solutions during the wash will not cause significant deviations in the HTC trace.

5.2.3 Effect of nitric acid concentration.

The effect of the addition of nitric acid the CIP solution on the HTC was investigated to determine whether the process fluid heat transfer resistance (R_p) was significantly affected by the presence of nitric acid. A clean plate with a HF sensor attached was installed in module 2 to measure the HTC. The heat transfer coefficient of water from 40 to 85°C was first measured to provide a baseline for comparisons with the nitric acid solutions. Details of the plant operations during CIP experiment are given in section 4.5.5 (page 96).

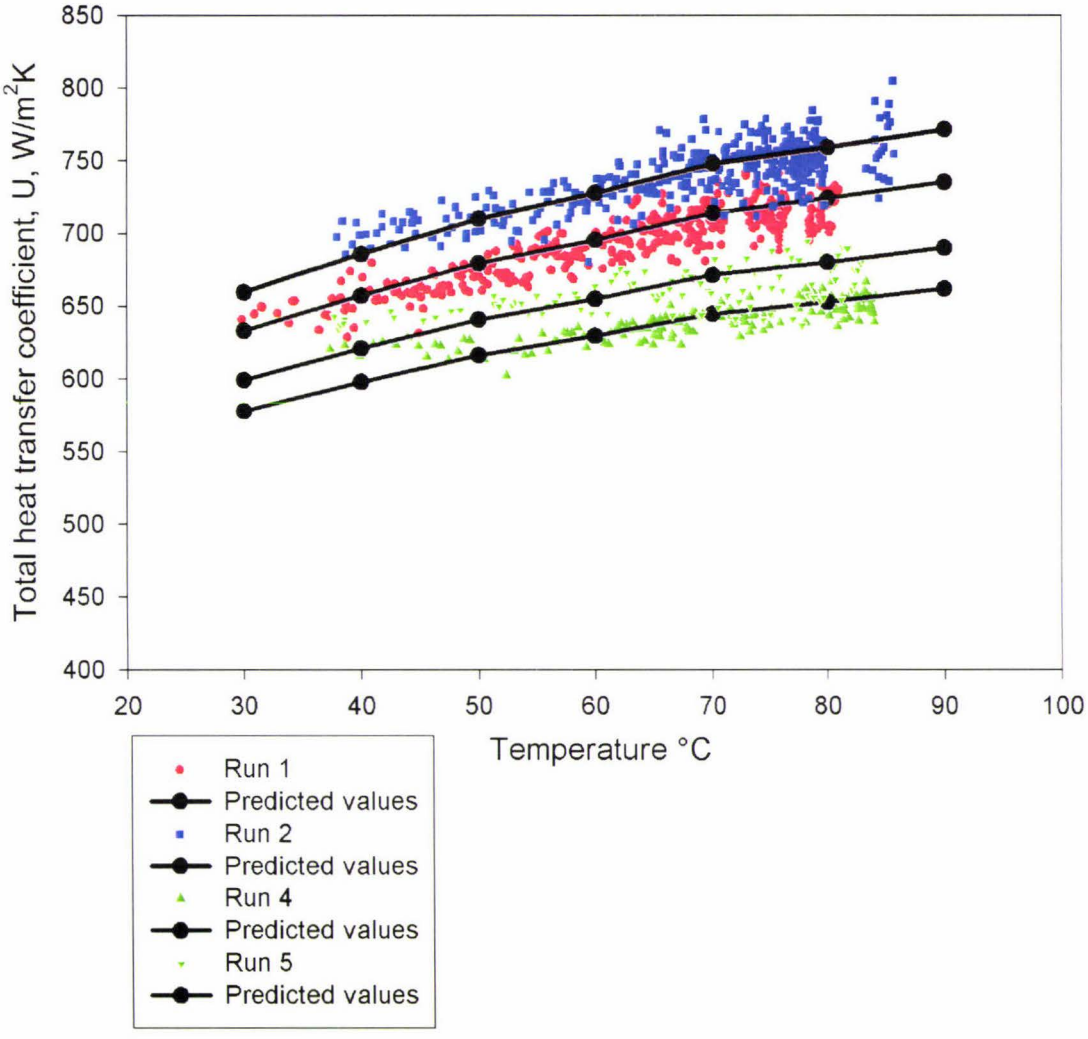

Figure 5.3: Plot of HTC (U) against temperature for four water runs. Predicted values of U are also shown for each water run. Water run 3 has been removed as the data overlaps run 2 making the plot too cluttered.

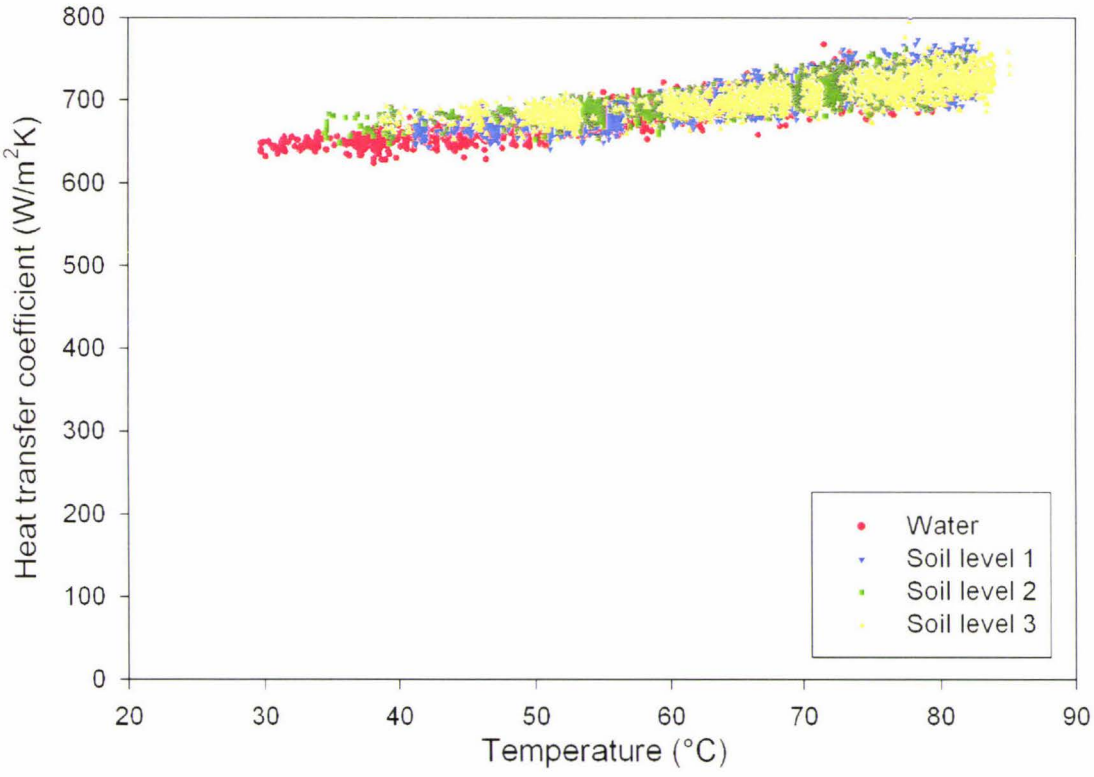

Figure 5.4: Plot of HTC against temperature for 4 solutions containing increasing concentrations of soiled caustic (retentate).

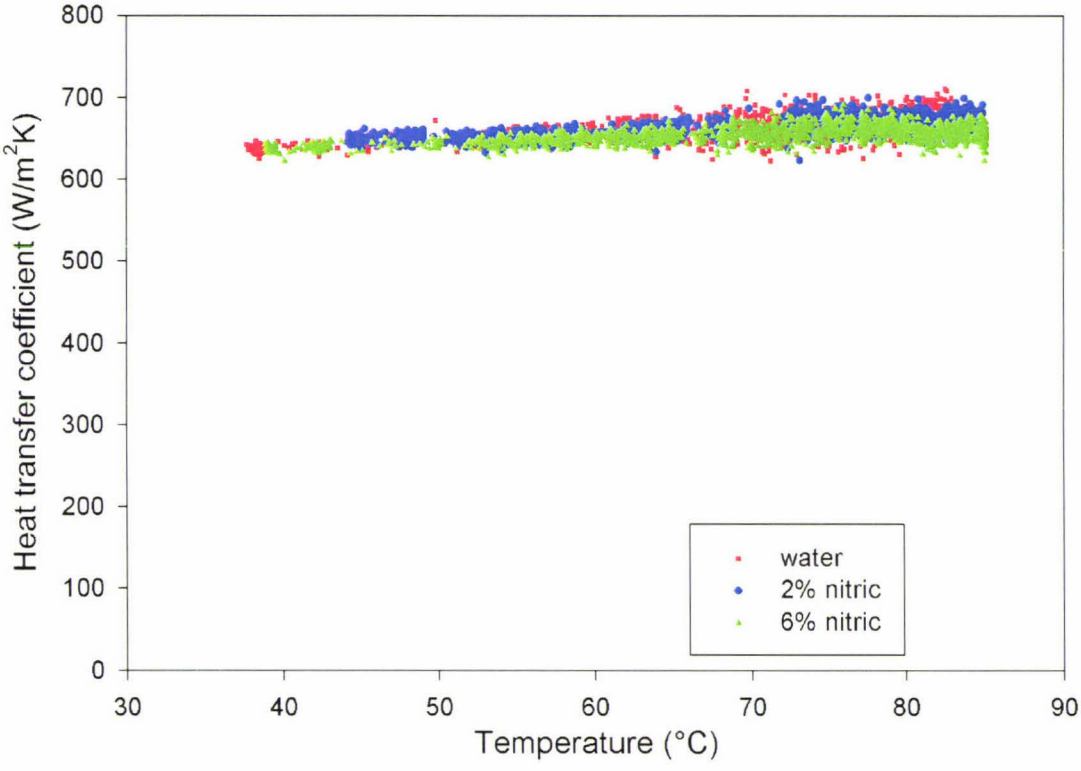

Figure 5.5: Plot of HTC against temperature for 3 solutions containing increasing concentrations of nitric acid.

Figure 5.5 (Run 33) shows the HTC of the three solutions containing 0%, 2% and 6% nitric acid respectively over a temperature range from 40 to 85°C. No significant difference can be seen seen between the 2% nitric solution and water. There may be a very small reduction in HTC for nitric concentrations of 6% at high temperatures but this difference is very small and a concentration of 6% nitric acid is higher than the values used in most milk powder plants which typically introduce nitric acid solutions into the plant at around 0.5%.

5.2.4 Effect of caustic concentration

The effect of caustic soda concentration on the HTC was investigated using three caustic solutions: 2%, 4% and 6% w/w. The caustic solutions were passed over a clean plate installed in fouling module 2. Details of the experimental method used are given in section 4.5.5.

Figure 5.6 (Run 38) shows a plot of HTC against temperature for three caustic solutions compared against water. It can be seen that the addition of caustic to the solution lowers the HTC only slightly for a temperature range of 45 to 75°C. At 60°C the HTC of 2% caustic was 5% lower than the HTC of water. There is no significant difference between the HTCs of the four solutions at temperatures greater than 75°C.

The results suggest that a small decrease in the HTC will be seen when caustic is added to the CIP solution and the temperature of the caustic solution is less than 75°C. A compensation method for this effect was not developed because the effect is quite small and the effect appeared not to vary greatly with increases in caustic concentration of 2% to 6%. A small step change in the HTC during caustic cleaning would not greatly affect the interpretation of the CIP monitor trace as it would not prevent the determination of cleaning rate (slope) or cleaning time of the fouled surface.

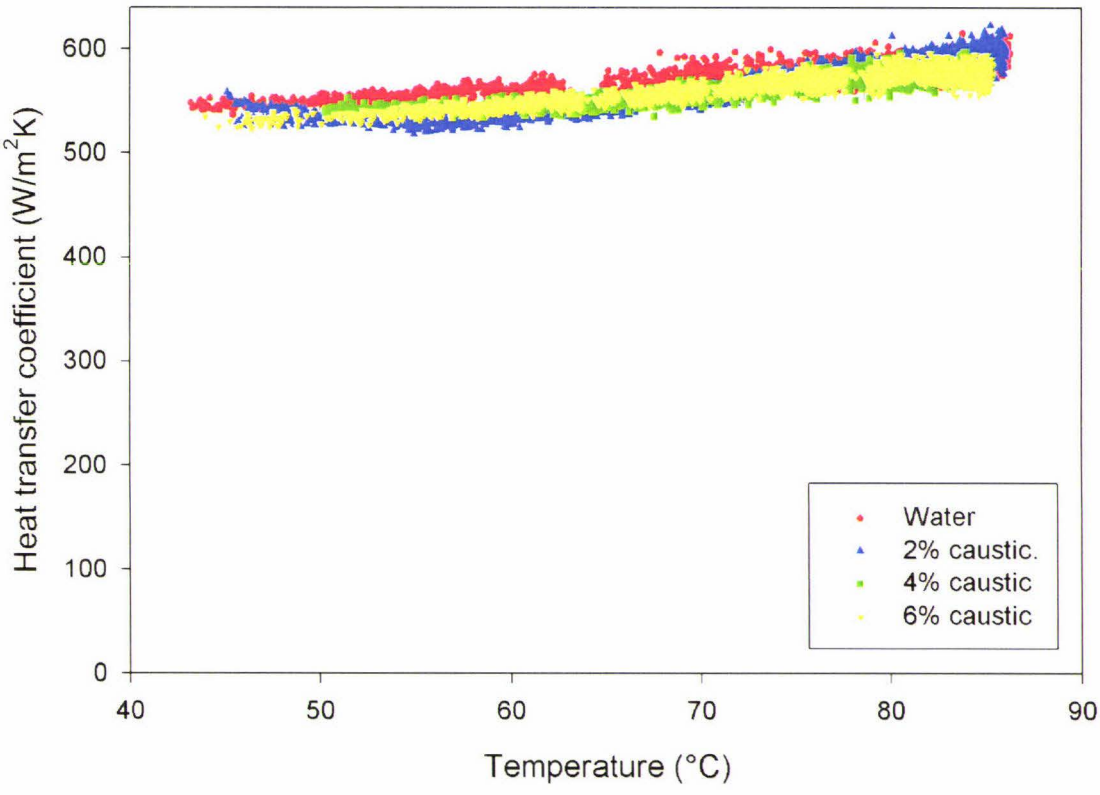

Figure 5.6: Plot of HTC against temperature for 4 solutions of increasing concentrations of caustic.

5.3 Effect of flowrate on HTC.

The effect of flowrate on the HTC was measured using a clean plate, with a HF sensor attached, installed in fouling module 1. The HTC of the clean plate system was measured for 2% caustic, 2% nitric, soiled caustic (Level 1, 0.52% protein, 0.036% fat and 0.34% caustic) and water. The temperature of all solutions was kept as constant as possible so that temperature effects on the HTC would be kept to a minimum. The actual temperature of the process fluids varied between 19 and 24°C during experimentation. The flowrate of the process fluid was reduced gradually from the maximum flowrate of 1.5m^3/s to 0.4m^3/s.

Figure 5.7 (Run 39) shows a plot of the heat transfer coefficient of the four CIP fluids over a range of flowrates. The plot shows that the HTC increased with flowrate. Variation between the HTC profiles of the four fluids was very small. Only the soiled caustic solution had a significantly lower profile than the other CIP solutions and this difference was only seen at flowrates below 1.0m^3/hr. The response of the HTC to flowrate diminished with increasing flowrate. The HTC is not strongly affected by flowrate in the upper region of the plot where CIP experiments were conducted.

Theoretical predictions of the HTC for different flowrates in the turbulent region were made using equation 5.8. An example calculation is given below.

Example calculation.

Fouling module properties. Dimensions: 0.022m x 0.026m x (L) 0.047m. Hydraulic diameter:

$$D_H = \frac{\text{4x cross sectional area}}{\text{wetted perimeter}} = \frac{4(0.022)(0.026)}{2(0.022)+2(0.026)} = 0.02383\text{m} \qquad (5.13)$$

Water properties.

The properties of water at various temperatures were taken from Cooper and Le Fevre (1975). For water at 20°C:

Viscosity	(μ)	$= 1.003 \text{ x } 10^{-3}$ Pa.s
Density	(ρ)	$= 998$ kg/m^3
Specific heat capacity	(C_p)	$= 4182$ J/kgK
Thermal conductivity	(k)	$= 0.603$ W/mK

Volumetric flowrate for a flow velocity of 0.5 m/s:

$$Q = (\text{cross sectional area})(u) = (0.022)(0.026)(0.5)(3600 \text{ sec/hr}) = 1.0296 \text{ m}^3\text{/hr} \qquad (5.14)$$

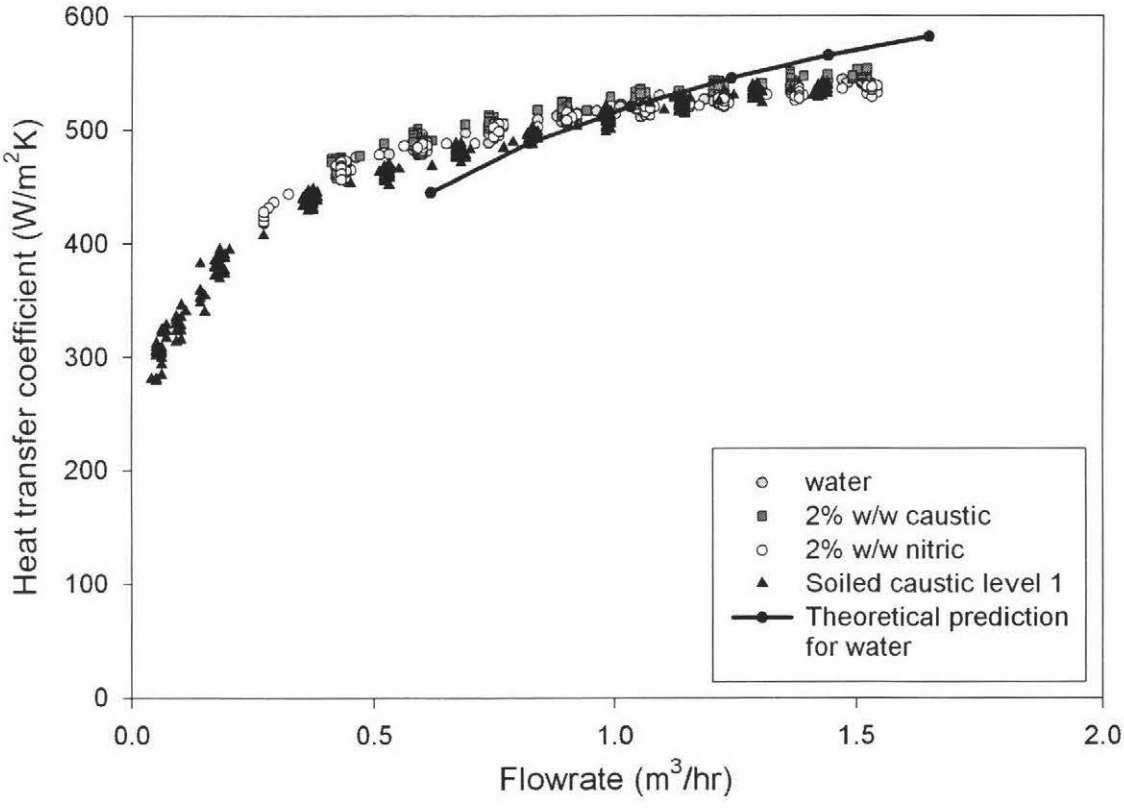

Figure 5.7: Plot of HTC against flowrate for four fluid types used in CIP. A theoretical prediction for water is also plotted.

Reynolds number:

$$Re = \frac{\rho u D_H}{\mu} = \frac{(998)(0.4856)(0.02383)}{1.002 \text{ x } 10^{-3}} = 11,867 \tag{5.15}$$

$$Pr = \frac{C_p \mu}{k} = \frac{(4182)(1.002 \text{ x } 10^{-3})}{0.603} = 6.95b \tag{5.16}$$

$$L/D_H = \frac{0.047}{0.02383} = 1.972 \tag{5.17}$$

$$Nu = 0.036(11,867^{0.8})(6.95)^{\frac{1}{3}}(1.972^{-0.054}) = 120.36 \tag{5.18}$$

The heat transfer coefficient of the process fluid can be calculated from the Nusselt number (Nu):

$$h_p = \frac{Nu.k}{L} = \frac{(120.36)(0.603)}{0.047} = 1544.3 \text{ W/m}^2\text{K} \tag{5.19}$$

The total resistance to heat transfer is therefore:

$$\frac{1}{U} = \frac{1}{U_c} + \frac{1}{h_p} \tag{5.20}$$

If the theoretical value of h_p is assumed to be accurate then U_c can be calculated using the experimental value of U at a single flowrate. This estimation of h_p at a flow velocity u of 0.5 m/s was used to calculate an estimation of U_c (the heat transfer resistances that remain constant during experimentation, defined on pg. 103).

$$U = 520.63 \text{ W/m}^2\text{K at u } = \text{ 0.5 m/s} \tag{5.21}$$

$$\frac{1}{U_c} = \frac{1}{U} - \frac{1}{h_p} \tag{5.22}$$

$$\frac{1}{U_c} = \frac{1}{520.63} - \frac{1}{1544.3} = \frac{1}{785.4} \tag{5.23}$$

Then

$$\frac{1}{U} = \frac{1}{785.4} + \frac{1}{h_p} \tag{5.24}$$

Estimates of U for flow velocities of 0.4, 0.5, 0.6, 0.7 and 0.8 m/s are shown in Table B.1 in the Appendix and plotted against the experimental data in Figure 5.7 (pg. 113).

The gradient of the predicted response of U to temperature is greater than the measured response. This means that the theoretical equations used do not predict the

response of U to flowrate accurately. The equation used was recommended for values of (L/D) greater than 10 (Perry and Green, 1984 pg. 10-17). The length of the fouling module is very short with an (L/D) value of just 2.0. The equation may not therefore fully take account of entrance effects within the fouling module.

5.4 Sensitivity of the HF sensor to the presence of fouling.

A series of experiments were conducted to develop techniques for interpreting the HTC trace during CIP in terms of kinetics and the efficiency of cleaning.

5.4.1 Comparison of the traces of clean and fouled plates.

Two fouled plates were installed in fouling modules alongside a clean plate during a complete CIP run. The clean plate was present to provide a comparison between the HTC of a plate without fouling compared to those with fouling initially present. The heat transfer resistance of the clean plate would be equal to the sum of the following resistances:

$$\frac{1}{U} = R_s + R_{\text{HTP}} + R_{\text{wall}} + R_p \tag{5.25}$$

The heat transfer resistance of the fouled plates would be equal to the same resistances plus the resistance due to fouling (R_f).

$$\frac{1}{U} = R_s + R_{\text{HTP}} + R_{\text{wall}} + R_p + R_f \tag{5.26}$$

Water rinse 1.

Figure 5.8 shows the normalised overall heat transfer coefficient (NHTC) of each plate. The method used to calculate the NHTC is described in section 5.1.1. During the first water rinse both of the fouled plates (F1 & F2) had a lower NHTC than the clean plate (C). These low values of NHTC were due to the additional heat transfer resistance of fouling present on the plates (R_f) during rinsing. The traces of the fouled plates did not increase greatly during the water rinse indicating that little, if any, cleaning was done during the rinse. Video footage of another CIP cleaning run supports this argument. (section 5.4.3).

Cleaning rate and cleaning time.

When the CIP solution changed from water to caustic the NHTCs of both of the fouled plates began to increase steadily. The trace of F1 increased at a faster rate than that

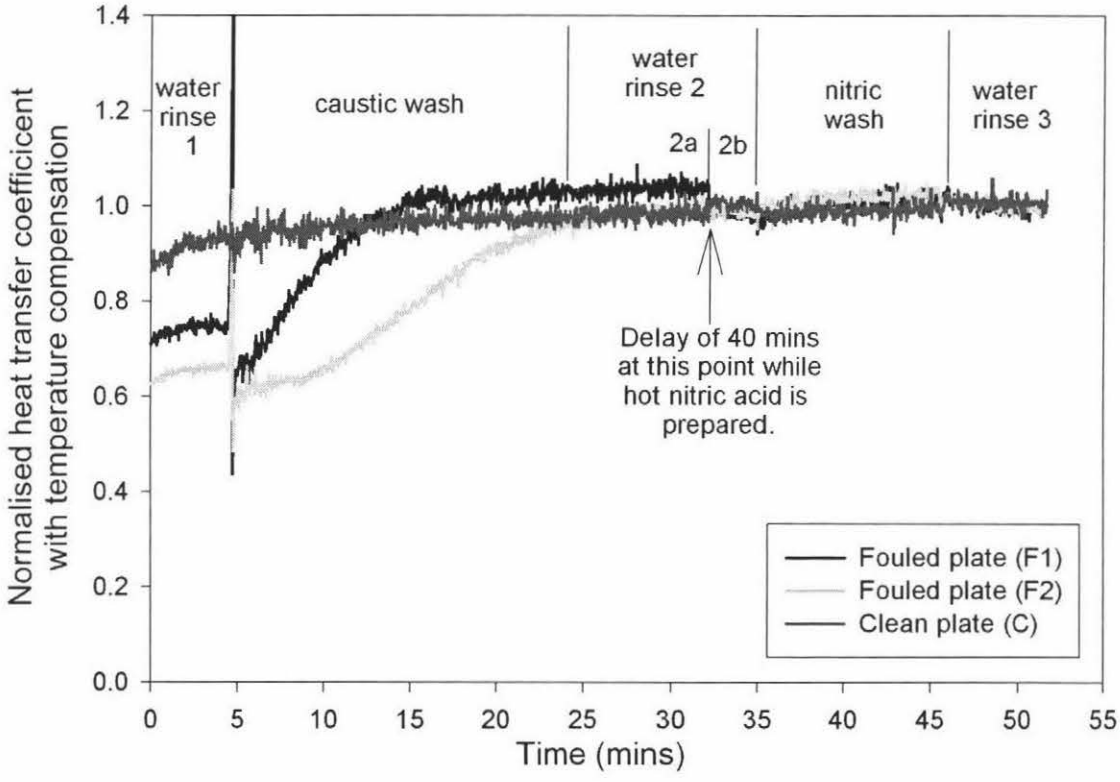

Figure 5.8: Normalised and temperature corrected HTC traces of three plates during a complete CIP cycle. Cleaning of two fouled plates (F1 & F2) and a clean plate (C).

of plate F2 indicating that fouling were removed at a faster rate. The trace of F1 began to level off quite sharply after about 16 minutes. The NHTC at this point is close to 1.0 indicating that the plate is almost clean.

The NHTC of plate 2 still increasing at the end of the caustic wash although its value was close to 1.0. This indicates that the plate F2 took longer to clean than F1. The lower NHTC of plate F2 relative to plate F1 during the first rinse indicated that it was fouled to a greater extent.

The cleaning rates of both plates were low during this caustic wash compared to other measured cleaning runs (for example Figure 5.2, pg. 104). This was possibly due to the low flowrate of 1.0 m^3/hr that was used for this cleaning run as opposed to the maximum speed of 1.4m^3/hr which was used in Figure 5.2. The lower flowrate allowed differences in cleaning rate to be observed as the cleaning rate at 1.4m^3/hr was so rapid that differences in the cleaning rates of two plates were hard to distinguish.

Post caustic rinses.

The NHTC values of all plates are close to 1.0 at the end of the caustic wash indicating that they as mostly clean. The traces of all three plates do no change much during water rinse 2, the nitric wash and the final water rinse. This shows that very little, if any, fouling is removed after the caustic wash.

5.4.2 Estimate of fouling thickness from the HTC trace.

An experiment was designed to determine if the presence of fouling could be determined using a HF sensor during CIP. This was achieved by making a comparison between clean and fouled plates during the same CIP run. Three plates were installed in three fouling modules. Two of the plates were fouled while the other was clean. A thermocouple was used to measure the temperature of the of the process fluid.

Figure 5.9 shows the heat transfer coefficient of three plates as measured during the rinses before and after cleaning. At the beginning of the CIP run two plates were covered with a fouling layer and the other was clean. All HTC traces have been normalised such that the HTC for the plate in its clean state during the final rinse is equal to 1.0.

During water rinse 1 the NHTC of the fouled plates is much lower than that of the clean plate due to the extra thermal resistance of the fouling present. The NHTC of both the clean and fouled plates remain reasonably constant during the pre-caustic rinse because water rinsing does not remove fouling solids from the plate surface. Small drifts in

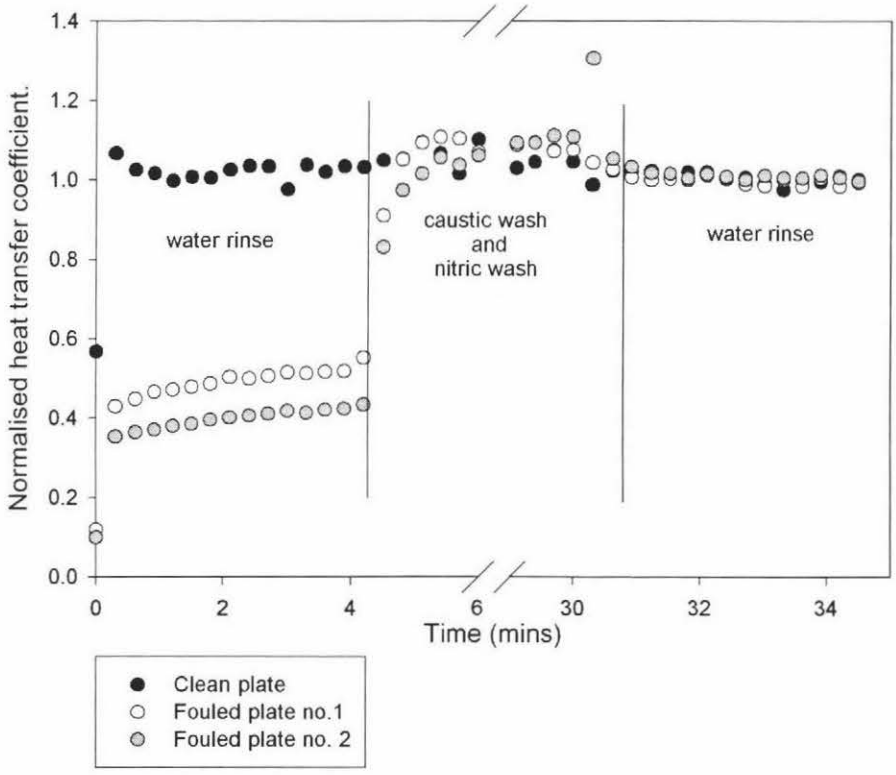

Figure 5.9: Plot of NHTC before and after cleaning. The NHTC was measured during the rinses before and after cleaning.

the NHTC of a fouled plate during cleaning may be due to either the removal of milk from the porous fouling layer or the re-wetting of a dry fouling layer. The fouled plates shown in Figure 5.9 had been in air at room temperature for several hours before they were cleaned. Because the plates came out of the fouling modules hot they dried quite quickly while being photographed and would undergo re-wetting in the early stages of CIP.

The NHTC of the clean plate remained virtually unchanged after cleaning the plates with a caustic wash and then a nitric wash. This result was expected as the physical properties of the heat exchange system had not been altered by the cleaning process. The NHTC of the initially fouled plates after cleaning had, however, more than doubled due to the removal of fouling from the plates surfaces. The NHTC of all plates coincided at a value of 1 after the caustic wash indicating the fouling layers had been removed.

Figure 5.9 also shows that the NHTC of plate no.2 was lower than plate no.1. Because the NHTC values are normalised for differences in the variables other than fouling for the plates the lower value of NHTC for plate no.2 during water rinse 1 indicates that it has a greater amount of fouling at the sensor location. If the value of U_c remained constant from run to run, as would occur with a permanent probe attachment in an industrial setting, then the value of NHTC during the water rinse 1 would allow the degree of fouling on the measured surface to be determined and compared with previous runs.

5.4.3 Fouling resistance and visual observations.

A video of a fouled plate being cleaned with a 1.0% caustic solution was taken using a special fouling module that contained a window on the process side and a 3Com WebCam digital video camera (Run 35). During the cleaning the CIP monitor was used to record heat transfer through the plate. The cleaning involved a water rinse 1, a caustic wash and then water rinse 2. Details of the experimental method used are given in section 4.5.5. The experiment allowed the HTC trace and an estimate of the fouling resistance (R_f) to be compared against a visual record of the cleaning process.

The heat transfer resistance ($R_f = 1/h_f$, where h_f is the heat transfer coefficient of the fouling (W/m^2K)) was estimated as shown in the sample calculation in section 5.2.1. Then the fouling resistance was calculated from:

$$R_f = R_T - \frac{1}{U_c} - R_p \tag{5.27}$$

Mathematical analysis.

First a theoretical value of the convection heat transfer coefficient (h_p) was calculated for water flowing through the fouling module at 1.44 m^3/hr and at temperatures of 20 to 90°C in 10°C steps. A linear regression of these values gave a linear relationship between temperature and h_p.

$$h_p = 23.386\theta_p + 1587.2 \quad R^2 = 0.9962 \tag{5.28}$$

This equation allowed values between the calculated heat transfer coefficients to be interpolated. U_c was estimated using the method described in section 5.3 (pg. 112). A value of h_p was then calculated for each data point in the cleaning run using equation 5.28. The sum of U_c and the convection HT coefficient gives an estimate of the overall heat transfer coefficient less the fouling resistance.

$$U_{\text{clean}} = \frac{1}{U_c} + \frac{1}{h_p} \tag{5.29}$$

An estimate of R_f is then the measured HTC (U) minus the clean HT coefficient.

$$R_f = \frac{1}{U} - \frac{1}{U_{\text{clean}}} \tag{5.30}$$

The results of this analysis are shown in Figure 5.10. The numbers along the trace indicate the timing of the still images taken from the video that are shown in Figures 5.11 to 5.21. A plot of the overall heat transfer coefficient U during cleaning is shown in Figure 5.23 (page 129).

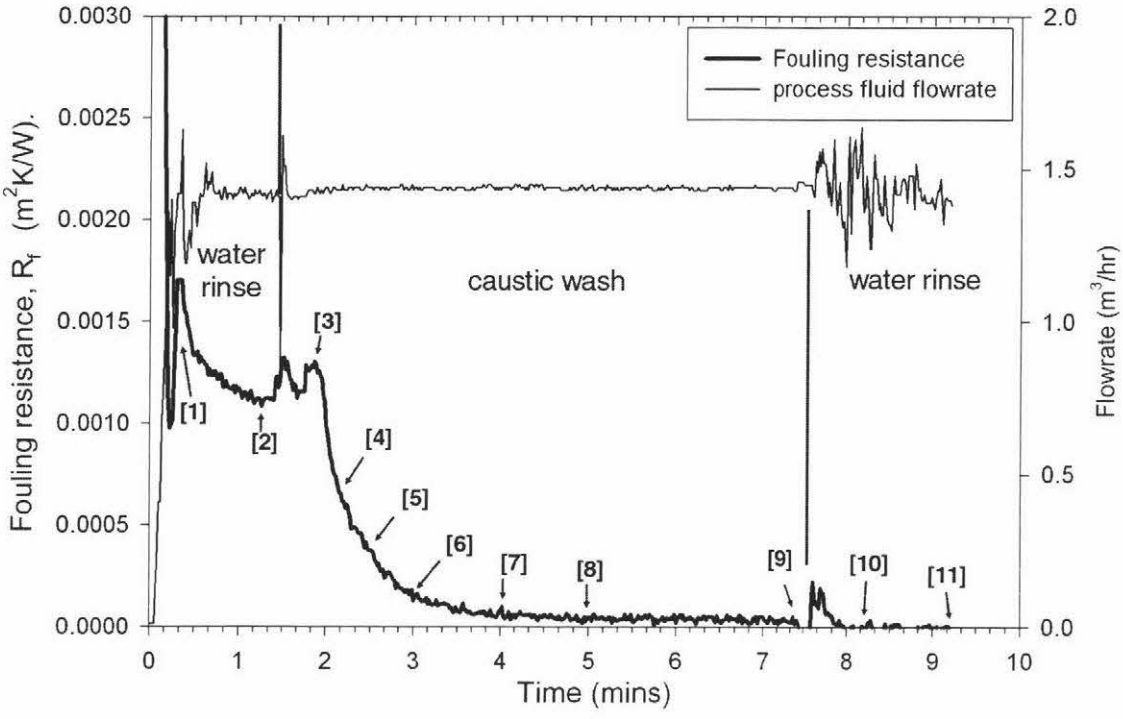

Figure 5.10: A plot of estimated fouling resistance against time for Run 35. The flowrate is also plotted. The numbers from [1] to [11] refer to the stills reproduced from Figure 5.11 to 5.21

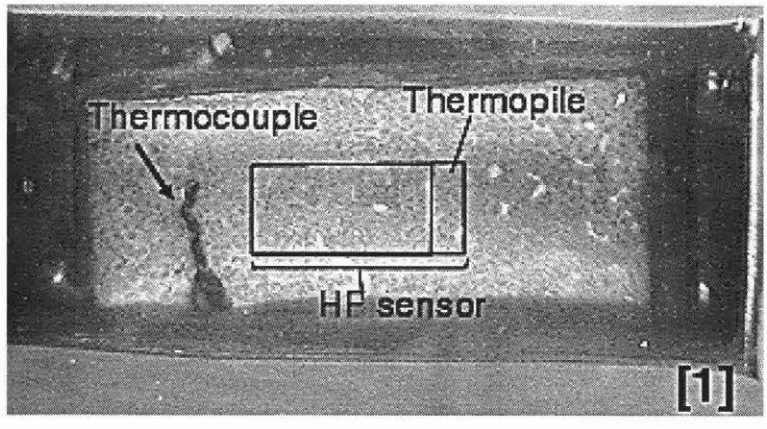

Figure 5.11: 1st rinse. Time 0:22s. White areas indicate positions where there is no fouling and the stainless steel plate shines through. Light grey indicates fouling. The black frame indicates the location of the HF sensor on the opposite side of the plate.

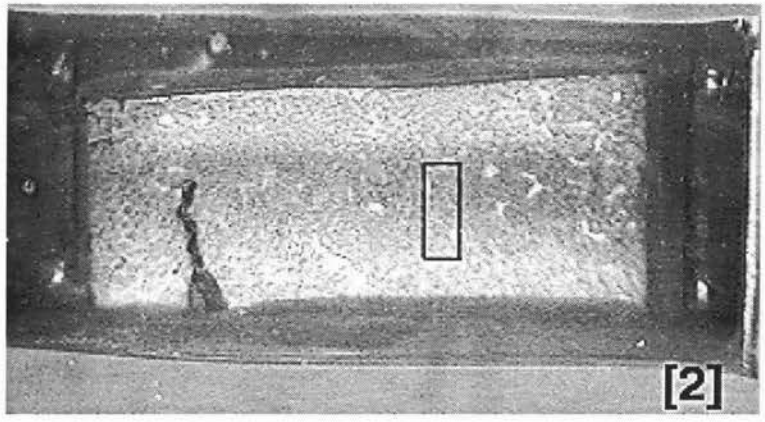

Figure 5.12: 1st rinse. Time 1:17s. Note that the white areas have not changed.

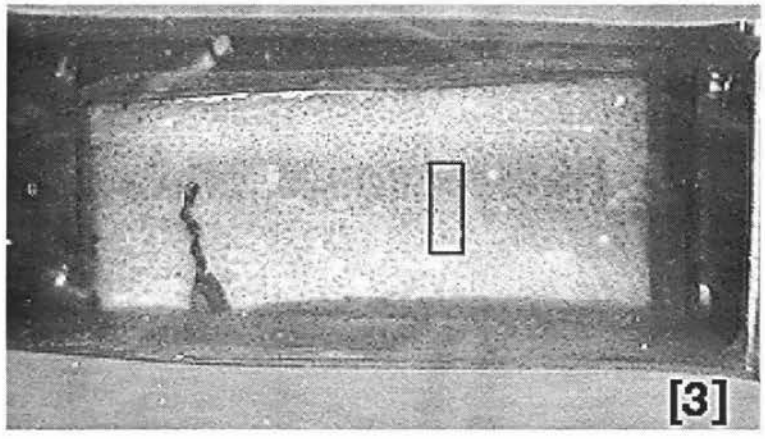

Figure 5.13: Caustic wash. Time 1:51s. Note that the white areas have decreased in area. Right at the probes thermopile location they have disappeared altogether. This is due to swelling of the fouling layer.

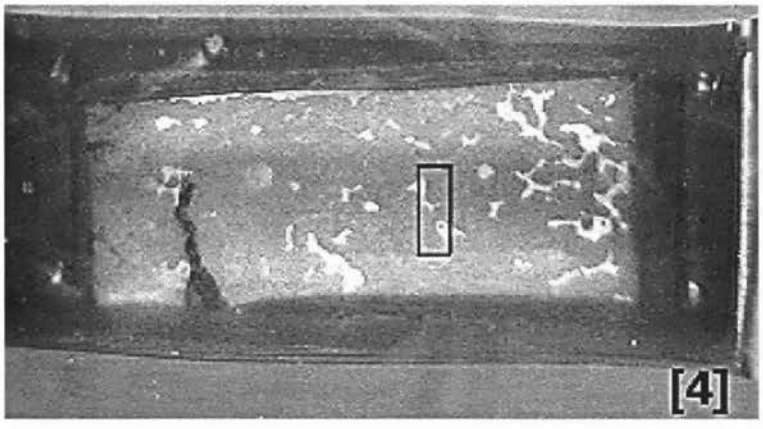

Figure 5.14: Caustic wash. Time 2:11s. Note that white areas have expanded indicating that cleaning has begun. The white areas during the caustic wash are at the same position as was observed during water rinse 1. Cleaning expands the white areas.

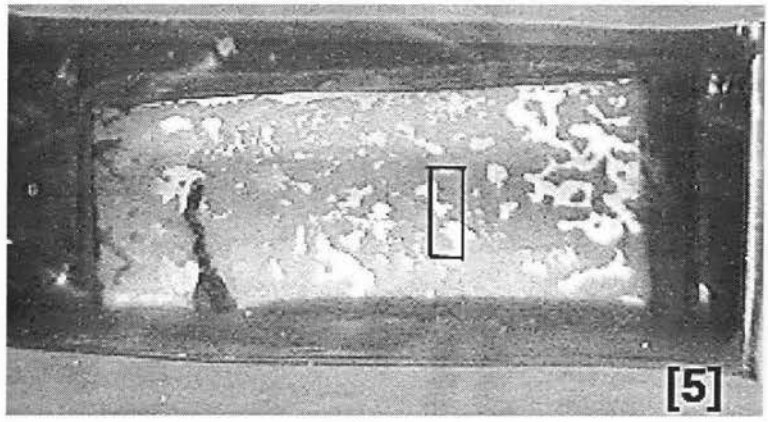

Figure 5.15: Caustic wash. Time 2:30s. White areas have expanded significantly from their original size.

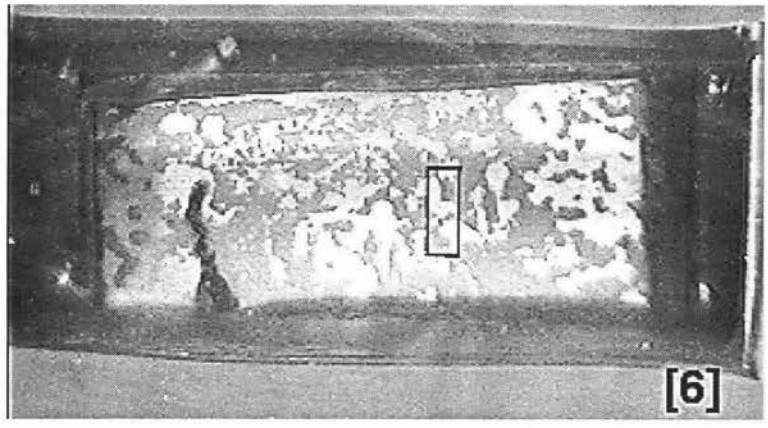

Figure 5.16: Caustic wash. Time 3:01s.

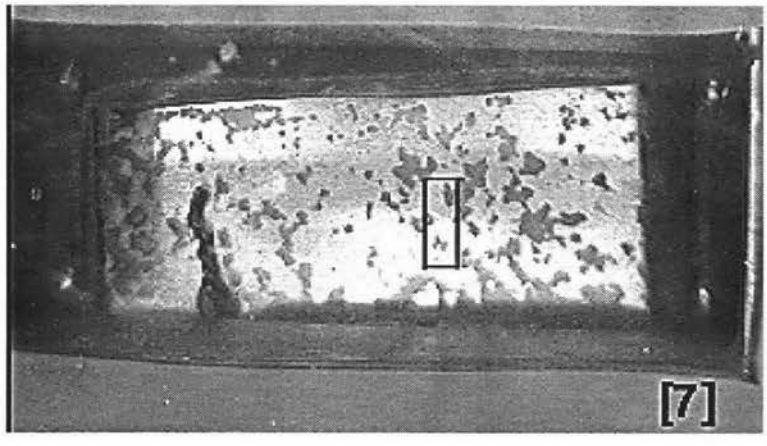

Figure 5.17: Caustic wash. Time 4:01s.

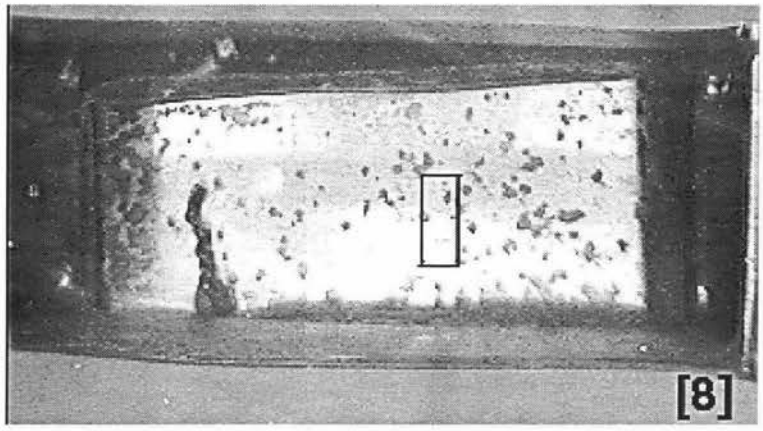

Figure 5.18: Caustic wash. Time 5:00s.

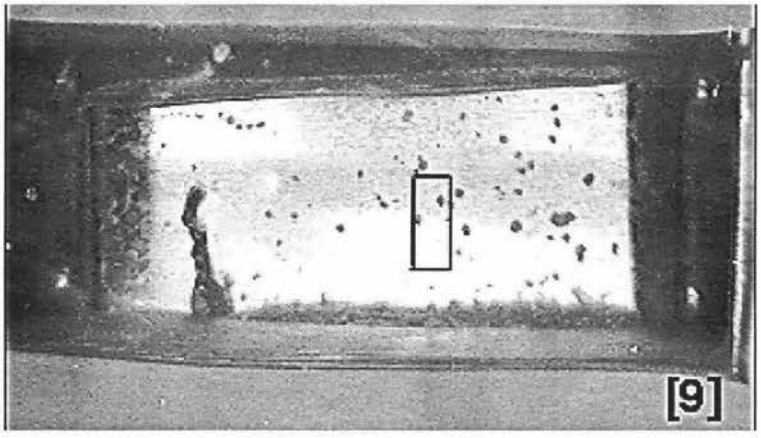

Figure 5.19: Caustic wash. Time 7:26s. Near the end of the caustic wash.

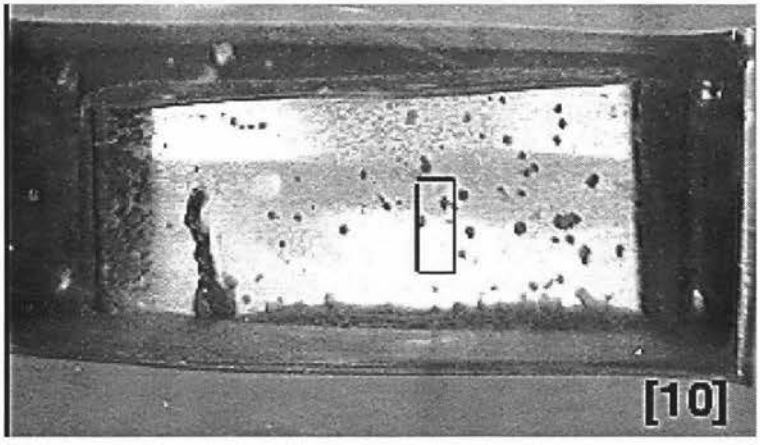

Figure 5.20: Water rinse 2. Time 8:11s. Note that the grey specs are no longer shrinking. The water rinse does not clean any further.

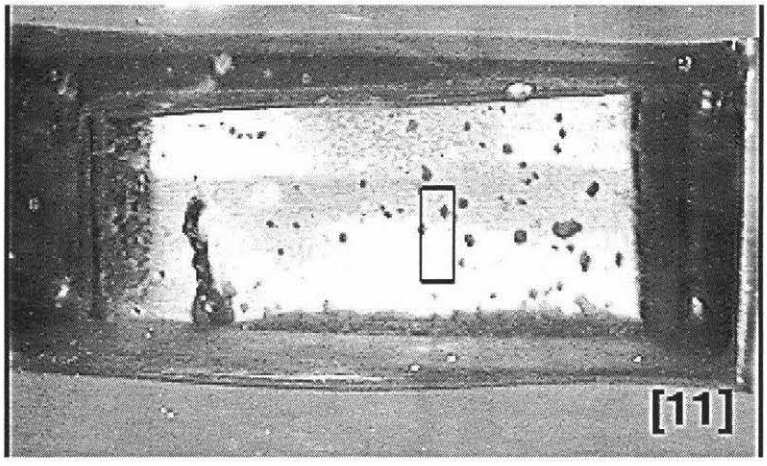

Figure 5.21: Water rinse 21. Time 9:17s.

The first water rinse

Figure 5.11 [1] shows the fouling at the beginning of the first water rinse. Figure 5.12 [2] shows the fouling near the end of the water rinse. The position of the HF sensor on the other side of the plate is marked in Figure 5.11. The small box at the right hand end of the marked HF sensor is the area that contains the thermopile, the transducer that measures heat flux. This small box does not mark the exact area where the HF sensor actually measured the heat flux as the size of this area is unknown. The box should only be taken as a approximate indication of the measured area.

During the first water rinse no visible changes to the fouling layer can be seen. The fouling was initially dry as it was a fouled plate that was made the previous day and no milk can be seen leaching from it during the first rinse. This is not the normal situation for fouling in an industrial plant so this experiment does not show what the usual effects of rinsing on fouling are.

The fouling resistance (R_f) decreases during the first rinse. This may be due to the re-wetting of the fouling which might cause the average thermal conductivity of the fouling layer to increase.

The caustic wash.

During the first 30 seconds of the caustic wash the R_f increases to a peak at 1:51s. This is marked [3] on the R_f trace and a photo of [3] is shown in Figure 5.13. A comparison of [3] with photos [1] and [2] shows that the small holes in the fouling layer have closed up indicating that the fouling is swelling in the presence of the caustic solution.

After this point the fouling begins to be visibly removed from the plate (Figure 5.14 [4]). Fouling is removed fastest where the CIP solution enters the fouling module (the right hand side). This is possibly due to the turbulence caused by entrance effects. R_f falls rapidly after [3] and continues to fall until the trace has almost levelled out at 4m 30s into the caustic wash [8]. Photos [4], [5], [6] and [7] show that the amount of steel plate visible increases as R_f falls. No clumps of fouling can be seen breaking off the fouling layer during cleaning. This differs from the cleaning process described by Bird (1997c) who reported that material left the surface in aggregates rather than uniformly. This difference in cleaning mechanism was possibly due to differences in the fouling layer type being studied. The fouling layers used by Bird were formed using whey protein concentrates.

At minute 5, photo [8], only small islands of fouling are left visible on the plate.

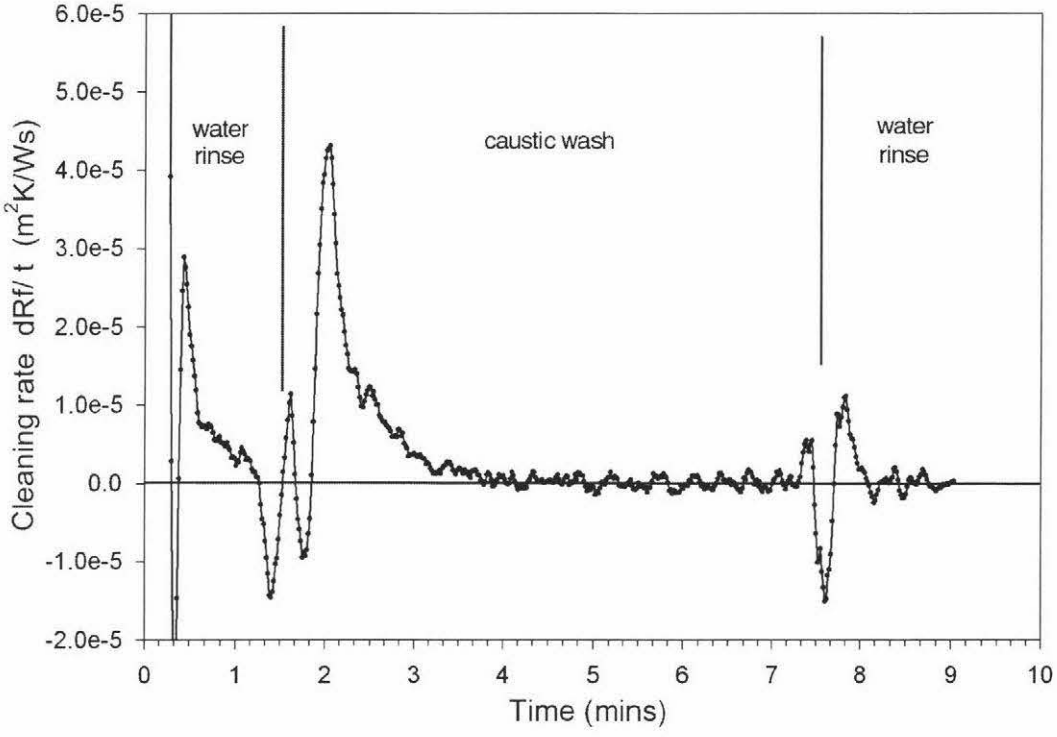

Figure 5.22: A plot of cleaning rate against time for Run 35.

Some of these islands have been removed by the end of the caustic wash but some still remain. Two islands of fouling can be seen remaining in the area estimated to be measured by the HF sensor.

Water rinse 2 (post-caustic rinse).

Photos [10] and [11] show that the fouling does not visibly change during the post-caustic rinse. The fouling resistance R_f reads around zero during the water rinse as a result of the method used to calculate R_f. The small decrease in estimated R_f from the end of the caustic wash to the water rinse may be due to a small change in R_p as the concentration of caustic in the process fluid falls to zero.

Cleaning rate.

Figure 5.22 shows a plot of the cleaning rate against time for Run 35. The cleaning rate is defined here as the gradient of the line R_f as plotted in Figure 5.10. The results show a similar pattern to the data presented by Gallot-Lavallee (1984a) and Bird (1997b). Although the trace is unstable during the swelling period of the trace the cleaning rate does,

on average, climb to a peak and then fall away.

Change in fouled area during cleaning.

The images captured from the video show that the thickness of the fouling layer varies greatly with respect to position during cleaning. The fouling layer began with a number of small holes revealing bare steel. The fouling surrounding these holes was the first to be removed causing the areas of clean steel to grow and merge with one another over time.

These results show that fouling surface area is an important parameter affecting the overall cleaning rate. As fouling is removed the surface area of the fouling decreases as parts of the steel surface become visibly clean. This reduction in surface area would probably reduce the amount of soil being entrained in the caustic solution. It has been assumed by some workers that the surface area of the interface between fouling and the CIP solution is constant throughout cleaning for the purpose of developing mathematical cleaning models (Gallot-Lavallee et. al. (1984a), Bird (1997b)). This greatly simplifies a model as it allows a one-dimensional analysis. However because the thickness of the fouling layer varies with position during cleaning a one-dimensional analysis cannot be assumed to be realistic.

5.4.4 Visual evidence of the end of the caustic wash.

A level trace does not necessarily indicate a clean plate. Figure 5.24 shows a photograph of the plate cleaned in the video discussed above (Run 35) after it had been cleaned with caustic and rinsed with water . Small islands of fouling can be seen remaining on the plate. In addition to the small islands of fouling a very thin broken layer of white material can be seen distributed across the plate. This is possibly the lower mineral rich layer described by other workers (Tissier and Lalande (1986)).

The fouling remaining on the bottom and right hand edge was due to that portion of the fouling layer being covered by the gasket in the fouling module. This small area of fouling was not therefore exposed to the cleaning solution.

Figure 5.23 shows the HTC trace of the plate during cleaning. It can be seen that the trace has levelled out by minute 5. Figure 5.18 (pg. 124) shows that the plate is not yet clean at this point. The HTC trace does not increase significantly from minute 5 onward. The photo of the plate after cleaning (pg. 130) shows that the level HTC does not necessarily indicate a completely clean plate.

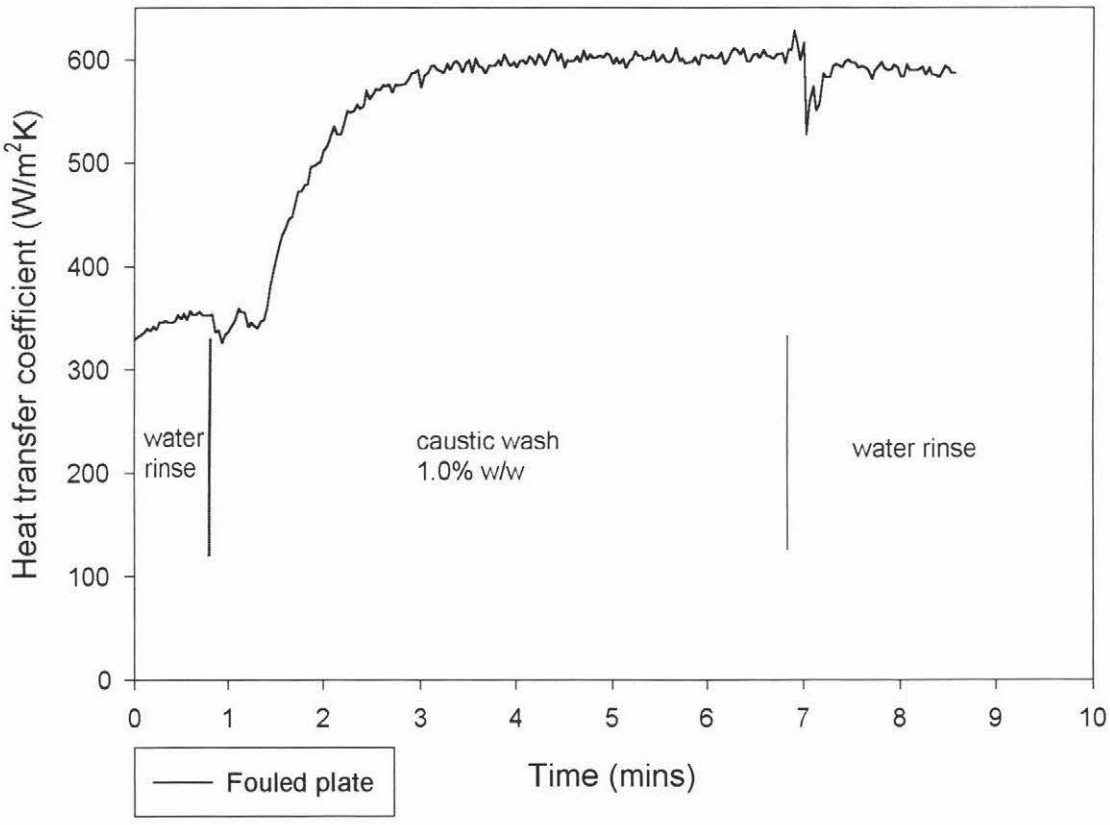

Figure 5.23: HTC trace of a initially fouled plate during a caustic wash cycle.

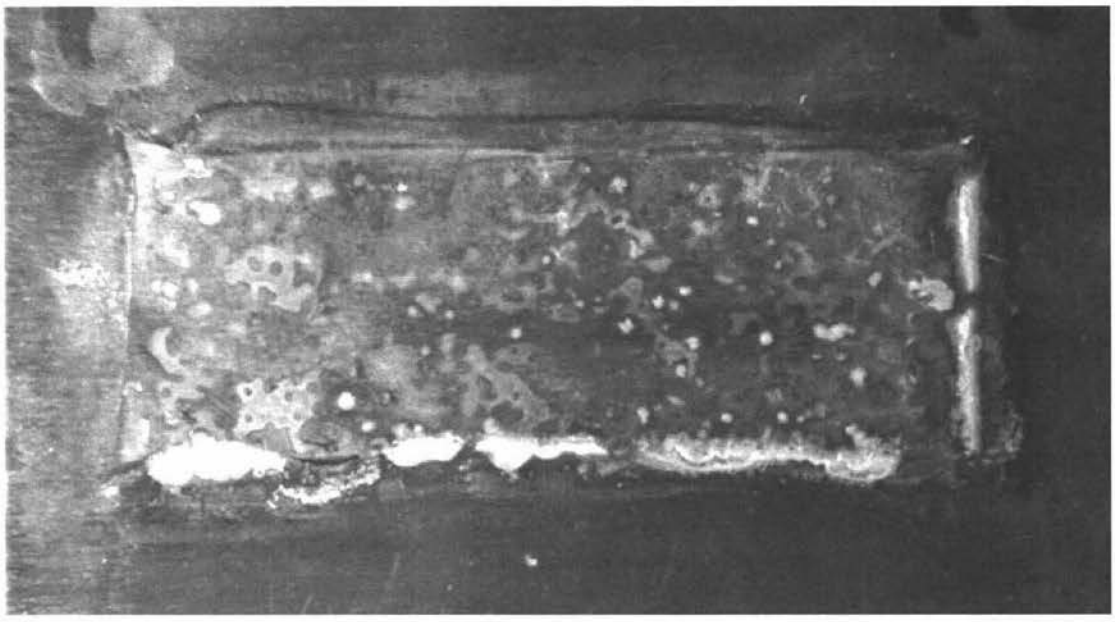

Figure 5.24: Photograph of the plate (Run 35) after the post-caustic rinse. Some fouling can be seen still remaining of the plate after cleaning.

5.5 Effect of lag in process temp measurement on monitor performance

Figure 5.25 shows a comparison of two temperature sensors at close proximity measuring the same flow. The two temperature sensors are less than 1cm apart. The sensor represented by the dotted line is a thermocouple. The solid line shows that temperature as measured by a resistance temperature detector (RTD) shrouded in a stainless steel sheath. Figure 5.26 shows a photograph of the two sensors. It can be seen from the photograph that the shielded RTD has a greater thermal mass than the thermocouple due the stainless steel sheath that surrounds the RTD located within the tip.

The event being recorded was the first phase of a CIP clean: the pre-caustic rinse, the caustic wash and the post-caustic rinse (Run 21). Both sensors were measuring the temperature of the process fluid in a fouling module containing a clean plate.

The traces in Figure 5.25 show that the RTD is has a much slower response time to temperature changes than the thermocouple. The increased lag time of the RTD is due to its increased thermal mass in comparison to the thin thermocouple. Figure 5.27 shows the HTC of the flow system as calculated using each of the temperature sensors data.

The HTC calculated using the thermocouple (the solid line) was almost level with

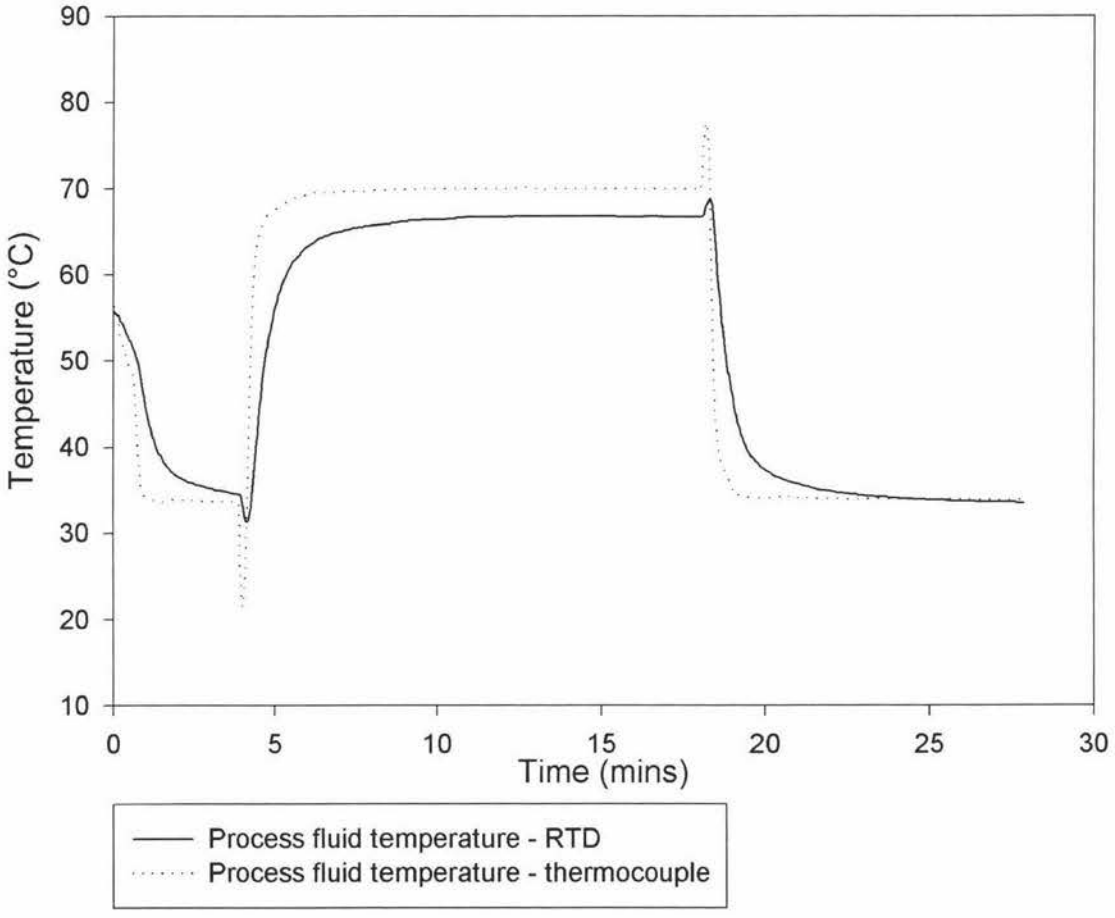

Figure 5.25: Comparison of two temperature sensor types. Both sensors are measuring the same flow. The RTD suffers from both a long response time and an offset error caused by heat loss.

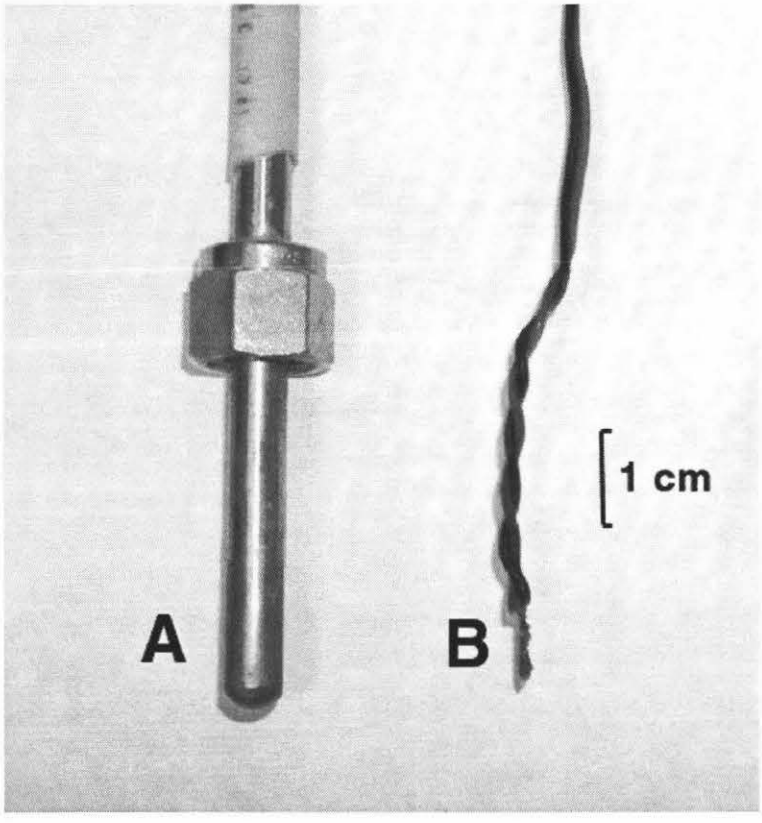

Figure 5.26: Photograph of the two sensor types used. Sensor A is a RTD shielded in a stainless steel sheath. Sensor B is a T-type thermocouple with plastic insulation.

only very small step changes when the fluid type is changed. The HTC as measured by the RTD (the dashed line) was not level however. Each time there is a step change in temperature the HTC obtained from the RTD responds slowly due to the lag in the temperature. The HF sensor responds reasonably quickly to changes in temperature in the process fluid. If the temperature sensor measuring the process fluid is significantly slower than the response time of the HF sensor then the measurements used for the calculation of the HTC to become un-synchronised.

When a naked thermocouple with approximately the same thermal mass as the on-board thermocouple as the HF sensor was used the measurements were more synchronised. The effect of different temperature sensors on the HTC calculated are shown in Figure 5.27. The commercial RTD used introduces artifacts into the HTC trace and makes any estimate of cleaning time very misleading. As a result of these experiments thermocouples were used to measure process fluid temperatures in the fouling modules thereafter.

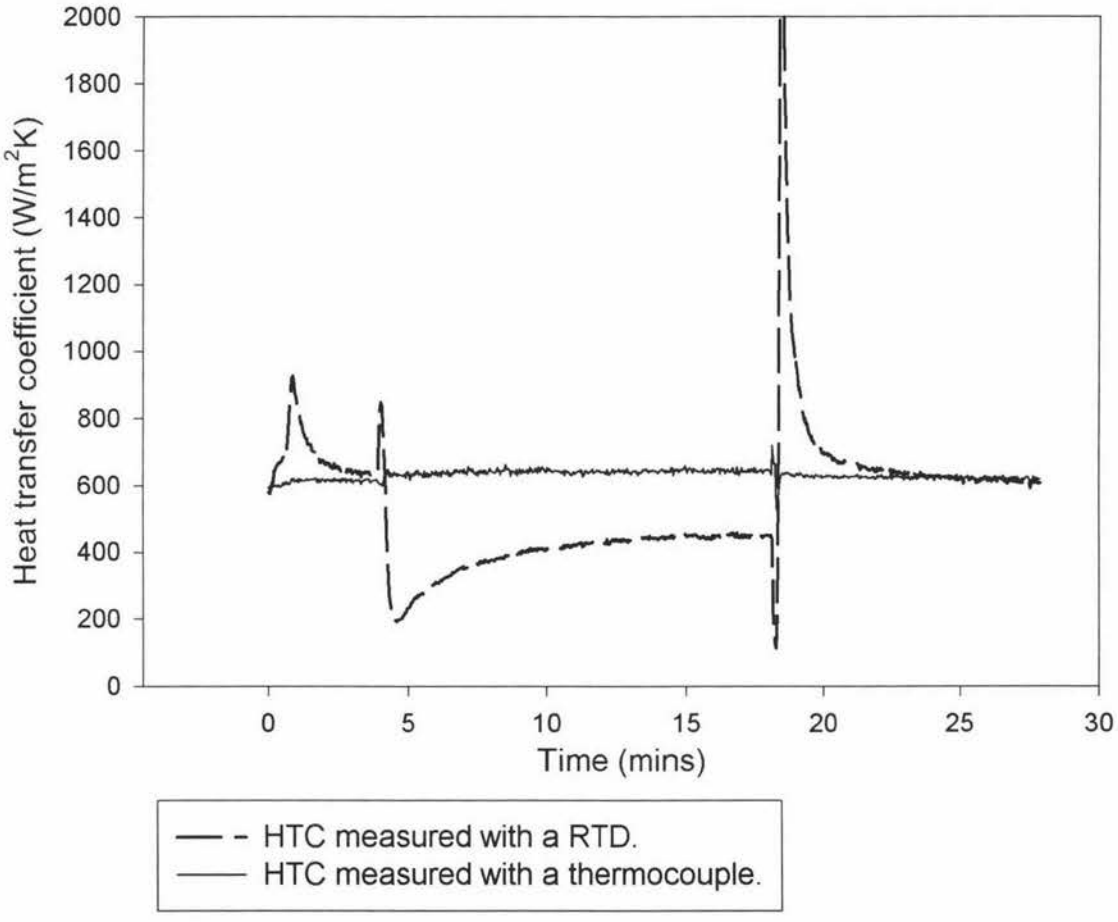

Figure 5.27: Comparison of HTC traces on a clean plate as measured by two different temperature probes: a thermocouple and an RTD.

Chapter 6

Industry Trial

Once the technology for use of the CIP probe and interpretations of its HTC trace had been developed in the pilot plant trials an industry trial was organised. This chapter describes the location of the trial, the experimental setup and the results obtained.

6.1 The trial site.

The trial was conducted at Kiwi Dairies Coop. Ltds Pahiatua Milk Powder Factory. The site contained two milk powder factories. The trial was performed on the larger of the two factories; a 5 tonne per hour powder plant.

The position within the plant chosen for monitoring was the pipe directly following the direct steam injection unit used to pre-heat milk from the plate heat exchanger to 94°C before it entered the evaporator. The position was chosen because the heat flux sensor (HF sensor) could be non-invasively attached to plant and the area was known to foul considerably. From a heat transfer point of view the position was not ideal as the heat was moving from the process fluid to air which is not a very effective coolant. This results in small and unstable heat fluxes. Trialing the HF sensor in a more favourable position such as within a plate heat exchanger would have required modifications to the plant, which were beyond the scope of this trial.

6.2 Sensor setup and data collection

6.2.1 Attachment of the heat flux sensor to the DSI.

A heat flux sensor (HF sensor No. 4 from the pilot plant, RDF Corp. Model 27036-3) was attached to the top of the pipe following the Direct Steam Injection unit (DSI). At the exit of the DSI there was a reducing nipple that connected the DSI to a straight pipe. The HF sensor was attached to the top side of this reducer.

The HF sensor was attached to the pipe using the same materials used in the pilot plant (described on page 83). A 5 by 7 cm strip of aluminium tape was used to hold the HF sensor to the pipe surface. The HF sensor was placed with the long edge running parallel with the flow so that the effect of the curvature of the pipe on contact with the flat HF sensor would be minimised.

6.2.2 Data logger.

The data logger used was a Campbell Scientific CR10X. The CR10X was chosen because of its flexibility in terms of programming and also the range of sensors that could be connected to it. The data logger was powered by two 6V batteries. Both the data logger and the batteries were protected by a plastic box which kept the setup free from the dusty additives that would settle on surfaces throughout the plant. The box was placed on a gangway in a corner of the plants evaporator room midway between the DSI and the nearby control room.

Thermistor ice-point.

An electronic ice-point (thermistor) was used to provide a zero-point for the thermocouple on-board the heat flux sensor. The thermistor was held in firm contact with the wiring board of the data logger with aluminium tape to ensure isothermal conditions between the two objects. The thermistor was powered by a 12V supply from the data logger and the differential voltage across it measured by channel 1 of the data logger every 8 seconds and the value held in the data loggers memory as a reference point for thermocouple measurements.

6.2.3 Data collected.

Five variables were measured and recorded in the plant. Two of these were the measurements made by the heat flux sensor; heat flux and HF sensor temperature. The

other three recorded variables were measurements made by existing plant sensors that were part of the control system:

- The temperature of the milk / CIP solution leaving the Direct Steam Injection unit. More precisely this was the temperature of the process fluid approximately 6 meters down stream from the exit of the Direct Steam Injection unit.
- The process fluid feed flowrate to the evaporator. This was the flowrate of process fluid throughout the pre-heating system including the Direct Steam Injection unit.
- The conductivity of the process fluid entering the pre-heating section of the milk powder plant.

Connection of the HF sensor to the Data Logger.

The data logger was located more than 8 metres from the Direct Steam Injection unit. Therefore a 4-core shielded signal wire of 10 metres length was used to connect the HF sensor to the data logger. Only two of the wires were used, the other two were simply trimmed back. Running such a long length of signal wire from the HF sensor to the data logger was not desirable because it increased the chances of electrical noise within the plant interfering with the weak voltage developed by the sensor. The use of shielded signal wire was aimed at reducing the effects of this possible problem.

Thermocouple wire of the same length was used to connect the on-board thermocouple of the HF sensor to the data logger. This cable was not electrically shielded.

6.2.4 Plant sensors.

Flowrate, DSI exit temperature and conductivity. Three sensors from the plants control system were monitored by the data logger and their values recorded every 8 seconds. Access to these measurements was accomplished with the help of a site electrician who extended the 4 - 20 mA signal loops of the three sensors and brought them alongside the data logger. Because the data logger could not measure current a resistor was installed in each 4 - 20 mA loops to provide a point of known resistance. The data logger was then used to measure the voltage difference across the resistors. The current could then be calculated from these values.

$$I = \frac{V}{R} \tag{6.1}$$

Where: I = current (A)

V = voltage (V)

R = resistance of the resistor (Ω)

This method of logging data from the three plant sensors allowed the data logger to sample the plant sensors at a rate independent of the plant control system. It also allowed all the recorded data to be handled directly by the data logger instead of attempting to extract the data from the plant database at a later time.

Calculation of real values from the voltage readings.

Calculating the real values measured (temperature, conductivity and flowrate) from the voltages read by the data logger involved two steps. First the voltage was converted back to a current in mA. The resistance of each of the resistors inserted into the 4 - 20 mA sensor circuits was measured using a multimeter before they were installed in the plant. The second step was to convert this current to the real value using a linear relationship between current and the desired units. A table of the correlations between current and the measured values is given in Table 6.1 below. Also shown in the table is the gradient and intercept of the linear equation that relates current to the property that each sensor was measuring.

Table 6.1: Plant sensor signal outputs, resistors and linear equations.

Sensor	4 mA =	20 mA =	Resistor (Ohms)	gradient	intercept
Flowmeter	0 L/hr	50,000 L/hr	99.66	3125	-12500
Temperature	0°C	150°C	119.74	12500	-50000
Conductivity	0 μ S	200,000 μS	119.9	9.375	-37.5

An example calculation for the flowrate sensor is given below.

$$I = \frac{V}{R} = \frac{2123 \text{ mV}}{119.92 \text{ Ohms}} = 17.703 \text{ mA} \tag{6.2}$$

The flowrate was obtained as:

$$\text{Flowrate} = (17.703)(3125) - 12500 = 42,822 \text{ l/hr} \tag{6.3}$$

6.2.5 Data storage.

Variables logged and sample rate.

- Heat flux: logged every 4 seconds at high resolution (5 digits, 4 bytes per data point).

- HF sensor temperature: logged every 4 seconds at high resolution.
- Flowrate: logged every 8 seconds at low resolution (4 digits, 2 bytes per data point).
- DSI exit temperature: logged every 8 seconds at low resolution.
- Conductivity: logged every 8 seconds at low resolution.
- Julian day (DD): logged every 8 seconds. (2 bytes)
- Time (HHMM): logged every 8 seconds. (2 bytes)
- Seconds (SS.SS): logged every 8 seconds. (2 bytes)

Data management.

The data logger used a ring-memory system that once full would begin to overwrite old data. Because the data logger was sampling five sensors at a rate of either 4 or 8 seconds 24 hours a day a sufficient amount of data was collected to fill the memory of the data logger in several days. As the monitoring setup was to be left for longer than that period of time a laptop micro-computer (Intel 486 processor running Windows 95) was used to retrieve data from the data logger at regular intervals.

The laptop computer was kept in the control room of the factory and left running continuously. It was connected to the data logger using a 15 metre electrically shielded serial cable designed for sending data over distances up to 150 metres (Black Box Cable ED12-C). The computer was running the Campbell Scientific 'Telcom' software that was configured to retrieve data from the data logger every 20 minutes.

The program running the data logger was designed to be fairly efficient in terms of its use of memory. As described above only the two measurements from the HF sensor were logged at a 4 second interval with other variables including time being logged at 8 second intervals. This resulted in data downloaded from the data logger not being in plain columns. The data could be easily arranged into columns by recording a simple macro in Microsoft Excel if the data followed a continuous pattern. In fact the data recorded was found not to be continuous so organising the data required an extra step. The methods used to sort the data are discussed in the following section.

6.3 Data manipulation.

Before data from the data logger could be plotted it needed to be arranged into columns. Because more than 180,000 lines of data were collected this process was automated using Visual Basic macros in Microsoft Excel.

Data from the data logger was unfortunately not continuous. Loss of data either during measurement and storage in the data logger or during transmission from the data logger to the computer resulted in lines of data missing from the data file retrieved from the laptop computer. Because the data could not be sorted in regular columns by a simple script if the data did not follow a continuous pattern the data was first organised into a continuous pattern by either deleting or inserting blank lines. A Visual Basic script was written to do this. The source code for this is shown in the Appendix (C.2.1, page 169). After this process the data was organised as follows:

Key:

Program table no.	HFS temperature	HF					
Program table no.	HFS temperature	HF					
Program table no.	flowrate	conductivity	RTD temp	day	time	sec	
...							

```
103     94.534  0.06829
103     94.605  0.0411
205     2157    434.2   1677    88      2247    4.125
103     94.463  0.10044
103     94.605  0.04243
205     2157    434.4   1677    88      2247    8.13
103     94.747  0.05105
103     94.605  0.04757
205     2164    434.6   1677    88      2247    12.13
...
```

After the data had been made into a continuous pattern using this macro the data was filtered so that the extra 4 second interval measurements of heat flux and HF sensor temperature were removed from the data. The script used to do this is given in Appendix C.2.2 (page 171). Following this the data had the following format:

```
103     94.605  0.0411
205     2157    434.2   1677    88      2247    4.125
103     94.605  0.04243
205     2157    434.4   1677    88      2247    8.13
103     94.605  0.04757
```

```
205     2164    434.6   1677    88      2247    12.13
...
```

After this manipulation the data was sorted into plain columns using the recorded macro shown on page 171 to give:

```
        Temp-TC HF      flow    cond    temp    day     time    sec
103     94.605  0.0411  2157    434.2   1677    88      2247    4.125
103     94.605  0.04243 2157    434.4   1677    88      2247    8.13
103     94.605  0.04757 2164    434.6   1677    88      2247    12.13
...
```

6.4 Results and Discussion.

6.4.1 Interference and noise in the collected data.

Much of the data collected from the HF sensor and the process fluid temperature sensor contained significant noise or interference. Figure 6.1 shows a plot of process fluid temperature over a period of about 11 hours. Three periods of significant interference can be seen in the data.

The cause of the interference is unknown but it was most likely due to electrical interference from powerful electrical devices operating in the plant. A similar effect can be seen in the measured heat flux although in this case the noise is more severe (Figure 6.2). Heat flux measurements were significantly more noisy during cleaning-in-place. The larger sensitivity of the HF measurements to interference was likely due to the very weak signal developed by the HF sensor, typically 0.05mV. It is likely that the signal from the HF sensor will need signal conditioning if it is to be sent over several meters of cable to a data logger or Programmable Logic Controller. This may involve amplifying the voltage produced by the HF sensor to improve the signal to noise ration or converting the voltage to a 4 - 20 mA current before sending it through the plant.

The data loggers clock.

Figure 6.3 shows a plot of the time reported by the data loggers clock during three days of the trial. The plot shows many step changes in the plot and also periods where the clock appears to be suspended at a particular time. The cause of this phenomena is not understood but it is possible that the clock suffered electrical interference from its surroundings or that it malfunctioned. The plant room was expected to be electrically noisy.

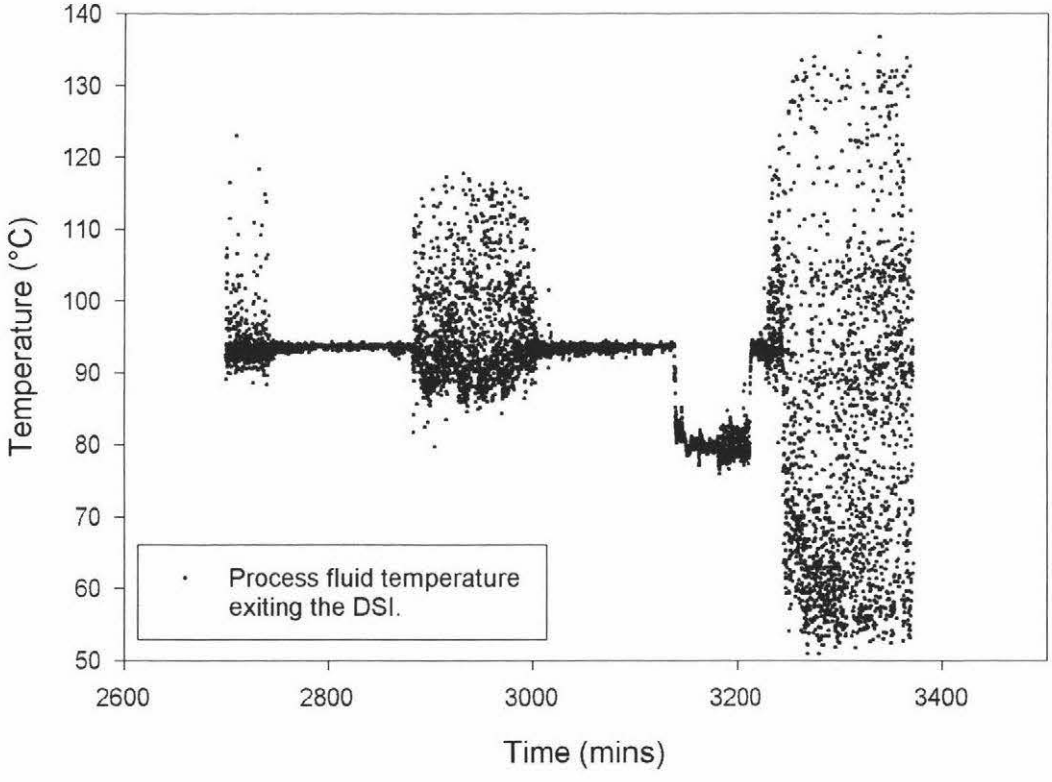

Figure 6.1: A plot of process fluid temperature against time. The data shows three periods of severe interference in the data.

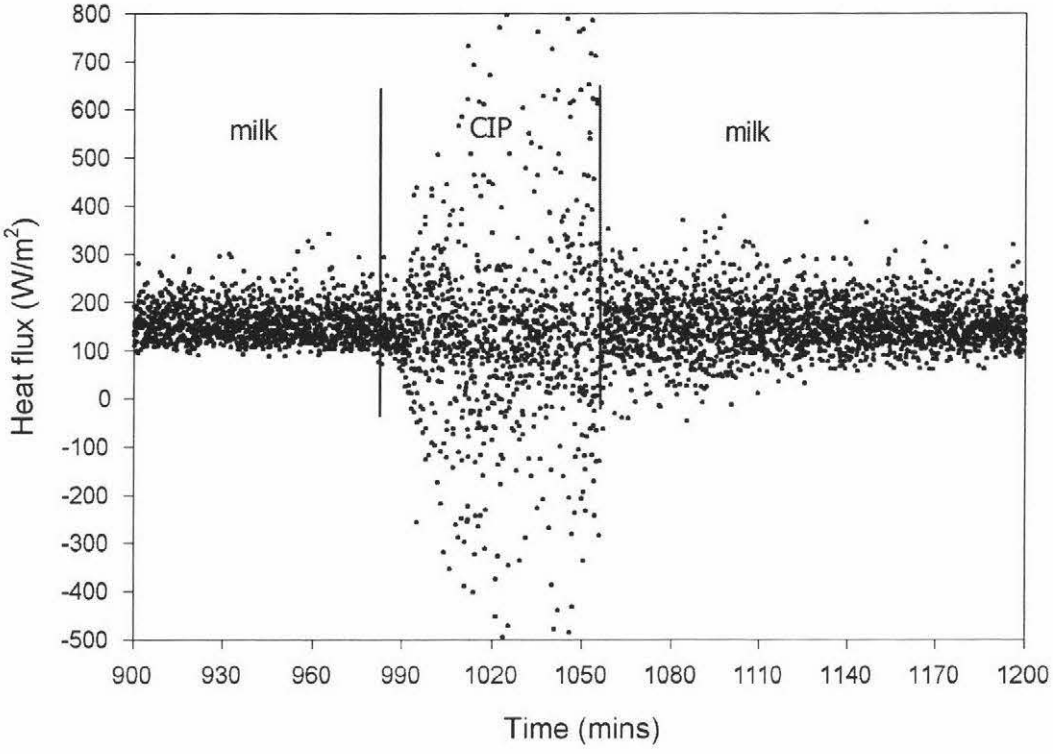

Figure 6.2: A plot of heat flux against time. The plot shows that the noise levels in the HF data increase during cleaning-in-place.

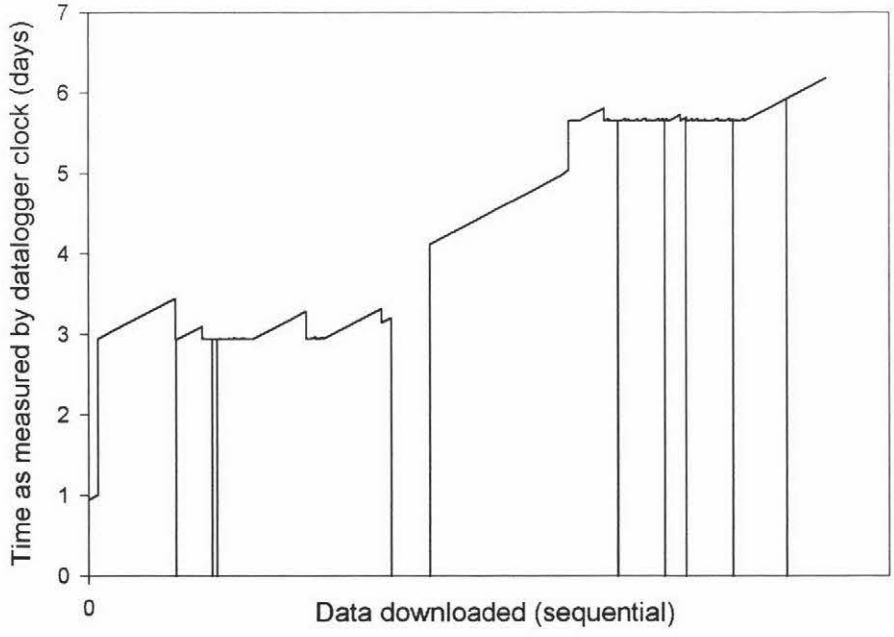

Figure 6.3: Plot of the time (in days) recorded by the data logger. Step changes in the recorded time suggest that the data loggers clock suffered interference or malfunctioned during the trial.

Because the times recorded by the data logger were erratic they were not used for the analysis of the data. The data was instead assumed to continuous with each data point being 4 seconds later than the previous point. As data from the data logger was downloaded and appended to a text file on the laptop computer every 20 minutes it is unlikely that the data recorded on the laptop was not sequential. It was however found that the downloaded data contained holes of missing information. This was discussed in section 6.3.

Instability of the DSI during CIP.

During milk processing the temperature and flowrate of the milk remained very constant. This greatly aided HF sensor measurements as changes in the thermal conditions of the process fluid would move as a wave through the measured system affecting the HF sensor and the process fluid temperature sensor at different times.

During cleaning-in-place (CIP) however the DSI system was subject to regular disturbances that affected both the flowrate and the temperature of the process fluid making accurate measurement of the overall heat transfer coefficient (U) impossible with the experimental set up used for the trial. The disturbances were independent of process fluid temperature but always occurred when the process fluid flowrate was increased from 45,000 l/hr for milk to 49,500 l/hr for CIP. Figure 6.4 shows a plot of the HF sensor temperature, process fluid temperature and flowrate during a CIP clean. Figure 6.5 shows detail from the plot. It can be seen that the temperature of the process fluid oscillates by about 8°C with a period of about 1 minute. The temperature of both temperature sensors follow each other with little delay although it is possible that both measured temperature lag behind the true process fluid temperature due to the thermal mass between the process fluid and both of the sensor transducers.

Figure 6.5 also shows that the flowrate trace contains regular large spikes that correspond to peaks in the temperature traces. These disturbances can, however, only be seen at every second peak in the temperature measurements. These results indicate that the temperature of the process fluid and the flowrate are related. This was expected as the DSI is mixing a given amount of steam with a given amount of process fluid. The proportion of steam to water is one of the determining factors in the final temperature of the process fluid leaving the DSI. It is possible that the variations in temperature are due to sudden changes in process fluid flowrate.

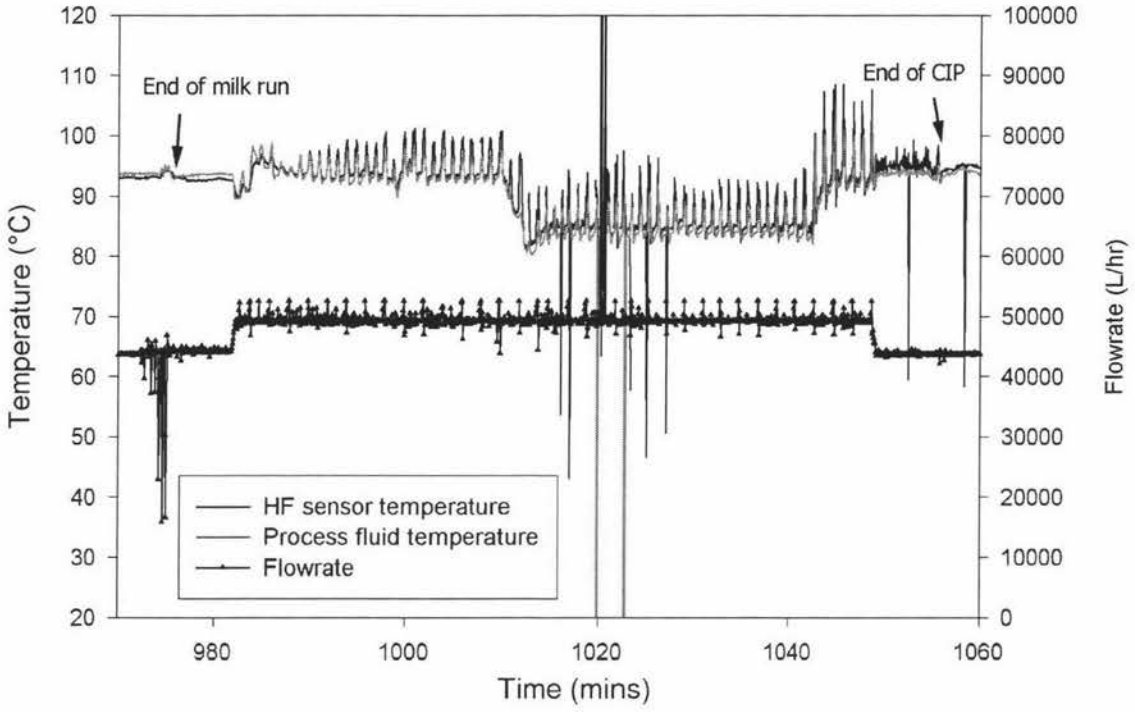

Figure 6.4: A plot of HF sensor temperature, process fluid temperature and flowrate during cleaning-in-place.

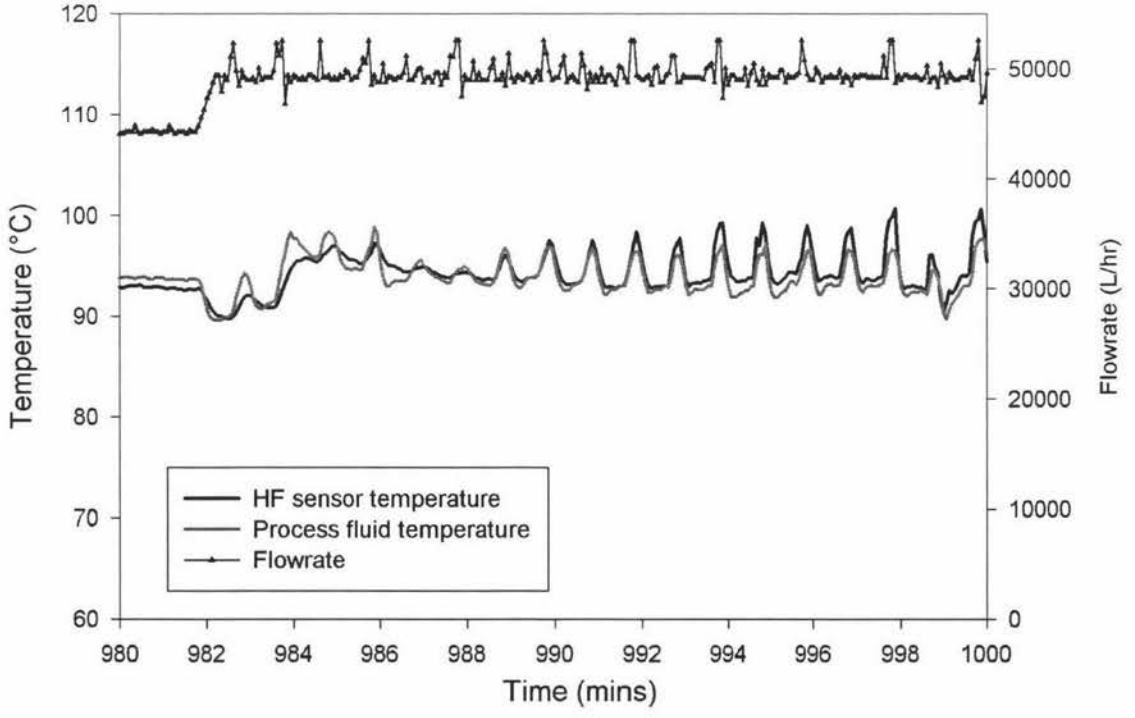

Figure 6.5: Detail of the plot of HF sensor temperature, process fluid temperature and flowrate during cleaning-in-place.

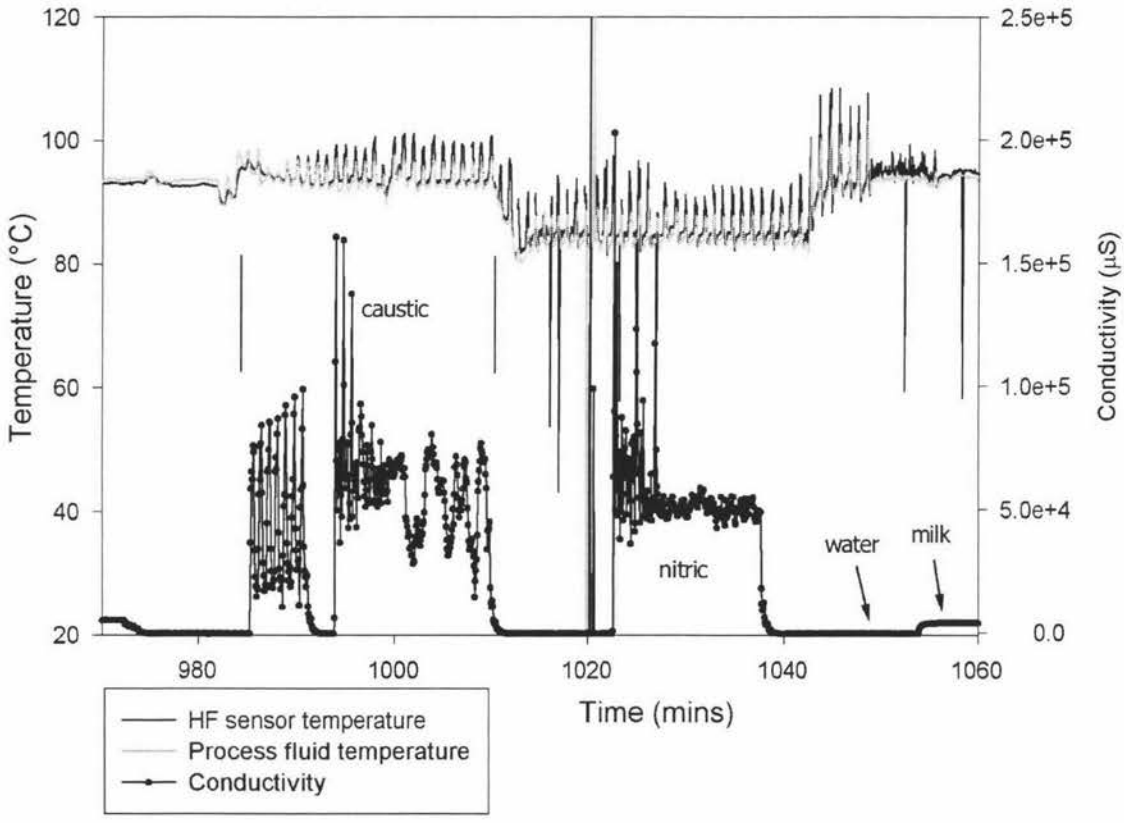

Figure 6.6: A plot of the conductivity of the process fluid along with the process fluid temperature and the HF sensor temperature during a CIP cycle.

DSI oscillations not affected by CIP fluid type.

Figure 6.6 shows the conductivity of the process fluid plotted with the two measured temperatures during a caustic wash. The conductivity of the process fluid allows the type of fluid passing through the plant to be determined (although caustic soda and nitric acid cannot be distinguished from one another). When the process fluid is milk the conductivity is 4000 and 5000μS. When the process fluid is water the conductivity is close to zero. The sudden increase in conductivity during periods of the CIP cleaning is due to the dosing of caustic soda or nitric acid into the process stream. The magnitude of the conductivity of the process fluid is proportional to the concentration of caustic soda or nitric acid present.

The first increase in conductivity (at 985 mins) is the beginning of the caustic wash. During this phase the caustic only passes through the plant once (no recycle). The conductivity rises and falls rapidly as slugs of caustic are dosed into the system. Then after a short rinse further caustic is dosed into the system except that this time the process fluid is recycled through the plant.

The third increase in conductivity during the CIP cycle is due to the addition of nitric acid to the process fluid. The stability of the conductivity during this phase indicates that the nitric solution is recycled through the plant.

It can be seen that the dosing of concentrated CIP solutions into the plant did not affect the disturbances in the temperatures or flowrate. The disturbances remained when the flowrate was high whether or not caustic or nitric was present in the process fluid.

6.4.2 Sensitivity of the HF sensor to fouling.

When measurements from the HF sensor were not subject to significant noise the build up of fouling on the measured surface was apparent in two ways. The most clear of these was a fall in HF sensor temperature during milk processing despite a constant milk temperature at the exit of the DSI. Figure 6.7 shows a plot of the HF sensor temperature and the milk temperature during a milk processing run of 14 hours. It can be seen that the temperature of the HF sensor (approximately the temperature of the surface of the pipe) falls from 94°C to below 93°C as fouling develops during the course of the milk run.

Figure 6.8 shows a plot of the overall heat transfer coefficient (U) of the pipe during the milk run. To calculate the U values for this plot 2°C was added to each of the measured process fluid temperature values. This was done as the temperature of the HF sensor at the beginning of the milk run was equal to or slightly higher than the measured

process fluid temperature. As the temperature of the outside of the pipe must have been lower than the milk on the inside of the pipe the measurements indicate that one of the two temperature sensors (or both) had an error large enough to report this obviously inaccurate reading.

- *HF sensor temperature.* This sensor was a T type thermocouple. The American National Standards Institute has established limits of error for standard thermocouple wire to be $\pm 1.0^{o}$C (ANSI MC 96.1, 1975). The accuracy of a CR10 voltage measurement is specified as 0.2% the full scale range used to make the measurement. In the environmental temperature range with voltage measured on the appropriate scale the error in temperature due to the voltage measurements is a few hundredths of a degree.

- *Process fluid temperature.* The process fluid temperature sensor was located more than 4 metres downstream from the HF sensor. The sensor used was a RTD housed in a stainless steel sheath. Section 5.5 (pg. 130) discusses an issue with some RTD sensors mounted in stainless steel sheaths that results in the sensor reporting a temperature several degrees lower than the real value. It is possible that the RTD measuring the process fluid temperature exiting the DSI is reporting a slightly lower temperature than the true value.

Figure 6.8 shows that the overall heat transfer coefficient decreases over the period of the milk run indicating that fouling is building up on the pipe wall adjacent the HF sensor. Truong et al. (1998) reported similar results using the same technique. This however was not the main target of investigation which was the measurement of fouling during cleaning. The instability of the DSI during CIP confounded this objective due to the limitations of standard industrial temperature sensors used in dairy plants (as was discussed previously).

The effect of cleaning on temperature difference.

Figure 6.9 shows a plot of the process fluid temperature and the HF sensor temperature during a CIP cycle. At the end of milk processing and during the initial rinse of CIP the HF sensor temperature is about 3°C lower than the process fluid temperature. Note that 2°C has been added to each of the process fluid temperatures plotted in the graph. The difference between the two temperatures indicate there is fouling on the inside pipe wall adjacent to the HF sensor (section 6.4.2). During the initial rinse of the CIP cycle the difference between the two temperatures does not reduce. This indicates that little if

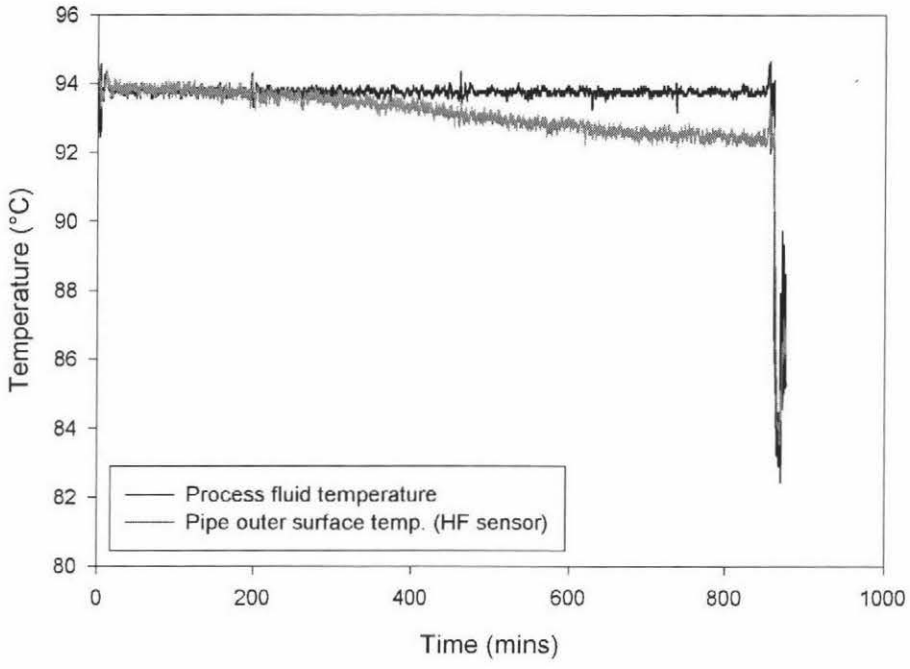

Figure 6.7: Plot of the temperature of the process fluid and the HF sensor during milk processing.

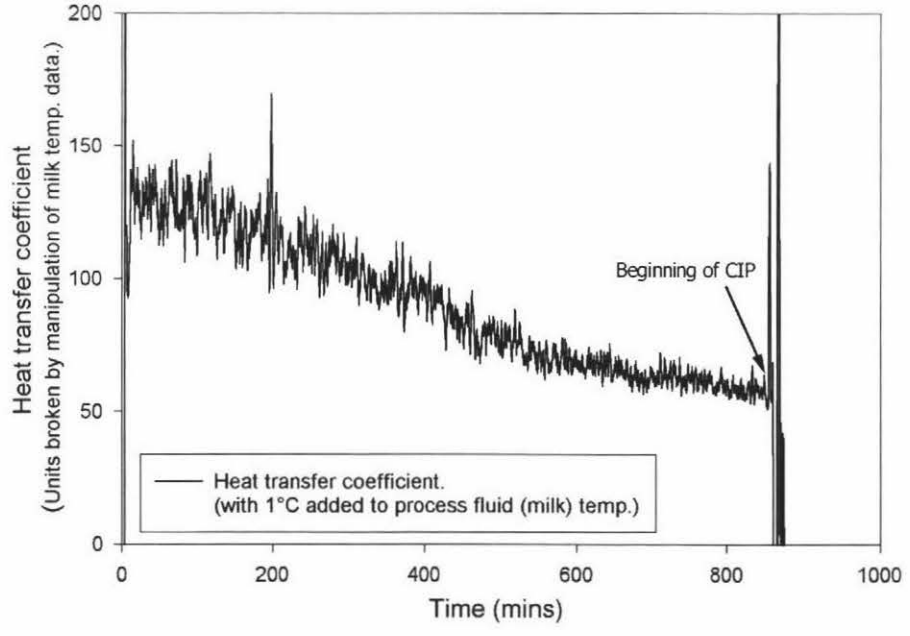

Figure 6.8: Plot of the overall heat transfer coefficient(U) of the pipe at the exit of the Direct Steam Injection unit during milk processing. Two (2) degrees K has been added to the temperature of the process fluid temperature for each calculation of U.

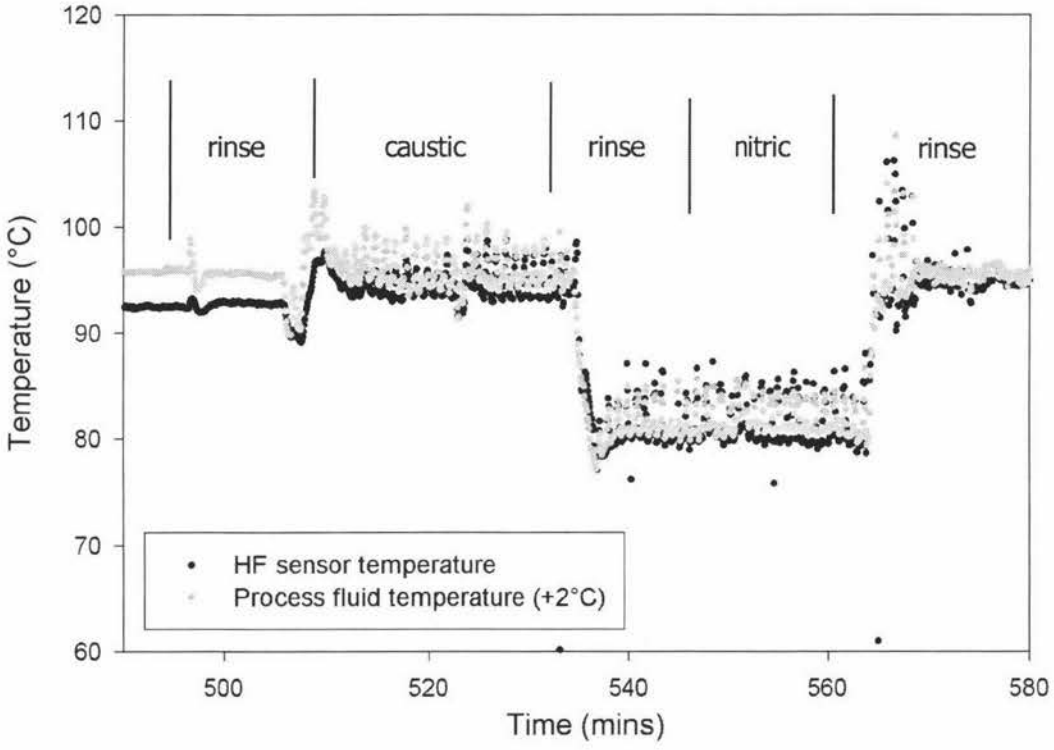

Figure 6.9: Plot of process fluid temperature and HF sensor temperature during a CIP cycle. The difference between the two temperatures provide an indication of the amount of fouling on the inside pipe surface adjacent to the HF sensor.

any fouling is removed during rinsing. Just before the caustic wash the temperature of the process fluid was increased and the DSI became unstable with the increase in flowrate. Accurate comparison of the traces becomes more difficult as this point but the results suggest that during the next rinse the two temperatures are much more similar indicating that most of the fouling has been removed.

At the end of the CIP cycle the two temperatures are however almost the same. This justifies the addition of 2^oC to each of process fluid measurements as the temperature of the HF sensor would have increased to become higher than that of the process fluid temperature without this modification. This is clearly not possible as the ambient temperature of the room was around 40^oC and process fluid 94^oC. Heat must have been leaving the pipe and therefore the temperature of the HF sensor (attached to the outside of the pipe) must have been lower than the temperature of the process fluid.

6.4.3 Summary discussion.

The results from this trial successfully showed that the HF sensor is sensitive to the presence of fouling on the adjacent side of a measured wall in factory situation as has also been shown by Truong et al. (1998).

Results from cleaning-in-place cycles, however, mostly illustrated the issues involved in bringing the method used in the pilot plant to an industrial setting. One of these issues had already been identified during development of the technique in the pilot plant. This was the need for accurate temperature sensors with suitably fast response times that ensure that the three measurements of heat flux, HF sensor temperature and process fluid temperature are correctly synchronised. The instability of the DSI during CIP highlighted the need for this.

Other confounding factors such as the effect of electrical interference on collected data highlighted problems that were not an issue in the pilot plant.

The factory trial showed that the key issues involved in bringing the HF sensor to industry as a CIP monitor were the performance and location of the process fluid temperature sensor and the careful handling of the sensor signals in an electrically noisy environment.

Chapter 7

Conclusions & Recommendations.

7.1 Conclusions

7.1.1 Performance of the heat flux sensor during CIP.

The heat flux sensor (HF sensor) has been shown to reflect changes to the fouling mass during cleaning-in-place. The heat transfer coefficient (HTC) was low in the presence of fouling on the measured surface. As fouling was removed during CIP the overall heat transfer coefficient would increase.

The probe allowed estimation of several parameters during CIP:

- Duration of the caustic wash. The end of this phase is indicated by a levelling out of the NHTC trace.
- The extent of fouling removed during cleaning. This allows us to map out the positions of excessive fouling in a plant.
- Rate of cleaning. This parameter is obtained from the slope of the NHTC during CIP. It seems to change only during the caustic wash. This parameter allows insight into the difficulty of cleaning different types of deposit. It also allows the testing of different CIP formulations and products.

Video footage of the cleaning process showed that the steady increase in overall heat transfer coefficient (OHTC) during the caustic wash matched the attrition of fouling from the measured surface. It could be seen that the application of caustic to the fouling layer caused it to swell and this swelling process could be seen in the OHTC trace.

Cleaning was found to be a relatively rapid process. Plates with approximately 1 mm of fouling would be almost clean after 5 minutes of washing with 1.0% w/w caustic.

Cleaning was a process of attrition and no lumps of fouling were seen breaking off the surface. Cleaning was most rapid at locations surrounding holes in the fouling layer. The front of cleaning therefore moves sideways as well as through the fouling layer.

7.1.2 Factors affecting the NHTC trace during cleaning.

- Changes in process fluid temperature (CIP solution) were found to have a much more significant effect on the convection heat transfer coefficient than changes in its composition. A method derived to compensate for changes in temperature improved the readability of the trace by reducing changes in the trace caused by temperature effects. The compensation has been justified by predictions calculated from fundamental heat transfer theory.

- The addition of nitric acid or milk fouling soil to the solution did not have a significant effect on the heat transfer coefficient.

- The addition of caustic soda to the solution caused a very small decrease in the heat transfer coefficient of the flow system.

Electrical noise in the industrial environment was found to cause significant interference in the heat flux readings especially during cleaning-in-place. The very small voltage generated by the HF sensor probably made it particularly sensitive to electrical noise. HF sensors produce a voltage significantly lower than a thermocouple. Therefore their HF signals need to be protected from interference in an industrial environment.

7.1.3 Performance of the process fluid temperature sensor.

The effect of lag in the process fluid temperature measurement on the accuracy of the heat transfer coefficient showed the need for synchronisation between the HF sensor and the process fluid temperature sensor measurements. When a RTD mounted in a stainless steel sheath was used to measure the process fluid temperature it was found to have a response time that was much slower than that of the HF sensor or thermocouples. This produced anomalies in the heat transfer coefficient trace. Such anomalies were not seen when the RTD sensors were replaced with thermocouples which had response times similar to that of the HF sensor.

7.1.4 Limitations of the sensor

The heat flux sensor was unable to detect fouling that consisted of only small islands of fouling on an otherwise visually clean plate. Theory suggests that the HF sensor will be less sensitive when attached to thicker walls. In the pilot plant experiments of this project the wall thickness of the plates monitored using the HF sensor was 0.6 mm which is quite thin. The walls of heat transfer surfaces in industry would not all be this thin so the sensitivity of the HF sensor in each situation would have to be considered.

7.2 Recommendations for further work.

7.2.1 Using the HF sensor to map fouling within a plant.

A series of HF sensors could be used to map the growth and removal of fouling from heated surfaces throughout milk powder plants or, indeed, other types of milk processing plants. The probe could be used to determine which surfaces within the plant foul the most and which surfaces within the plant take the longest to clean.

For further initial industrial work it is recommended that the HF sensor be installed on the utility side of a plate within a plate heat exchanger. This would allow the sensor to be tested in a fluid-to-fluid heat transfer system where it likely to produce the highest quality data.

7.2.2 Development of a data gathering and control system using the HF sensor.

To date the HF sensor has only been used as an experimental probe with customised data collection techniques. Large amounts of data were collected using the HF sensor and all of the data was analysed manually. Such a setup would not be feasible in an industrial setting. The amount of data collected by the HF sensor in the factory trial would be unmanageable over a long period of time and a person could not be expected to analyse it each day.

Automated data collection and processing techniques would have to be developed to provide a useful day-to-day CIP monitor for a dairy factory. Several probes would probably need to be used and a computer running quasi-intelligent software would be needed to monitor data from each of the probes, analyse it and record highlights or derived performance data. If the CIP monitor was installed in several plants that were managed by one

company (either a chemical supplier or dairy company) then networking of CIP monitors would provide essential access to data over long distances and the ability to compare sites from CIP cycle to CIP cycle. The CIP monitor system could be used to optimise the CIP process by using feed-back control to reduce cleaning times and concentrate cleaning efforts on trouble spots within the plant.

7.2.3 Development of fast-response temperature sensors.

If the heat flux sensor is to be used in a location where the process fluid temperature is unstable then a fast-response temperature sensor will be required. This is necessary so that the measurements of heat flux, HF sensor temperature and process fluid temperature are synchronised. Without this synchronisation the measured value of heat transfer coefficient will be unacceptably inaccurate.

To achieve the performance necessary the temperature sensor will need to have the transducer mounted in such a way that it is only affected by a very small thermal mass. This will improve the response time. To remove the problems of offset in temperature readings the sensors transducer will need to be thermally isolated from the probes external structure and surrounding piping. Despite these modifications, however, the probe will still need to be robust enough for industrial use.

Bibliography

[1] Anon. *CR10 Operator's manual.* Campbell Scientific, Inc., 1993.

[2] H. Bennett. Whole milk fouling on heated surfaces. Masters thesis, Massey University, Palmerston North, New Zealand, 2000. In press.

[3] M. R. Bird. Lecture 1: The need to clean. In *Cleaning and Disinfection in the Dairy and Food Processing Industries.* University of Auckland, Auckland, New Zealand, April 1997a.

[4] M. R. Bird. Lecture 3: Hard surface cleaning models. In *Cleaning and Disinfection in the Dairy and Food Processing Industries.* University of Auckland, Auckland, New Zealand, April 1997b.

[5] M. R. Bird. Lecture 4: Experimental cleaning results. In *Cleaning and Disinfection in the Dairy and Food Processing Industries.* University of Auckland, Auckland, New Zealand, April 1997c.

[6] New Zealand Dairy Board. http://www.nzdb.com/facts/figures-exports .html#revenues, May 2000.

[7] New Zealand Dairy Board. http://www.nzdb.com/facts/figures-industry.html, May 2000.

[8] H. Burton. Deposits from whole milk in heat treatment plant–a review and discussion. *Journal of Dairy Research*, 35:317–330, 1968.

[9] J. R. Carstens. *Electrical Sensors and Transducers.* Regents/Prentice Hall, New Jersey, USA, 1993.

[10] H. Chen. *Heat transfer and fouling in film evaporators with rotating surfaces.* PhD thesis, Massey University, Palmerston North, New Zealand., 1997.

[11] T.J. Davies, S.C. Henstridge, C.R. Gillham, and D.I. Wilson. Investigation of whey protein deposit properties using heat flux sensors. *Food and Bioproducts Processing*, 75(C2):106–110, 1997.

[12] T.J. Duddridge, C.A. Kent, and J.F. Laws. Effect of shear stress on the attachment of *pseudomonas fluorescens* to stainless steel under defined flow conditions. *Biotechnology and Bioengineering*, 24:153–164, 1982.

[13] P.J. Fryer and M.T. Belmar-Beiny. Fouling of heat exchangers in the food industry: a chemical engineering perspective. *Trends in Food Science and Technology*, 2(2):33–37, 1991.

[14] P.J. Fryer and A.M. Pritchard. A comparison of two possible fouling monitors for the food processing industry. In R.W. Field and J.A. Howell, editors, *Process Engineering in the Food Industry: Development and Opportunities*, London, UK, 1989. Elsevier Applied Science.

[15] P.J. Fryer and A.M. Pritchard. Factors which affect the kinetics of cleaning dairy soils. *Food Science and Technology Today*, 8(1):36–42, 1994.

[16] L. Fung. The effect of milk fat globule membrane damage in the absence of air on fouling in heat exchangers. Masters thesis, Massey University, Palmerston North, New Zealand., 1998.

[17] T. Gallot-Lavallee, M. Lalande, and G. Corrieu. A optical method to study the kinetics of cleaning milk deposits by sodium hydroxide. *Journal of Food Processing Engineering*, 5:131–143, 1982.

[18] T. Gallot-Lavallee, M. Lalande, and G. Corrieu. Cleaning kinetics modeling of holding tubes fouled during milk pasteurization. *Journal of Food Process Engineering*, 7:123–142, 1984a.

[19] P. Gilbert, G. Brown, and H. Dandwith. A novel method for cleaning high temperature-short time evaporators. *South African Journal of Dairy Technology.*, 11(2):57–59, 1979.

[20] A.S. Grandison. Factors of composition of milk which affect the formation of deposit during ultra high temperature (uht) processing. In *Fouling and Cleaning in Process Plant*, Oxford, UK, July 1988a. St. Catherines College.

[21] A.S. Grandison. Uht processing of milk: seasonal variation in deposit formation in heat exchangers. *Journal of the Society of Dairy Technology*, 41(2):43–49, 1988b.

[22] A. Grasshoff. A removal of firmly encrusted deposits in milk heaters using multi-stage cleaning. *Kieler Milchwirtschaftliche Forschungsberichte*, 45(1):67–80, 1993.

[23] A. Grasshoff. Cleaning of heat treatment equipment. *Bulletin of the International Dairy Federation*, 328:32–44, 1997.

[24] W.G. Jennings. Circulation cleaning iii: The kinetics of a simple detergent system. *Journal of Dairy Science*, 42:1763–1771, 1959.

[25] T.J.M. Jeurnink and D.W. Brinkman. The cleaning of heat exchangers and evaporators after processing milk of whey. *International Dairy Journal*, 4:347–368, 1994.

[26] A.D. Jones, N.J. Ward, P.J.R. Shreier, and P.J. Fryer. The use of a heat flux sensor in monitoring fouling. In P.J. Fryer, Hasting A.P.M., and Th.J.M. Jeurnink, editors, *Fouling and cleaning in food processing.* Jesus College, Cambridge, Directorate-General XII Science, Research and Development, Mar 1994.

[27] C. Ma and K.T. Trinh. The role of fat in milk fouling. In *Milk Powders for the Future 4.*, pages 99–105, 1999.

[28] W.R. Paterson and Fryer P.J. A reaction engineering approach to the analysis of fouling. *Chemical Engineering Science*, 43:1714–1717, 1988.

[29] M.N. Perlat, M. Lalande, and G. Corrieu. *Food engineering and process applications. Unit operations*, chapter Cleaning of UHT plants: influence of cleaning solutions according to deposit composition, pages 521–529. Elsevier Applied Science Publishers, Barking, Essex, U.K., 1986.

[30] R.H. Perry and D. Green, editors. *Perry's chemical engineers handbook.*, chapter 5. McGraw-Hill, rev. ed. of 5th edition, 1984.

[31] H.J. Schlussler. Zur reinigung fester oberflachen in der lebensmittelindustrie. *Milchwissenschaft*, 25(3):133–145, 1970.

[32] W. Smetana. *Handbook of sensors and actuators*, chapter Thick flim heat flux sensors, pages 151–165. Elsevier Science, B.V., 1994.

[33] R. Steinhagen, H.M. Muller-Steinhagen, and K. Maani. Heat exchangers applications, fouling problems and fouling costs in new zealand industries. Technical report, Market Information and Analysis Group, Energy and Resources Division, Ministry of Commerce, Wellington, New Zealand, 1990.

[34] D. Timperley, A.P.M. Hasting, and G. de Goederen. Developments in the cleaning of dairy sterilization plant. *Journal of the Society of Dairy Technology*, 47(2):44–50, 1994.

[35] D. Timperley and C.N.M. Smeulders. Cleaning of dairy htst plate heat exchangers: Comparison of single- and two-stage procedures. *Journal of the Society of Dairy Technology*, 40(1):4–7, 1987.

[36] D. Timperley and C.N.M. Smeulders. Cleaning of dairy htst plate heat exchangers: Optimization of the single-stage procedure. *Journal of the Society of Dairy Technology*, 41(1):4–7, 1988.

[37] J.P. Tissier and M. Lalande. Experimental device and methods for studying milk deposit formation on heat exchange surfaces. *Biotechnology Progress*, 2(4):218–229, 1986.

[38] J.P. Tissier, M. Lalande, and G. Corrieu. *Engineering and Food Vol. I. Engineering Sciences in the Food Industry*, chapter A study of milk deposit on heat exchange surface during UHT treatment, pages 49–58. Elsevier Applied Science Publishers, Barking, Essex, U.K., 1984.

[39] H.T. Truong. Design and development of a pilot-scale fouling rig and its evaluation. In B. Fenton and T. Murray, editors, *Proceedings of the 4th annual New Zealand Engineering and Technology Postgraduate Student Conference*, Hamilton, 1997. Univeristy of Waikato.

[40] T. Truong, S. Anema, K. Kirkpatrick, and K.T. Trinh. In-line measurements of fouling and cip in milk powder plants. In *Fouling and Cleaning in Food Processing*, Jesus College, Cambridge, U.K., 1998.

[41] P.M. Withers. Ultrasonic, acoustic and optical techniques for the non-invasive detection of fouling in food processing equipment. *Trends on Food Science and Technology*, 7(9):293–298, 1996.

[42] P.W. Wood and J. Middleton. *Physical properties of dairy products.* MAF Quality Management (N.Z.), 3 edition, 1996.

Appendix A

Abbreviations and Nomenclature

A.1 Abbreviations

CIP	cleaning-in-place
DPHE	double pipe heat exchangers
DSI	direct steam injection
HF	heat flux
HFS	heat flux sensor
HT	heat transfer
HTP	heat transfer paste
HTC	heat transfer coefficient
MPEC	mini plate heat exchanger
NHTC	normalised heat transfer coefficient
OHTC	overall heat transfer coefficient
P&ID	process and instrumentation diagram
PHE	plate heat exchangers
RTD	resistance temperature detector
SEM	scanning electron microscopy
TC	thermocouple
TCF	temperature correction factor
UHT	ultra heat temperature
WPC	whey protein concentrate

A.2 Nomenclature.

Symbol	Definition	Units
a	regression coefficient (dimensionless)	
b	regression constant	°C
A_m	cross-sectional area of milk flow in each fouling tube	m^2
A_T	cross-sectional area of milk flow through both fouling tubes	m^2
C_p	Specific heat capacity	J/kg.K
D_H	Hydraulic diameter of the duct	m
D_{io}	inner tube outer diameter.	m
D_{si}	shell tube inner diameter.	m
g	local acceleration due to gravity	m/s^2
HFQ	calibrated heat flux value	W/m^2
h_f	heat transfer coefficient of the fouling	(W/m^2K)
h_p	process fluid heat transfer coefficient	(W/m^2K)
I	electrical current	A
k	thermal conductivity of process fluid	W/mK
f	Fanning friction factor (dimensionless)	
L	Length of the duct	m
Le	equivalent pipe length	m
L_s	thickness of the HF sensor	m
Nu	Nusselt number (dimensionless)	
MF	voltage multiplication factor (heat flux)	W/m^2
Pr	Prandtl number (dimensionless)	
q	heat flux	W/m^2
R	electical resistance	Ω
R^2	correlation coefficient	
R_T	total heat transfer resistance	m^2K/W
R_c	constant heat transfer resistances (eq. 5.7)	m^2K/W
R_{milk}	heat transfer resistance of the milk	m^2K/W
R_s	heat transfer resistance of the HF sensor	m^2K/W
R_{HTP}	heat transfer resistance of the heat transfer paste or cement	m^2K/W
R_{wall}	heat transfer resistance of the wall	m^2K/W
R_p	heat transfer resistance of the CIP fluids	m^2K/W
R_f	heat transfer resistance of the fouling	m^2K/W
Re	Reynolds number (dimensionless)	
TMF	temperature multiplication factor (dimensionless)	
u	fluid velocity	m/s
U	Overall heat transfer coefficient between θ_p and θ_s	W/m^2K
U_0	Overall heat transfer coefficient attime zero.	W/m^2K
U_{60}	HTC at 60°C.	W/m^2K
U_{inf}	heat transfer coefficient of the flow system at the end of the final water rinse.	W/m^2K
U_c	sum of heat transfer resistances assumed to remain constant	W/m^2K
U_{clean}	overall heat transfer coefficient of the system with no fouling	W/m^2K
U_n	Normalised overall heat transfer coefficient.	
U_{nt}	HTC normalised to 60°C	
U_{tc}	HTC corrected for temperature effects.	
V	voltage	V
x_{HTP}	thickness of the heat transfer paste layer	m

Greek symbols

Symbol	Definition	Units
ΔP_{FRP}	pressure drop through fouling rig and surrounding piping.	Pa
$\Delta\theta$	$\theta_s - \theta_p$, the temperature difference between the heat flux sensor (θ_s) and the CIP solution (process fluid, θ_p)	K
ΔP_{FRP}	pressure drop through fouling rig and surrounding piping.	Pa
ΔP_{FT}	pressure drop across the fouling tubes	Pa
ΔP_{PHE}	pressure drop across the plate heat exchanger	Pa
ΔT	temperature difference across the HF sensor	K
ϵ	surface roughness	mm
λ_{HTP}	thermal conductivity of the heat transfer paste	W/mK
λ_p	thermal conductivity of the layer in the probe	W/mK
μ	Viscosity	Pa.s
λ_s	thermal conductivity of the HF sensor	W/mK
ϕ	heat flux	$\mathrm{W/m^2}$
$\phi_{50\mathrm{mV}}$	heat flux corresponding to a 50mV signal	$\mathrm{W/m^2K}$
ρ	Density	$\mathrm{kg/m^3}$
ΣR	Total HT resistance of the system at time zero	$\mathrm{m^2K/W}$
θ	reported temperature from sensor	°C
θ_0	reported temperature at 0°C	°C
θ_{100}	reported temperature at 100°C	°C
$\theta_{\mathrm{calibrated}}$	true temperature of the measured system	°C

Appendix B

Example Calculations.

B.1 Calculation of heat transfer coefficient for fouling modules.

Fouling module properties. Dimensions: 0.022m x 0.026m x (L) 0.047m. Hydraulic diameter:

$$D_H = \frac{\text{4x cross sectional area}}{\text{wetted perimeter}} = \frac{4(0.022)(0.026)}{2(0.022)+2(0.026)} = 0.02383\text{m} \tag{B.1}$$

Water properties.

The properties of water at various temperatures were taken from Cooper and Le Fevre (1975). For water at 60°C:

Viscosity	(μ)	$= 4.67 \text{ x } 10^{-4}$ Pa.s
Density	(ρ)	$= 983.3$ kg/m^3
Specific heat capacity	(C_p)	$= 4185$ J/kgK
Thermal conductivity	(k)	$= 0.653$ W/mK

Flow velocity:

$$u = \frac{\text{cross sectional area}}{\text{flowrate}} = \frac{(0.022)(0.026)}{2.777 \text{ x } 10^{-4}} = 0.4856 \text{ m/s} \tag{B.2}$$

$$Re = \frac{\rho u D_H}{\mu} = \frac{(983.3)(0.4856)(0.02383)}{4.67 \text{ x } 10^{-4}} = 24,365 \tag{B.3}$$

$24,365 > 10,000$ therefore flow is turbulent.

$$Pr = \frac{C_p \mu}{k} = \frac{(4185)(4.67 \text{ x } 10^{-4})}{0.653} = 2.99 \tag{B.4}$$

$$L/D_H = \frac{0.047}{0.02383} = 1.972 \tag{B.5}$$

$$Nu = 0.036(24,365^{0.8})(2.99)^{\frac{1}{3}}(1.972^{-0.054}) = 161.62 \tag{B.6}$$

The heat transfer coefficient of the process flow boundary layer can be calculated from the Nusselt number (Nu):

$$h_p = \frac{Nu.k}{L} = \frac{(161.62)(0.653)}{0.047} = 2245.5 \text{ W/m}^2\text{K} \tag{B.7}$$

Where: h_p = process fluid heat transfer coefficient = $1/R_p$ (W/m^{2}K)

B.2 Effect of flowrate on HTC.

Table B.1: Calculations of U for flow velocities of 0.4, 0.5, 0.6, 0.7 and 0.8 m/s.

Flowrate	0.82368	1.0296	1.23552	1.44144	1.64736
Velocity m/s	**0.4**	**0.5**	**0.6**	**0.7**	**0.8**
Temperature °C	20	20	20	20	20
Viscosity Pa.s	1.002E-03	1.002E-03	1.002E-03	1.002E-03	1.002E-03
Density kg/m^3	998	998	998	998	998
Cp J/Kg.K	4182	4182	4182	4182	4182
k W/mK	0.603	0.603	0.603	0.603	0.603
Re	9,494	11,867	14,241	16,614	18,988
Pr	6.95	6.95	6.95	6.95	6.95
L/D^-0.054	0.9640	0.9640	0.9640	0.9640	0.9640
Nu	100.69	120.37	139.27	157.55	175.31
h	**1291.80**	**1544.27**	**1786.77**	**2021.28**	**2249.16**
if Uc = 785.4	785.4	785.4	785.4	785.4	785.4
U	488.44	520.62	545.58	565.62	582.12

Appendix C

Computer Programming.

All source code presented here is also contained on the CD-ROM.

C.1 CR10X Datalogger program.

The following is the program run on the CR10X datalogger for collecting data from the Pahiatua site milk powder plant.

```
Program:
Flag Usage:
Input Channel Usage:
Excitation Channel Usage:
Control Port Usage:
Pulse Input Channel Usage:
Output Array Definitions:


*     1        Table 1 Programs
  01: 4        Sec. Execution Interval

01:  P2        Volt (DIFF)
  01: 1        Rep
  02: 31       2.5 mV 50 Hz rejection Range
  03: 3        IN Chan
  04: 3        Loc :
  05: -1       Mult
  06: 0.0000   Offset

02:  P14       Thermocouple Temp (DIFF)
  01: 1        Rep
```

```
  02: 3         25 mV slow Range
  03: 2         IN Chan
  04: 1         Type T (Copper-Constantan)
  05: 1         Ref Temp Loc
  06: 2         Loc :
  07: 1         Mult
  08: 0.0000    Offset

03:  P86        Do
  01: 10        Set high Flag 0 (output)

04:  P78        Resolution
  01: 1         High Resolution

05:  P70        Sample
  01: 1         Reps
  02: 2         Loc

06:  P70        Sample
  01: 1         Reps
  02: 3         Loc

07:  P86        Do
  01: 20        Set low Flag 0 (output)

08:  P          End Table 1


*      2        Table 2 Programs
  01: 8         Sec. Execution Interval

Page 2   Table 2


01:  P2         Volt (DIFF)
  01: 1         Rep
  02: 35        2500 mV 50 Hz rejection Range
  03: 1         IN Chan
  04: 1         Loc :
  05: 0.2       Mult
  06: -273.2    Offset

02:  P2         Volt (DIFF)
  01: 1         Rep
  02: 35        2500 mV 50 Hz rejection Range
  03: 4         IN Chan
```

```
  04: 4        Loc :
  05: 1        Mult
  06: 0.0000   Offset

03:  P2        Volt (DIFF)
  01: 1        Rep
  02: 35       2500 mV 50 Hz rejection Range
  03: 5        IN Chan
  04: 5        Loc :
  05: 1        Mult
  06: 0.0000   Offset

04:  P2        Volt (DIFF)
  01: 1        Rep
  02: 35       2500 mV 50 Hz rejection Range
  03: 6        IN Chan
  04: 6        Loc :
  05: 1        Mult
  06: 0.0000   Offset

05:  P10       Battery Voltage
  01: 7        Loc :

06:  P86       Do
  01: 10       Set high Flag 0 (output)

07:  P70       Sample
  01: 1        Reps
  02: 4        Loc

08:  P70       Sample
  01: 1        Reps
  02: 5        Loc

09:  P70       Sample
  01: 1        Reps
  02: 6        Loc

10:  P77       Real Time
  01: 111      Day,Hour-Minute,Seconds

Page 3   Table 2


11:  P86       Do
  01: 20       Set low Flag 0 (output)
```

```
12:  P        End Table 2


*     3       Table 3 Subroutines

01:  P        End Table 3


*     A       Mode 10 Memory Allocation
  01: 28      Input Locations
  02: 64      Intermediate Locations
  03: 0.0000  Final Storage Area 2


*     C       Mode 12 Security
  01: 0000    LOCK 1
  02: 0000    LOCK 2
  03: 0000    LOCK 3
```

Page 4 Input Location Assignments (with comments):

```
 Key:
 T=Table Number
 E=Entry Number
 L=Location Number

 T:  E:  L:
 2:  1:  1:  Loc :
 1:  2:  2:  Loc :
 1:  1:  3:  Loc :
 2:  2:  4:  Loc :
 2:  3:  5:  Loc :
 2:  4:  6:  Loc :
 2:  5:  7:  Loc :
```

C.2 Programs for arranging data from the industrial trial.

C.2.1 Program to patch raw data to make it a regular pattern.

The Visual Basic scripts listed below were used to sort data gathered from the factory trial. The first script (main function 'fix_data()') corrected the data to remove holes of lost data and bring it into a regular pattern. This was necessary so that the data could be then sorted by another program. Sorting the data manually would have been prohibitively time consuming as more than 180,000 lines of data were collected.

```
Sub fix_data()
' Fixes the holes in data from Pahiatua
' by deleting lines or inserting a blank line.
'
' 7/05/00
' by Richard Croy
' Keyboard Shortcut: Ctrl+y
'
For i = 1 To 1000

  While ActiveCell.Value <> 206
   move_down (1)
  Wend

    ActiveCell.Select
    If ActiveCell.Offset(2, 0).Range("A1").Value = 206 Then
        plus2 (0)
    ElseIf ActiveCell.Offset(3, 0).Range("A1").Value = 206 Then
        plus3 (0)
    ElseIf ActiveCell.Offset(4, 0).Range("A1").Value = 206 Then
        plus4 (0)
    ElseIf ActiveCell.Offset(5, 0).Range("A1").Value = 206 Then
        plus5 (0)
    Else
        Exit Sub
    End If

Next i

End Sub

Sub move_down(down)
' Move active down by [down] rows
    ActiveCell.Offset(down, 0).Range("A1").Select
End Sub
```

```
Sub move_up(up)
' Move active cell up by [up] rows
    ActiveCell.Offset(-up, 0).Range("A1").Select
End Sub

Sub plus2(dummy)
' Fix if only one 103 line between two 203 lines.  Adds a empty
' row.
' Won't waste time finding out why VB won't accept "plus2()" as
' a function.  Just pass zero as a dummy variable instead.
    move_down (2)
    ActiveCell.Rows("1:1").EntireRow.Select
    ActiveCell.Activate Selection.Insert Shift:=xlDown ActiveCell.Select
    move_up (1)

End Sub

Sub plus3(dummy)
' All is good
    move_down (1)
End Sub

Sub plus4(dummy)
' Delete a row
    move_down (2)
    ActiveCell.Rows("1:1").EntireRow.Select
    ActiveCell.Activate
    Selection.Delete Shift:=xlUps
    ActiveCell.Select
    move_up (1)
End Sub

Sub plus5(dummy)
' Delete two rows.
    move_down (2)
    ActiveCell.Rows("1:2").EntireRow.Select
    ActiveCell.Activate
    Selection.Delete Shift:=xlUps
    ActiveCell.Select
    move_up (1)
End Sub
```

C.2.2 Removing data recorded between 8 second intervals.

This recorded Visual Basic script was used to cut 4 second interval data (HF and HF sensor temp.) from the data leaving just the 8 second data.

```
Sub crop_to_8_secs()
'
' crop_to_8_secs Macro
' Macro recorded 31/03/00 by Richard Croy
' Removes every second line from the data.
'
' Keyboard Shortcut: Ctrl+f
'
 For i = 1 To 1000
    ActiveCell.Rows("1:1").EntireRow.Select
    Selection.Delete Shift:=xlUp
    ActiveCell.Offset(1, 0).Rows("1:1").EntireRow.Select
    Selection.Delete Shift:=xlUp
    ActiveCell.Offset(1, 0).Rows("1:1").EntireRow.Select
    Selection.Delete Shift:=xlUp
    ActiveCell.Offset(1, 0).Rows("1:1").EntireRow.Select
    Selection.Delete Shift:=xlUp
    ActiveCell.Offset(1, 1).Range("A1").Select
 Next i

End Sub
```

C.2.3 Organising data into straight columns.

This recorded Visual Basic script was used organise Pahiatua data into a plain table with each variable in only one column. This is just a set of cut and paste and row-delete operations.

```
Sub sort_pahiatua()
'
' sort_pahiatua Macro
' Macro recorded 30/03/00 by Richard Croy
'
' Organises Pahiatua data into plain columns.
' Keyboard Shortcut: Ctrl+g
'
 For i = 1 To 1000
    ActiveCell.Offset(2, 0).Range("A1:F1").Select
    Selection.Cut
```

```
    ActiveCell.Offset(-1, 2).Range("A1").Select
    ActiveSheet.Paste
    ActiveCell.Offset(1, 0).Rows("1:1").EntireRow.Select
    Selection.Delete Shift:=xlUp
    ActiveCell.Offset(2, 0).Range("A1:F1").Select
    Selection.Cut
    ActiveCell.Offset(-1, 2).Range("A1").Select
    ActiveSheet.Paste
    ActiveCell.Offset(1, 0).Rows("1:1").EntireRow.Select
    Selection.Delete Shift:=xlUp
    ActiveCell.Offset(2, 0).Range("A1:F1").Select
    Selection.Cut
    ActiveCell.Offset(-1, 2).Range("A1").Select
    ActiveSheet.Paste
    ActiveCell.Offset(4, -2).Range("A1:F1").Select
    Selection.Cut
    ActiveCell.Offset(-1, 2).Range("A1").Select
    ActiveSheet.Paste
    ActiveCell.Offset(-2, 0).Rows("1:1").EntireRow.Select
    Selection.Delete Shift:=xlUp
    ActiveCell.Offset(2, 0).Rows("1:1").EntireRow.Select
    Selection.Delete Shift:=xlUp
    ActiveCell.Offset(2, 0).Range("A1:F1").Select
    Selection.Cut
    ActiveCell.Offset(-1, 2).Range("A1").Select
    ActiveSheet.Paste
    ActiveCell.Offset(1, 0).Rows("1:1").EntireRow.Select
    Selection.Delete Shift:=xlUp
    ActiveCell.Offset(2, 0).Range("A1:F1").Select
    Selection.Cut
    ActiveCell.Offset(-1, 2).Range("A1").Select
    ActiveSheet.Paste
    ActiveCell.Offset(1, 0).Rows("1:1").EntireRow.Select
    Selection.Delete Shift:=xlUp
    ActiveCell.Select

    Next i

End Sub
```

Appendix D

Chemical analysis.

D.1 Mojonnier method for fat. AACC Method 30-10.

D.1.1 Apparatus.

- Water bath.
- Beaker, 50 ml.
- Mojonnier fat extraction apparatus.
- Steam bath.
- Steam bath.
- Drying oven.
- Centrifuge.

D.1.2 Reagents.

- Ethyl alcohol (95%)
- Hydrochloric acid solution (25 ml conc Hcl plus 11 ml water).
- Diethyl ether, free from residue on evaporation.
- Petroleum ether, boiling point below 60^{o}C.
- 35^{o}C w/w ammonium hydroxide.
- 2% phenolphthalein.

D.1.3 Preparation of flour, bread or baked cereal products.

1. Place 2 g flour in 50 ml beaker, add 2 ml ethyl alcohol and stir to moisten particles. Moistening of the sample with alcohol prevents lumping on addition of acid. Add 10 ml HCl mix well. Set beaker in a boiling water bath and stir at frequent intervals for 30-40 minutes. Cool. Add 10 ml alcohol and mix.

2. Transfer mixture to Mojonnier fat extraction tube. Rinse beaker into extraction tube with 25 ml of diethyl ether in three portions. Stopper flask and shake gently for about 1 minute.

D.1.4 Majonnier fat extraction procedure (all samples).

1. Remove the stopper and add 25 ml petroleum ther, using the first few ml to rinse the stopper and the neck of the tube, allowing the rinsings to run into the tube.

2. Replace the stopper, again wetted with water, and rock carefully for 30 seconds.

3. Centrifuge Mojonnier flask for 2 minutes at 600 RPM.

4. Examine the tube to see if the interface of the liquid is in line with the upper junction of he neck of the tube. If it is below this, it should be raised by the addition of a little water run down the side of the tube.

5. Remove the cork and carefully decant as much as possible of the organic solvent layer into a preweighed short-necked flask by gradually bringing the cylindrical bulb of the tube into a horizontal position.

6. Add 5 ml of ethyl alcohol and mix. The helps prevent emulsions forming and is in accord with the AOAC method.

7. Repeat the extraction using 15 ml of diethyl ether and 15 ml of petroleum ether (steps 1 to 5). Add second extract into the same flask as used in step (5).

8. Use a steam bath to evaporate solvent and dry the flask in the oven at 100^{o}C for 90 minutes, taking precautions to remove all traces of solvent vapour prior to placing in the oven.

9. Allow the flask to cool to room temperature. Do not use a desiccator.

10. Weigh the flask, and record the fat content of the sample.

11. At the same time as the above procedure is carried out, make a blank determination with 10 ml of water in place of the sample. Use a similar extraction apparatus, the same reagents and the same technique throughout. Correct the apparent weight of fat for the change, if any, in the weight of the flask used for the blank determination.

D.1.5 Results - fat content.

Table D.1: Retentate fat content results.

Sample	sample weight (g)	Fat extracted (g)	fat content (%)
1	5.1643	0.0375	0.73
2	5.4049	0.0411	0.76
3	5.365	0.0395	0.73
4	4.961	0.0358	0.72
		mean fat content	0.74

D.2 Protein Analysis - Kjeldahl Method.

The quantitative determination of total organic nitrogen in foods is often used for estimating the total protein content but the method will include other nitrogenous compounds present usually in minor proportions. The crude protein is calculated by multiplying the total nitrogen by an empirical factor (for dairy products, 6.38). It should be borne in mind, however, that such a figure for protein often includes some non-protein nitrogenous compounds and also that nitrogen in certain forms (e.g. nitrates, nitrites and nitroso compounds) is not estimated in the Kjeldahl process.

D.2.1 Apparatus.

Kjeltec 1026 system (Tecator Sweden).

D.2.2 Reagent.

- Concentrated H_2SO_4.
- Kjeltabs
- 4% boric acid solution.
- 250 ml conical flask

- 0.1 M HCl.

D.2.3 Digestion.

1. Accurately weigh about 0.5 g sample into the digestion tube.
2. Add two Kjeltabs (each containing 3.5 g K_2SO_4 and 0.0035g Se) and then 15 ml concentrated H_2SO_4.
3. Carry on a blank digestion at the same time (no sample, but all other reagents). Set up block digester unit and digest samples at 420°C for 40 minutes or until clear.
4. Remove the tubes carefully from the heating unit, leaving the exhaust manifold in place and water aspirator about half on. Allow to cool until the tops of the tubes are cool to touch.
5. Add approximately 70 ml hot distilled water to each tube and shake gently to mix. Ensure all solids have been dissolved.

D.2.4 Distillation and titration.

1. Add 25 ml 4% boric acid solution to 250 ml conical flask.
2. The distilling unit has been prepared for distillation and is set on "automatic".
3. Connect the digestion tube with the first sample to be distilled in position.
4. Place the receiver flask and boric acid solution on the platform and raise it to its upper position. To avoid contamination don't touch the glass outlet tube with your fingers. Hold it by its plastic tubing.
5. Close the safety door. The distillation automatically starts.
6. When the distillation is complete, the machine will "beep" several times. Remove the digestion tube and the receiver flask.
7. Titrate the sample with 0.1M HCl to grey-mauve end point.

Calculation.

$$\%N = \frac{(A)(B)(1400)}{1000(C)} \tag{D.1}$$

$$\%Protein = \%N(6.38) \tag{D.2}$$

Where: A = mls HCl used

B = exact molarity (normality) of HCl

C = weight of original sample taken (g)

D.2.5 Results - protein content.

Because sample one required only 0.1 ml of 0.1M HCl to reach its end-point the acid concentration for the following two samples was decreased to 0.01M. A burette of a smaller volume was also used for samples 3 and 3 to provide a more accurate reading.

Table D.2: Retentate protein composition results.

sample	sample weight (g)	mls HCl	% Nitrogen	(%N * 6.38)
1	1.0249	0.1ml (0.1M)	1.336	8.72
2	1.0152	1.20ml (0.01M)	1.165	10.56
3	1.0485	1.25ml (0.01M)	1.669	10.64
			Mean of 2 & 3	10.6

D.2.6 Caustic analysis - retentate.

The caustic concentration of the retentate was measured by titrating it against 0.1M HCl. Bromothymol Blue was used as the indicator. The results of the first six measurements were variable because the solution was not warm enough. If the sample was not warm enough the protein would coagulate.

Results

The final value was therefore 12.1 ml HCl (0.1M) required for 5.1 ml of retentate. The weight of NaOH (atomic mass 39.992) in the 5.1 ml of sample was therefore:

$$M_{\mathrm{NaOH}} = \frac{Atm_{\mathrm{NaOH}} V_{\mathrm{HCl}} MHCl}{1000 \text{ mls/L}} = \frac{(39.992)(12.1)(0.1)}{1000} = 0.04839g \tag{D.3}$$

Table D.3: Titration results for caustic concentration in the retentate.

Sample	Sample volume (ml)	Volume HCl (0.1M)
1	5.0	17.2
2	5.1	16.2
3	5.0	16.4
4	5.1	17.7
5	5.0	17.8
6	5.0	20.8
sample re-heated and mixed throughly		
7	5.1	12.1
8	5.1	12.1
9 7 5.1	12.1	

Where: Atm_{NaOH} = Atomic mass of caustic soda (g/mol)

V_{HCl} = volume of HCl (ml)

$MHCl$ = Molarity of HCl (Mol)

The density of the retentate was measured and found to be 0.9838 g/ml. The caustic composition by weight was then calculated.

$$\%caustic = \frac{M_{\mathrm{NaOH}}}{V_{\mathrm{NaOH}}\rho_{ret}} = 0.964\%\mathrm{w/w} \tag{D.4}$$

Where: M_{NaOH} = mols of NaOH in 5.1 ml sample.

V_{NaOH} = volume of NaOH (ml)

ρ_{ret} = density of the retentate (g/ml)

Appendix E

Contents of the CD-ROM

A CD-ROM is included that contains additional information belonging to the Appendix. The contents include:

- Experimental notes and data. The two videos made of CIP are also given in MPEG format.
- Electronic copies of the thesis. The thesis is given in PDF and Postscript form. Also provided are the LaTeX source files for the thesis and the individual figures in PDF form.
- Programs and Macros. The Visual Basic macros used to manipulate data are given in both Excel spreadsheets and in plain text. The program run on the datalogger is also provided.

Details of the contents of the CD-ROM are given in the ReadMe.txt file located in the root directory the CD-ROM itself.